DESIGN, SYNTHESIS AND CHARACTERIZATION OF EUMELANIN-INSPIRED SMALL MOLECULES AND POLYMERS AS NOVEL ORGANIC SEMICONDUCTORS

By

K. A. NIRADHA SACHINTHANI

Bachelor of Science in Chemistry
University of Kelaniya
Kelaniya, Sri Lanka
2010

Submitted to the Faculty of the
Graduate College of the
Oklahoma State University
in partial fulfillment of
the requirements for
the Degree of
DOCTOR OF PHILOSOPHY
July, 2017

DESIGN, SYNTHESIS AND CHARACTERIZATION OF EUMELANIN-INSPIRED SMALL MOLECULES AND POLYMERS AS NOVEL ORGANIC SEMICONDUCTORS

Dissertation Approved:

Dr. Toby Nelson

Dissertation Adviser

Dr. Richard Bunce

Dr. Jimmie Weaver

Dr. Jeffery White

Dr. Heather Fahlenkamp

ACKNOWLEDGEMENTS

First of all, I am grateful to the almighty God for giving me a wonderful time at OSU with good people and a healthy life.

Secondly, I would like to express my sincere appreciation and gratitude to my advisor Dr. Toby L. Nelson for all his support, guidance, kindness, trust and for all the opportunities I was given to conduct my research over these five years period. I was very lucky to have such a research environment with my colleagues under your supervision. Without your help and motivation, this dissertation would not have been possible.

Next, I would like to thank my advisory committee members Dr. Jeffery White, Dr. Richard Bunce, Dr. Jimmie Weaver and for my outside committee member Dr. Heather Fahlenkamp for their valuable suggestions and corrections they made in my PhD candidacy exam and in my dissertation defense. A special thanks goes to Dr. Darrell Berlin for his guidance and for revising my documents over the last five years.

I would love to thank my second family, Nelson's group and all of the members in our group. Starting with Dr. Subhashini Selvaraj, I thank Dr. Devang Khambhati, Raianna Hopson, Daniel Pankratz, Santosh Adhikari, Fathima Pary, Susan Pham and my undergraduates Reagan Chambers, Ray Martin and Charles Ault for their support and for making a nice, cooperative working environment in the laboratory.

I'm taking this opportunity to thank all of our collaborators, Prof. Joseph Shinar and Ruth

Shinar, for giving me a chance to visit their lab and learn OLED device fabrication techniques and for their time spent to collect data for my polymer project. I would like to thank my mentor at Ames Laboratory, Rajiv Kaudal, and my friends at Ames, Ravindu and Himashi Andaraarachchi, who provided me accommodations. At the same time, I thank Prof. Shanlin Pan and Nelly Kaneza at Louisiana State University for their enthusiasm do to ECL measurements for my polymers.

I also would like to thank all the faculty and staff members of the department of chemistry, Oklahoma State University, for being very helpful and friendly and for the department of chemistry for providing me a GTA position over five years and all the funding agencies who funded our research projects.

Finally, I would love to thank my dearest husband, Chaminda Pushpakumara, who sacrificed five years of his carrier life by being with me in Stillwater. Without you I could never have accomplished this dissertation. All your encouragement, help and understanding means a lot to me. A special thanks goes to my parents K. A. Wimalasena and K. L. Mary M. Perera and my mother-in-law Danwathie Abewickrama for staying with me the last three years and for taking care of my son while I worked at the university. Without their generous support it would have been impossible to accomplish this journey. A big thanks goes to my son, Senosh C. Appuhamividanaralalage for giving me much happiness and relieving all of my stress over the last three years.

Acknowledgements reflect the views of the author and are not endorsed by committee members or Oklahoma State University.

Name: K. A. NIRADHA SACHINTHANI

Date of Degree: JULY, 2017

Title of Study: DESIGN, SYNTHESIS AND CHARACTERIZATION OF EUMELANIN-INSPIRED SMALL MOLECULES AND POLYMERS AS NOVEL ORGANIC SEMICONDUCTORS

Major Field: CHEMISTRY

Abstract:
Over the past few decades, organic semiconductors (OSCs) have become a rapidly growing research field due to their diverse range of applications in electronics such as organic photovoltaics, organic light emitting diodes, organic field effect transistors, sensors and polymer batteries. These organic electronics offer several advantages over the conventional electronics because they are low-cost, flexible, optically transparent, light-weight and have low power consumption systems. Therefore, there is a high demand for high performance organic semiconductor materials. In the process of developing new OSCs, we have been inspired by materials that mother nature has created. One such nature's inspired material is Eumelanin, the major form of the natural pigment, Melanin. Melanin is found in all most all organisms and it is the primary determinant of the skin tone in humans. It is also found in hair, eyes, inner ears and brain of humans and acts as a photo-protective agent against the harmful radiation by converting it in to non-radiative pathways. Scientists have isolated natural eumelanin, a black-brown insoluble bio-macromolecule, from the ink sac of cuttlefish *Sepia*. It has been determined that the eumelanin is composed of two building blocks, 5,6-dihydroxyindole and 5,6-dihydroxyindole-2-carboxylic acid, but the exact structure of the eumelanin remains unsolved. Recently, Meredith and coworkers groundbreaking work established eumelanin as an electronic-ionic conductor rather than an organic semiconductor which opens the door to many bioelectronics applications. However, the current synthetic eumelanin materials have poor solubility, produce thin, brittle films with poor morphologies and are not well-suited for analysis and fabrication of electronic devices. Therefore, synthesizing well-defined, soluble eumelanin-inspired material is significant.

In my research, the synthesis of eumelanin inspired core (DBI), which is similar to the building blocks of natural eumelanin, will be discussed first. Secondly, the utilization of this core to synthesize blue-emitting polymers for organic light emitting diodes (OLEDs), with optoelectronic, physical and electro-generated chemiluminescence properties and as OLED device fabrication process will be reported. Finally, synthesis of eumelanin-inspired small molecules and polymers for the purpose of studying the structure-property-function relationships of natural eumelanin will be presented.

TABLE OF CONTENTS

Chapter Page

Chapter Page

Chapter Page

LIST OF TABLES

LIST OF FIGURES

Figure Page

Figure Page

LIST OF SCHEMES

Scheme Page

Scheme Page

CHAPTER I

INTRODUCTION AND BACKGROUND

1.0. INTRODUCTION

Mother nature is the best box of crayons. One such crayon is Melanin, the major pigment found in most organisms such as animals, including human, seeds, mushrooms and bacteria. Other than its two key features, coloration and photo-protection, melanin shows electrical conductivity in the semiconductor range. Recently it was recognized as an ionic-electronic hybrid conductor which opens the door of many bioelectronics. Applying nature's wisdom to our synthetic processes is a great task. Therefore, by utilizing eumelanin, new organic semiconductors can be developed. Mimicking the structure of this biopolymer will enable one to understand its structure-property-function relationships.

1.1. ORGANIC SEMICONDUCTORS

Semiconductor is a compound that is between the insulator and metal in its ability to conduct electric current. This ability can be selectively controlled by doping the materials with an impurity. Semiconductors are widely used in solid state electronic devices such as diodes, rectifiers,

transistors and integrated circuits (computer and memory chips). Semiconductors can be mainly divided in to two sub groups: organic semiconductors and inorganic semiconductors.[1]

Organic semiconductors (OSCs) are carbon-based materials which show properties such as higher electron conductivities, ion mobility, low band gaps, absorption and emission of light in the visible spectral range.[2-4] These materials hold promise for lightweight, inexpensive, flexible substrates that can be used and can be processed in solutions at low temperatures. Therefore, OSCs are highly applicable in electronic devices such as organic light emitting diodes (OLEDs)[5-7], organic photovoltaics (OPVs)[8-10], organic field effect transistors(OFETs)[11-13], electronic sensory devices[14-16] and polymer batteries[17-19]. Although, the OSCs have not reached the same level of electronic performance as their inorganic counterparts, the drive to produce organic electronics comes from the advantages afforded by the organic materials over the traditional silicon-based semiconductors. Most organic materials are much less expensive to generate than the highly crystalline, ultrapure inorganic semiconductors, and involve inexpensive device fabrication methods. In particular, most organics are soluble in one or more common organic solvents which allows for the possibility of solution processing, low cost, large area device fabrication techniques such as spin coating[20], inject-printing[21-22] and roll-to-roll screen printing[23]. Additionally, most inorganic semiconductor devices require an annealing step to reach to the high performance that is generally at high temperatures (at least 500 ^{o}C for silicon), but this is much less or not required for organic materials. The low annealing temperatures of organics allows for flexibility of the substrate choice for organic devices, such as transparent plastics, which is unable to withstand to the high annealing temperatures of silicon. The other advantage is the ability of tailoring the properties of the material for a specific applications by tuning the structures with the various groups.

OSCs are conjugated molecules having alternating single and double bonds in the entire structure and are planar with sp^2 orbital hybridization of the connecting carbons. The empty p_z orbitals of these sp^2 hybridized carbon atoms are perpendicular to the plane of the molecule. The overlapping

of p_z orbitals creates a system of delocalized π electrons among the molecules represented as an electron cloud. (**Figure 1.1.**)

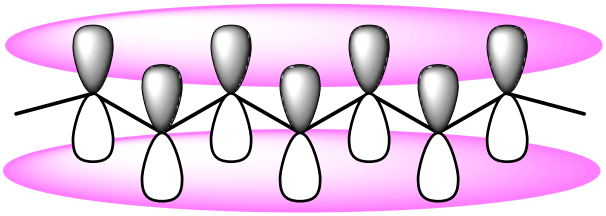

Figure 1.1. The electron cloud formed by the delocalized π electrons in p_z orbitals.

1.1.1. Band gap

The band gap is a characteristic property of OSCs. According to the Hückel theory, when two atomic orbitals combine, two types of new molecular orbitals are formed. They are bonding orbitals and anti-bonding orbitals. Similarly, in an ethylene molecule, two p_z atomic orbitals of the carbon atoms form two molecular orbitals which is shown in **Figure 1.2.** In the 1,3-butadiene molecule,

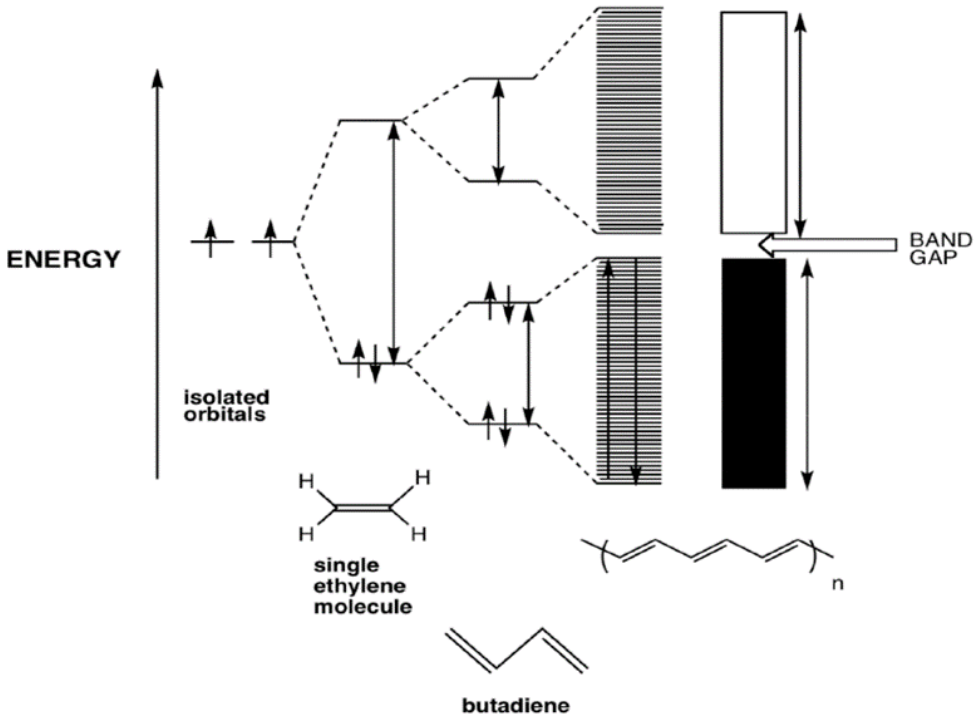

Figure 1.2. Band gap formation

four molecular orbitals are formed, and the energy gap between the highest occupied molecular orbital (HOMO) and lowest unoccupied molecular orbital (LUMO) has been reduced when compared to the ethylene. When conjugation increases, the number of p_z orbitals are increased which overlap and generates series of bonding and anti-bonding orbitals. These orbitals are energetically very close to each other and form two bands called a valence band and a conduction band. The valence band is full of electron filled bonding orbitals while the conduction band is a collection of antibonding orbitals. The gap between these two bands is referred as the band gap. One can also define the gap as between the HOMO and LUMO energy levels.

The band gap of a conductor is zero due to the overlapping of the valence and conduction bands while for an insulator it is very large. Generally, a material to be considered as a semiconductor, the band gap should be less than 3.5 eV. The band gap comparisons of metals, semiconductors and insulators is shown in **Figure 1.3.**

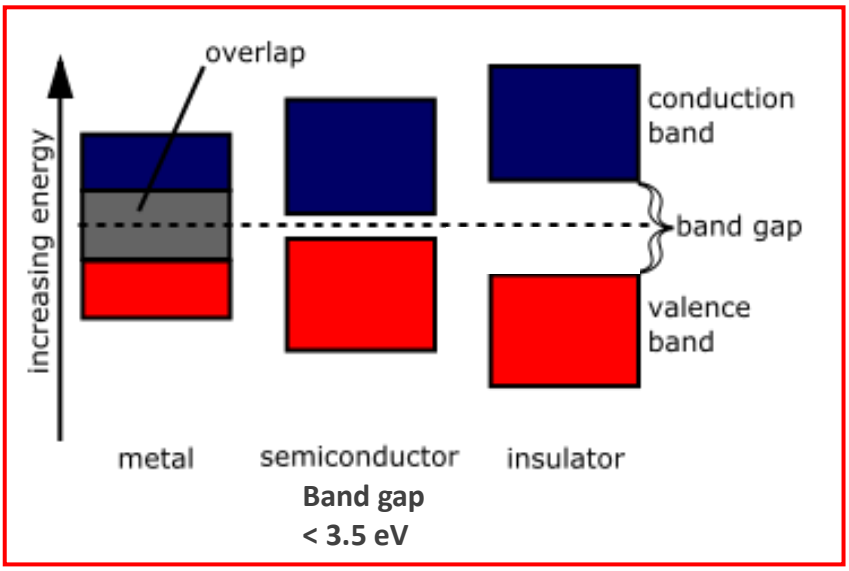

Figure 1.3. The band gap of metal, semiconductor and insulator

1.2. CLASSIFICATION OF ORGANIC SEMICONDUCTORS

OSCs are generally classified in two major groups: conjugated small molecules and conjugated polymers.

1.2.1. Conjugated small molecules

Conjugated small molecules can be either a single molecule or an oligomer. Some of the conjugated small molecules used in the electronic devices are shown in **Figure 1.4.** Conjugated small molecules have several advantages over conjugated polymers. They have a higher degree of structural homogeneity and higher purity. They can be reproduced easily since the exact structure is known.

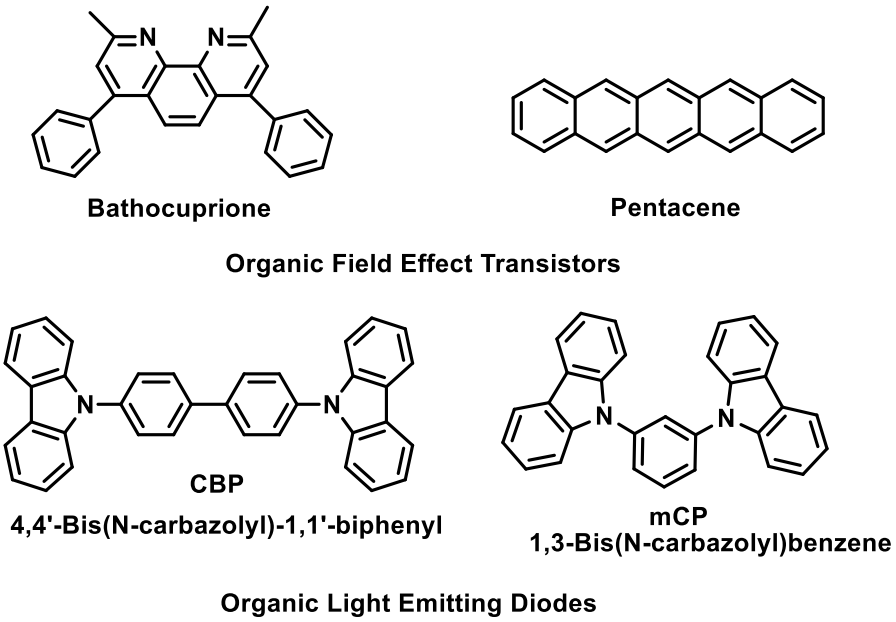

Figure 1.4. Some conjugated small molecules used in organic electronics.

Some conjugated small molecules are highly crystalline and not very soluble in common organic solvents. Therefore, techniques such as thermally evaporated vapor deposition, is used with them to fabricate electronic devices. The CBP and mCP [24-25]are the host materials used in the emissive

layers of the OLEDs and bathocuprione[26] and pentacene[27] are commonly used compounds in OFETs.

1.2.2. Conjugated polymers

The extended conjugation along the backbone of a conjugated polymer enables proper charge transportation and optical absorption of these polymers. When the backbone is functionalized with the solubilizing groups such as alkyl chains and alkoxy chains, solution processable polymers can be achieved and lead to low cost fabrication techniques for organic electronics.[28] The extent of conjugation, number averaged molecular weight (M_n) of the polymer and polydispersity index (PDI) are some of the common parameters which govern the optical, physical and electronic properties of the polymers.

1.3. TYPES OF CONJUGATED POLYMERS

1.3.1. Poly(aryleneethynylene)s

Poly(aryleneethynylene)s (PAEs) are a class of conjugated polymers which displays a robust and rigid nature due to the backbone. These polymers are generally luminescent in both solution and solid states. The optical and electrical properties of these polymers can be tuned by altering either the arylene unit or through the attachment of side chains. These polymers are highly used in sensors[29], supramolecular assemblies[30] and molecular wires[31]. PAEs are mostly synthesized by the Sonagoshira polycondensation method. The polymerization involves the Pd(0) catalyzed cross coupling between an sp^2 hybridized carbon and an sp-hybridized carbon which creates a new sigma bond by extending the conjugation. This polymerization reaction can be accomplished under mild reaction conditions and enables a large functional group tolerance with high yields. This reaction uses catalytic amounts of Pd and Cu and stoichiometric amounts of base.[32] A model reaction is shown in **Scheme 1.1.**

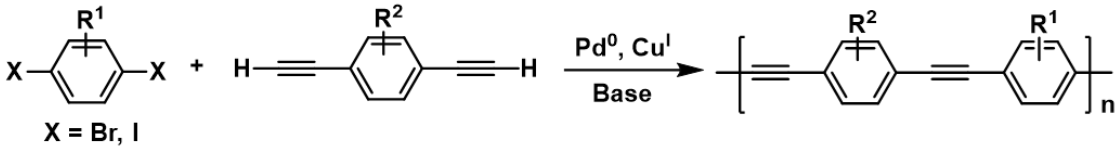

Scheme 1.1. The Sonagoshira coupling polymerization.

1.3.2. Polyarylenes

Polyarylenes are the major group of conjugated polymers which are widely applied in organic electronics. The most commonly used conjugated polyarylenes are shown in **Figure 1.5.** Polyarylenes are generally rigid-rod polymers having good chemical stabilities and useful physical properties.

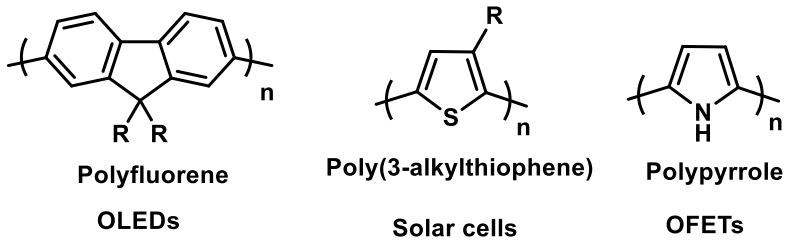

Figure 1.5. Common conjugated polyarylenes used in organic electronics

With the early development of the conjugated polymer field, well-defined conjugated polymers, such as poly(3-akylthiophene)s, poly(p-phenylene)s, poly(fluorene)s and poly(pyrrole)s gained extensive attention.[32] Not only homopolymers but polyarylene copolymers are also playing a crucial role in performances of the electronic devices. Through the appropriate choice of an arylene repeat unit, polymers can be designed and synthesized with electron rich and electron deficient properties for the stabilization of holes and electrons. The band gaps of these polymers can be tuned for specific light absorption and emission. The lower band gap polymers can be used to harvest light in solar cells[33] while higher band gap polymers can be applied as blue emitters in OLEDs.[34]

1.4. SYNTHETIC TOOLS FOR POLYARYLENES

Polyarylenes can be prepared by conventional synthesis methods such as Grignard metathesis, Suzuki, Stille and Yamamoto coupling reactions. These techniques allow a connection between two sp^2-hybridized C atoms more efficiently.

1.4.1. Grignard Metathesis (GRIM)

In 1999, the GRIM technique was developed to synthesize regioregular poly(3-alkylthiophene)s (rrP3ATs) by McCullough group.[35] These rrP3ATs showed excellent electronic properties due to their ability to order three dimensions, such as conformational ordering along the backbone, π-stacking of flat polymer chains, and lamellar stacking between chains. Therefore, this was a great invention was successfully applied to synthesize polyphenylenes[36], polyfuorenes[37] and thiophene based di block, triblock copolymers[38-39].

When the 2,5-dibromo-3-alkylthiophene is reacted with one equivalence of Grignard reagent, it forms two regiochemical isomers namely, 2-bromo-3-alkyl-5-bromomagnesiothiophene (**A**) and 2-bromomagnesio-3-alkyl-5-bromothiophene (**B**) in an 85:15 ratio. However, only major isomer **A** is initialized the polymerization reaction due to steric effects which lead to > 99% regioregular poly(3-alkylthiophene).[40] The GRIM reaction of poly(3-hexylthiophene) is shown in **Scheme 1.2.**

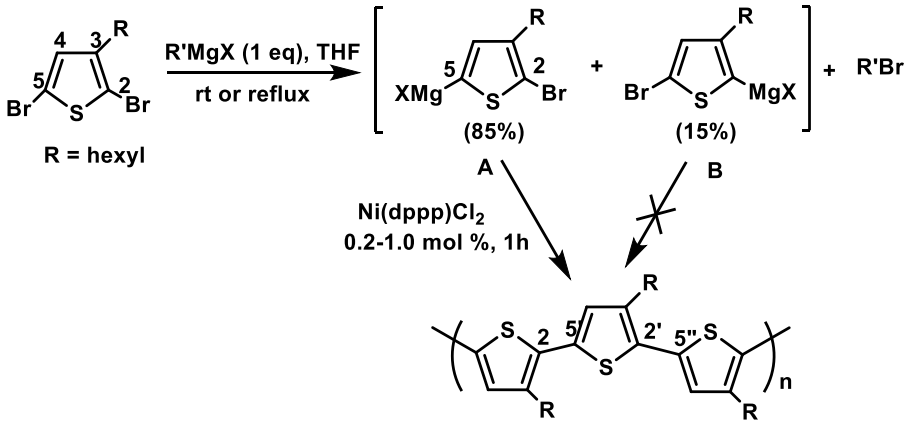

Scheme 1.2. The synthesis of poly(3-hexylthiophene) using GRIM reaction

This is a Ni(II) initiated quasi-"living" chain growth polymerization technique which offers narrower molecular weight distributions and defined chain-ends. Moreover, higher molecular weights can be achieved by controlling the ratio between the Ni(II) catalyst and the monomer.[40] The mechanism for the repetitive transformation of the Ni complex to the chain end for further propagation of the polymer is still unclear.[41]

1.4.2. Suzuki-Miyaura polymerization

The Suzuki-Miyaura cross coupling reaction was invented by Suzuki, Miyaura and coworkers in 1979. This is a very versatile synthetic tool used to make a C-C bond between the aryl or vinyl boronic acid with an aryl or vinyl halide catalyzed by Pd(0) complexes. Later, this method was widely used to synthesize conjugated polymers. Suzuki-Miyaura polymerization is a step growth type polymerization and offers several advantages over other conventional cross coupling polymerizations. The process uses milder reaction conditions, reactants are commercial availabile such as diverse boronic acids/esters, and the overall method is environmentally safer. Moreover, the removal of boron containing byproducts is task when compared to other organometallic reagents. The mechanism of the Suzuki-Miyaura polymerization is consists of three main steps; 1). Oxidative addition and metathesis 2). transmetallation and 3). reductive elimination.[42] A Pd^0 catalyzed Suzuki-Miyaura polymerization of polyfluorene[43] is shown in **Scheme 1.3.**

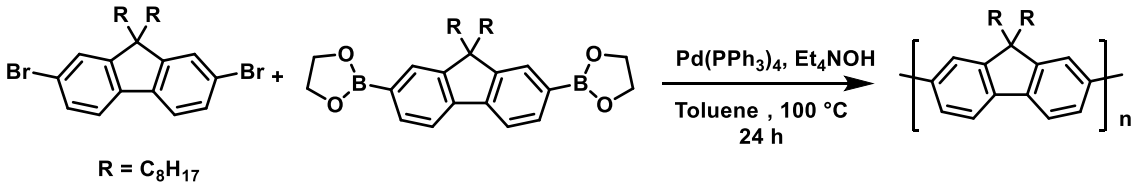

Scheme 1.3. The Suzuki-Miyaura polymerization of polyfluorenes

To synthesize aryl boronic acid/ester monomers, techniques, such as transition metal catalyzed borylation and lithiation followed by the borylation, can be applied. Ir catalyzed C-H borylation has successfully been used for heteroarenes such as indoles, pyrroles, quinolones and pyridines.[44]

Ir catalyzed nitrogen directed aryl borylation at the 7-position of 2-substituted indoles[45] is shown (**Scheme 1.4.**) which has been used to synthesize indole dimers via a Suzuki-Miyaura cross coupling reaction.

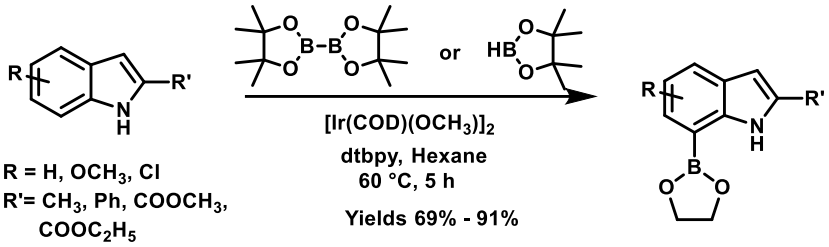

Scheme 1.4. Ir catalyzed nitrogen directed borylation of 2-substituted indoles

1.4.3. Yamamoto polycondensation

Yamamoto polycondensation is a dehalognative condensation of dihaloaromatic compounds, promoted by a Ni(COD) complex.[46-47] This is a step growth polymerization technique. The advantage of this technique is dihalo arylenes can be directly polymerized without preparing any organometallic monomers such as in Suzuki and Stille polymerizations. There are some drawbacks of this tool such as lower yields of polymers and uncontrolled regioregularity for unsymmetrical monomers. A polymerization of 2,7-dibromocarbazole[48] is shown in **Scheme 1.5.**

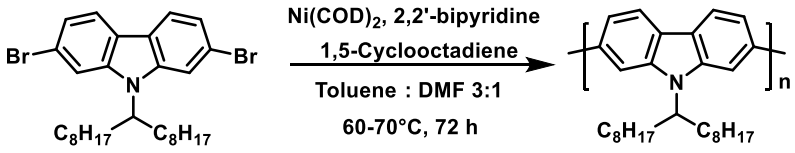

Scheme 1.5. The Yamamoto polycondensation of 2,7-dibromocarbazole.

1.5. APPLICATIONS OF OSCS: ORGANIC LIGHT EMITTING DIODES

1.5.1. Brief history of OLEDs

The first true OLED was developed by Tang et al. in 1987 at Eastman Kodak with a luminous of over 1000 Cd/m^2 at a driving voltage of ~ 10 V.[49] The device was a two-layered structure having a

separate hole transporting layer (N,N'-diphenyl-N,N'-bis (3-methylphenyl) 1,1'-biphenyl-4, 4' diamine (TPD)) and an electron transporting layer (tris(8-hydroxyquinoline) aluminum (Alq3)). The electron and hole recombination and light emission both occured at the interface of the two organic layers which resulted in a lower drive voltage for the device and higher overall performance. This invention opened the doors to the OLED field. Since then a variety of OLEDs that emit full spectrum of visible colors have been developed.[50-52]

1.5.2. The general architecture and the working principle of OLED

A general OLED device schematic is shown in **Figure 1.6.** A typical device is consists of a transparent electrode made of indium tin oxide (ITO) deposited as a thin layer on a transparent substrate (which is mostly glass), a hole transporting layer (HTL), an emissive layer(EML), an electron transporting layer (ETL), and a cathode.

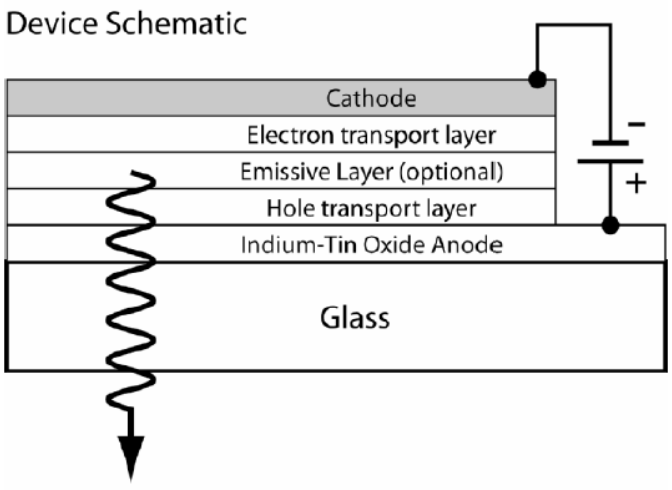

Figure 1.6. The device schematic of OLED.

When voltage is applied across the device, the cathode is negative and anode is positive with respect to the cathode. Therefore, a current of electrons flow from the cathode to the anode by injecting electrons into the LUMO of the ETL and withdrawing electrons from the HOMO of the HTL at the anode. In short, injecting holes into the HTL. Generally holes having higher mobility compared to

the electrons. Therefore, the electrons and holes are recombined at the EML/ETL interface to form an excited state particles called excitons. Some excitons decay via energy radiative routes, leading to light emission. The color of the emitted light depends upon the photon energy which is determined by the band gap of the emitting material. In this case, the bandgap of the conjugated polymer is utilized.

Guest-host OLEDs are famous in the OLED research field due to their higher performance. In such systems, a semiconducting small molecule or polymer is used as the "host" and is doped with the small amounts of an emitting material. Researchers have made different OLEDs with a wide variety of emissive materials, including small molecules and conjugated polymers.[53-55] A variety of host materials have been reported. The CBP[56] and mCP structures in **Figure 1.4.** are some of the small molecules used as hosts while poly(*N*-vinylcarbazole) (PVK) is the most common polymer host.[54-55] Guest-host OLEDs are more efficient than neat-film devices because the host disrupts π-stacking induced aggregation of the guest. Guest aggregations cause concentration quenching in the emissive films and decrease the quantum yield of the emitters. Introducing large flexible side chains, such as linear or branched alkyl groups to the back bone or incorporating asymmetric moieties to the backbone can prevent the efficient π-stacking of the polymers.[57]

1.5.3. Measurements of OLEDs

There are several standard methods for measuring device quality of an OLED. These standard measurements provide valid comparisons between the different devices with varied materials.

1). Brightness – This refers to the human eye response, or photonic response to the emitted light which strongly depends upon the emission spectrum. The photonic response varys through the visible range. The photosensitivity of the human eye peaks at 555 nm and vanishes above ~700 nm and below ~390 nm[58] (**Figure 1.7.**). Therefore, the brightness of the blue and red is comparatively lower than the brightness of green.

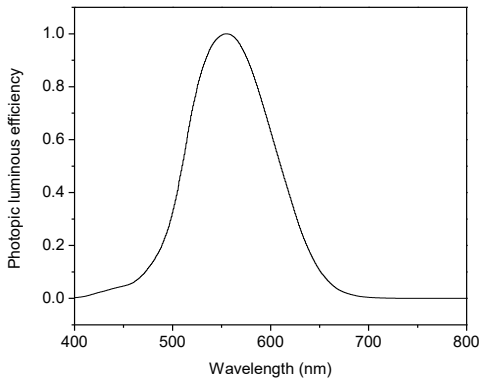

Figure 1.7. The photopic response of human eyes

2). External quantum efficiency (EQE) – This is defined as the ratio of the number of photons emitted by the OLED to the number of electrons injected. EQE represent with η_{exe}[59]

$$\eta_{ext} = \frac{\pi e}{k_m hc} \eta_L \frac{\int g(\lambda)\lambda d\lambda}{\int g(\lambda)k(\lambda)d\lambda}$$

Where $\pi e / k_m hc$ is a constant with a value of 3.703×10^{-5}

η_L is the luminous efficiency

g(λ) is the relative electroluminescence (EL) intensity wavelength λ

k(λ) is the Commision International de I'Ecairage chromaticity (CIE)

3). Luminous efficiency (η_L) – This is equivalent to EQE with the exception of that the luminous efficiency is considered the emitted photons according to the photopic response of the eye. The η_L can be calculated using the equation[59] below and the units are candelas per ampere (Cd/ A)

$$\eta_L = \frac{L}{J_{OLED}}$$

Where L is the brightness (in [Cd/m^2])

J_{OLED} is the current density (in [A/m^2])

4). CIE coordinates - CIE coordinates reflects the exact color emitted by the OLED device.[34] The CIE chromaticity diagram (**Figure 1.8.**) is the standard for primary colors which was established in 1931. Using the x and y coordinates, the color can be determined.

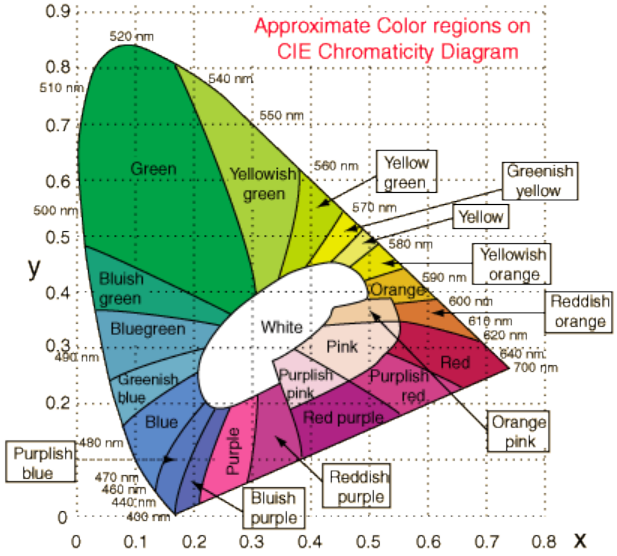

Figure 1.8. 1931 CIE chromaticity diagram

1.5.3. Applications of OLEDs

OLEDs are currently commercialized in different applications such as flat-panel displays and solid state lighting. Flat panel displays having OLEDs can be divided into two categories, small screens, such as in mobile phones, car radios, digital cameras and portable digital displays, and wrist watch displays, and large screens, such as in televisions. OLEDs are used in many Samsung, Motorola and HTC mobile phones and the recently introduced (2015) Apple wrist watches. Fujifilm GFX and 50S Sony a99 Mark II are some of the digital cameras recently introduced with OLED displays. LG is the pioneering company for the manufacturing of OLED TVs. In 2017, LG introduced 77" Smart OLED 4K Ultra HD TV with HDR. OLEDs have been used in solid state lighting as well as in flexible signs. Philips and Siemens Osram has made OLED lighting samples and white OLED panels for sale.

1.5.4. Advantages and challenges of OLEDs

OLEDs offer several advantages over conventional liquid crystal displays (LCDs). Since thin layers of organic materials are used to generate light, these displays are thinner and lighter compared to LCD displays which use backlighting and color filters. Since OLED displays are thinner, they can be fabricated on lighter surfaces, such as plastic substrates. Moreover, OLEDs do not require backlight. Thus, OLEDs consumes less energy when compared with LCD and are good for battery operated devices, such as mobile phones. Light emited from an OLED is omni-directional and unpolarized, Therefore, displays made from OLEDs have much wider viewing angels than LCDs. OLEDs use all generated light to make a displayed image which creates higher contrast ratios and brighter black images compared LCD, which use a backlight and liquid crystal pane that blocks most of the generated light.

Although, an OLED has amazing properties, it faces many challenges such as higher manufacturing costs, lower life span, lower efficiencies of blue OLEDs and the possibility of devices to be damaged over water.

1.6. BIO-INSPIRED MATERIALS AS OSCS

1.6.1. Bioinspired materials

Bioinspired materials are the synthetic materials which have structural properties or mimic the function of nature's materials or living matters. A few examples are light harvesting materials which mimics photosynthesis[60], superhydrophobicity which mimics the lotus leaf, and synthetic adhesives which inspired by the suction cups found in octopus tentacles.[61] Mother Nature is a great source materials that are rough, stronger, more flexible and more resilient than anything humans have made. There is a great demand on high performance, novel organic semiconductors. In terms of chemical and functional diversity, nature is a great source of new building blocks of

bioinspired-organic semiconductors. One such nature-inspired organic semiconductor is Melanin, a natural pigment found in many organisms.

1.7. MELANIN AND EUMELANIN

1.7.1. Melanin

Melanin is a class of naturally occurring pigments found in vertebrate animals, plants and bacteria. It is the primary determinant of the skin tone in human.[62] It also found in hair, inner ear, eyes and brain of human beings. Melanin is profound and fascinating material of interest to fields of chemistry, physics, biology and medicine.[63] Melanin has sub groups called Eumealnin, pheomelanin, neuromelanin and mixed melanin. Melanins are biologically synthesized in epidermal pigmentary cells, called melanocytes by the enzyme catalyzed oxidation (tyrosinase or T'ase) of tyrosine which is shown in **Figure 1.9.**

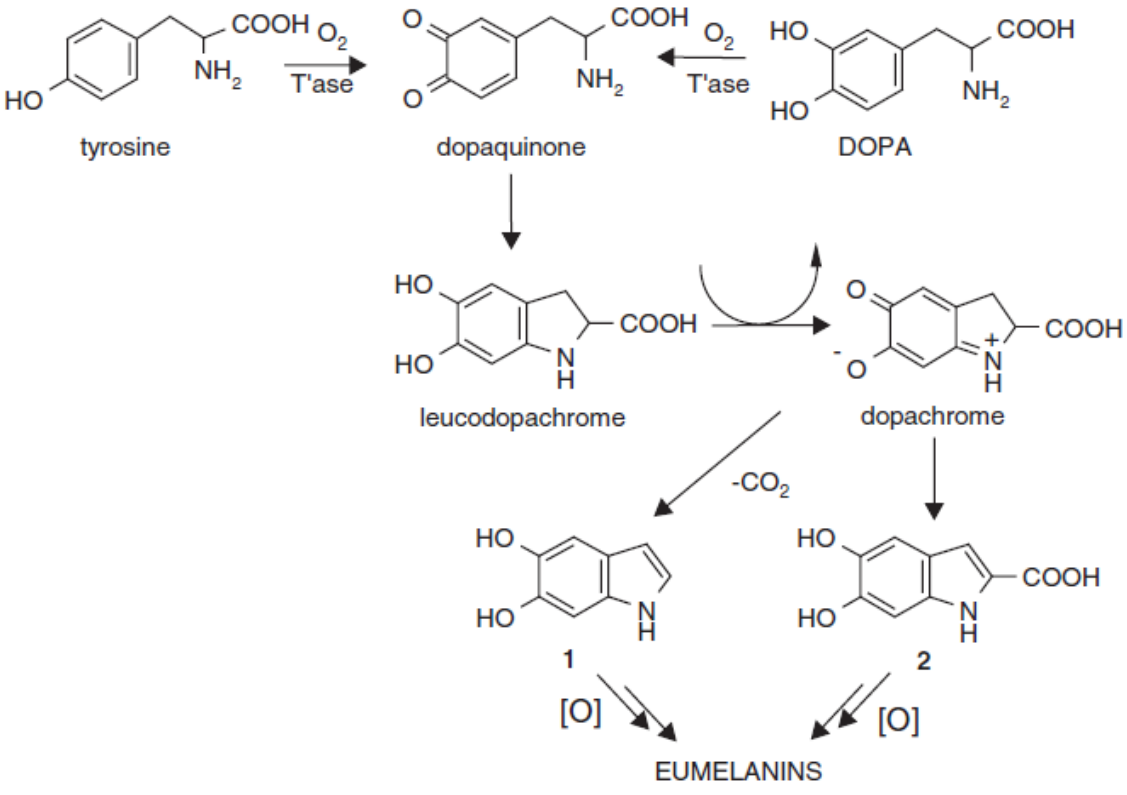

Figure 1.9. The biosynthesis pathway of eumelanin.[64]

This process forms two final precursor monomers, namely 5,6-dihydroxyindole (DHI) and 5,6-dihydroxyindole-2-carboxylic acid (DHICA). By the oxidative polymerization of these two precursor monomers, eumelanin is produced and is a major sub group of natural melanin.

1.7.2. Eumelanin

Eumelanin is the black-brown variety of the melanin and it is a heterogeneous macromolecule. Although, the basic structural units of eumelanin have been identified as DHI and DHICA (**Figure 1.10.**), the exact structure of eumelanin is still a mystery.[62-63, 65]

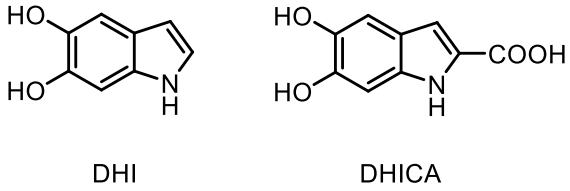

Figure 1.10. The structural units of eumelanin

Natural eumelanin was isolated from the ink sack of cuttlefish, *Sepia officinali*. Synthetic eumelanin materials have been synthesized by the enzymatic (tyrosinase, peroxidase) or chemical (ferricyanide) oxidation of tyrosine, L-dopa, DHI or DHICA. Therefore, the materials may significantly differ, depending on the substrate and oxidation conditions. Scanning Electron Microscopy (SEM) studies have been done[66] to investigate the similarity of the structures of natural eumelanin and the synthetic eumelanin which were made by the tyrosinase-catalyzed oxidative polymerization of L-Dopa.[67] The synthetic eumelanin is mostly consists of DHI-derived units. From this study, researchers realized that natural eumelanin is a significantly ordered structure when compared to the synthetic one which appeared to be an amorphous solid. Eumelanin shows interesting optical, electronic and radical scavenging properties.

1.7.3. Optical properties of Eumelanin

Natural eumelanin shows two key features, coloration and photoprotection. Both functions are related to the optical properties of the structure. Eumelanin has a broad band, featureless, monotonic

light absorption starting from near UV through the near IR regions. This type of absorption is atypical for organic molecule chromophores, since there's no distinct peaks shown for the transitions between the electronic states. Earlier, researcher believed this monotonic, broadband absorption was due to Mie and Rayleigh scattering.[68] Later, it was found under typical spectroscopic conditions, scattering contributes < 6% to the total optical attenuation across all wave lengths in the UV and visible.[69] A quantitative study on isolated sepia melanin solutions was performed, and it was found to have a scattering contribution of only about 12–13.5% at visible wavelengths.[70]

There is a common phrase "Eumelanin does not fluoresce" which has proven to be untrue. Eumelanin does emit but its fluorescence quantum yield is extremely low. The research was done on the radiative relaxation quantum yields of synthetic eumelanin and were found to have a value of $< 7 \times 10^{-4}$.[71] This means 99.9% of the absorbed photon energy is released via non-radiative pathways, such as heat. This is how eumelanin protects our skin by converting the 99.9% of absorbed harmful UV radiation into heat.

1.7.4. Electronic properties of Eumelanin

The groundbreaking work done by McGinness and coworkers established eumelanin as an organic semiconductor.[72] Since then, the electronic properties of eumelanin have been widely investigated. Eumelanin exhibits maximum electrical conductivity of 10^{-5} S/cm. This conductivity is at the relative humidity of 100%, and the conductivity values vary with the relative humidity. In vacuum, the conductivity is 10^{-13} S/cm.[73]

Recently, Meredith showed, that eumelanin is an electronic-ionic hybrid conductor rather than an amorphous semiconductor.[74] They measured the electrical conductivity, muon spin relaxation, and electron paramagnetic resonance by varying the environmental humidity. They demonstrated that, upon absorption of water, eumelanin produced free radicals (electrons) and hydronium ions (protons) via a com-proportionation reaction shown in **Figure 1.11.**

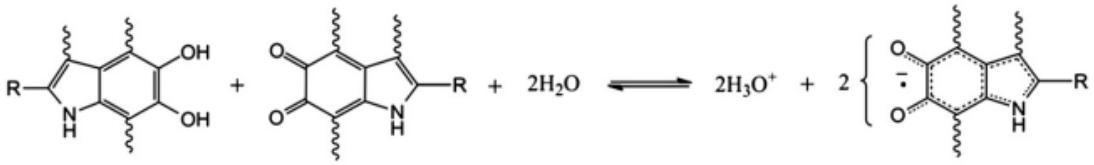

Figure 1.11. The com-proportionation reaction of Eumelanin.

They have suggested that this electronic-ionic hybrid conducting nature of the eumelanin opens the door to many bioelectronics applications such as in biocompatible implantable devices. However, the current synthetic eumelanin materials show poor solubilities and high heterogeneity. Therefore, they are not suitable for the above mentioned applications. Consequently, well-defined, soluble eumelanin-inspired materials need to be synthesized.

1.8. REFERENCES

1. Myers, J. D.; Xue, J., Organic semiconductors and their applications in photovoltaic devices. *Polymer Reviews* **2012,** *52* (1), 1-37.
2. Natelson, D., Organic semiconductors: carrier characteristics. *Nat Mater* **2010,** *9* (9), 703-704.
3. Friedman, L., Transport properties of organic semiconductors. *Physical Review* **1964,** *133* (6A), A1668-A1679.
4. Köhler, A.; Bässler, H., *Electronic processes in organic semiconductors: An introduction*. Wiley: 2015. New Jersey
5. Burroughes, J.; Bradley, D.; Brown, A.; Marks, R.; Mackay, K.; Friend, R.; Burns, P.; Holmes, A., Light-emitting diodes based on conjugated polymers. *Nature* **1990,** *347* (6293), 539-541.
6. Friend, R. H.; Gymer, R. W.; Holmes, A. B.; Burroughes, J. H.; Marks, R. N.; Taliani, C.; Bradley, D. D. C.; Santos, D. A. D.; Bredas, J. L.; Logdlund, M.; Salaneck, W. R., Electroluminescence in conjugated polymers. *Nature* **1999,** *397* (6715), 121-128.
7. Ma, D.; Chen, Y., *Organic Semiconductor Heterojunctions and its application in organic light-emitting diodes*. Springer Berlin Heidelberg: 2018.
8. Hadziioannou, G.; Malliaras, G. G., *Semiconducting polymers: chemistry, physics and engineering*. Wiley: 2007.
9. Cheng, Y.-J.; Yang, S.-H.; Hsu, C.-S., Synthesis of conjugated polymers for organic solar cell applications. *Chem. Rev.* **2009,** *109* (11), 5868-5923.
10. Scharber, M. C.; Mühlbacher, D.; Koppe, M.; Denk, P.; Waldauf, C.; Heeger, A. J.; Brabec, C. J., Design rules for donors in bulk-heterojunction solar cells—towards 10 % energy-conversion efficiency. *Advanced Materials* **2006,** *18* (6), 789-794.
11. Facchetti, A., Semiconductors for organic transistors. *Materials Today* **2007,** *10* (3), 28-37.

12. Allard, S.; Forster, M.; Souharce, B.; Thiem, H.; Scherf, U., Organic semiconductors for solution-processable field-effect transistors (OFETs). *Angewandte Chemie International Edition* **2008,** *47* (22), 4070-4098.
13. Zhang, X.; Xiao, C.; Zhang, A.; Yang, F.; Dong, H.; Wang, Z.; Zhan, X.; Li, W.; Hu, W., Pyridine-bridged diketopyrrolopyrrole conjugated polymers for field-effect transistors and polymer solar cells. *Polymer Chemistry* **2015,** *6* (26), 4775-4783.
14. Bernards, D. A.; Owens, R. M.; Malliaras, G. G., *Organic semiconductors in sensor applications*. Springer Berlin Heidelberg: 2008.
15. McQuade, D. T.; Pullen, A. E.; Swager, T. M., Conjugated polymer-based chemical sensors. *Chem. Rev.* **2000,** *100* (7), 2537-2574.
16. Alvarez, A.; Costa-Fernández, J. M.; Pereiro, R.; Sanz-Medel, A.; Salinas-Castillo, A., Fluorescent conjugated polymers for chemical and biochemical sensing. *TrAC Trends in Analytical Chemistry* **2011,** *30* (9), 1513-1525.
17. Muench, S.; Wild, A.; Friebe, C.; Häupler, B.; Janoschka, T.; Schubert, U. S., Polymer-based organic batteries. *Chem. Rev.* **2016,** *116* (16), 9438-9484.
18. Song, C. K.; Eckstein, B. J.; Tam, T. L. D.; Trahey, L.; Marks, T. J., Conjugated polymer energy level shifts in lithium-ion battery electrolytes. *ACS Applied Materials & Interfaces* **2014,** *6* (21), 19347-19354.
19. Nishide, H.; Oyaizu, K., Organic batteries. In *Innovations in Green Chemistry and Green Engineering: Selected Entries from the Encyclopedia of Sustainability Science and Technology*, Anastas, P. T.; Zimmerman, J. B., Eds. Springer New York: New York, NY, 2013; pp 235-246.
20. Chang, J.-F.; Sun, B.; Breiby, D. W.; Nielsen, M. M.; Sölling, T. I.; Giles, M.; McCulloch, I.; Sirringhaus, H., Enhanced mobility of poly(3-hexylthiophene) transistors by spin-coating from high-boiling-point solvents. *Chemistry of Materials* **2004,** *16* (23), 4772-4776.
21. Hebner, T. R.; Wu, C. C.; Marcy, D.; Lu, M. H.; Sturm, J. C., Ink-jet printing of doped polymers for organic light emitting devices. *Applied Physics Letters* **1998,** *72* (5), 519-521.
22. Kawase, T.; Shimoda, T.; Newsome, C.; Sirringhaus, H.; Friend, R. H., Inkjet printing of polymer thin film transistors. *Thin Solid Films* **2003,** *438*, 279-287.
23. Søndergaard, R.; Hösel, M.; Angmo, D.; Larsen-Olsen, T. T.; Krebs, F. C., Roll-to-roll fabrication of polymer solar cells. *Materials Today* **2012,** *15* (1), 36-49.
24. Kim, S. H.; Jang, J.; Lee, J. Y., High efficiency phosphorescent organic light-emitting diodes using carbazole-type triplet exciton blocking layer. *Applied Physics Letters* **2007,** *90* (22), 223505.
25. Wu, S.; Li, S.; Sun, Q.; Huang, C.; Fung, M.-K., Highly efficient white organic light-emitting diodes with ultrathin emissive layers and a spacer-free structure. *Sci. Rep.* **2016,** *6*, 25821.
26. Lili, D.; Xiao, L.; Zhanwei, W.; Jianping, Z.; Lei, S.; Wenli, L.; Yao, L.; Feiyu, Z.; Junkang, Z.; Qiang, R.; Fobao, H.; Hongquan, X.; Yingquan, P., A striking performance improvement of fullerene n-channel field-effect transistors via synergistic interfacial modifications. *Journal of Physics D: Applied Physics* **2015,** *48* (40), 405105.
27. Yi, M.; Guo, J.; Li, W.; Xie, L.; Fan, Q.; Huang, W., High-mobility flexible pentacene-based organic field-effect transistors with PMMA/PVP double gate insulator layers and the investigation on their mechanical flexibility and thermal stability. *RSC Advances* **2015,** *5* (115), 95273-95279.
28. Facchetti, A., π-Conjugated polymers for organic electronics and photovoltaic cell applications. *Chemistry of Materials* **2011,** *23* (3), 733-758.
29. Thomas, S. W.; Joly, G. D.; Swager, T. M., Chemical sensors based on amplifying fluorescent conjugated polymers. *Chem. Rev.* **2007,** *107* (4), 1339-1386.
30. Hoeben, F. J. M.; Jonkheijm, P.; Meijer, E. W.; Schenning, A. P. H. J., About supramolecular assemblies of π-conjugated systems. *Chem. Rev.* **2005,** *105* (4), 1491-1546.

31. James, D. K.; Tour, J. M., Molecular wires. In *Molecular Wires and Electronics*, Springer Berlin Heidelberg: Berlin, Heidelberg, 2005; pp 33-62.
32. Leclerc, M.; Morin, J. F., *Design and Synthesis of Conjugated Polymers*. Wiley: 2010.
33. Bundgaard, E.; Krebs, F. C., Low band gap polymers for organic photovoltaics. *Solar Energy Materials and Solar Cells* **2007,** *91* (11), 954-985.
34. Zhu, M.; Yang, C., Blue fluorescent emitters: design tactics and applications in organic light-emitting diodes. *Chemical Society Reviews* **2013,** *42* (12), 4963-4976.
35. Osaka, I.; McCullough, R. D., Advances in molecular design and synthesis of regioregular polythiophenes. *Accounts of Chemical Research* **2008,** *41* (9), 1202-1214.
36. Miyakoshi, R.; Shimono, K.; Yokoyama, A.; Yokozawa, T., Catalyst-transfer polycondensation for the synthesis of poly(p-phenylene) with controlled molecular weight and low polydispersity. *J. Am. Chem. Soc.* **2006,** *128* (50), 16012-16013.
37. Huang, L.; Wu, S.; Qu, Y.; Geng, Y.; Wang, F., Grignard metathesis chain-growth polymerization for polyfluorenes. *Macromolecules* **2008,** *41* (22), 8944-8947.
38. Iovu, M. C.; Jeffries-El, M.; Sheina, E. E.; Cooper, J. R.; McCullough, R. D., Regioregular poly (3-alkylthiophene) conducting block copolymers. *Polymer* **2005,** *46* (19), 8582-8586.
39. Zhang, Y.; Tajima, K.; Hirota, K.; Hashimoto, K., Synthesis of all-conjugated diblock copolymers by quasi-living polymerization and observation of their microphase separation. *J. Am. Chem. Soc.* **2008,** *130* (25), 7812-7813.
40. Loewe, R. S.; Ewbank, P. C.; Liu, J.; Zhai, L.; McCullough, R. D., Regioregular, head-to-tail coupled poly(3-alkylthiophenes) made easy by the GRIM method: Investigation of the Reaction and the Origin of Regioselectivity. *Macromolecules* **2001,** *34* (13), 4324-4333.
41. Sheina, E. E.; Liu, J.; Iovu, M. C.; Laird, D. W.; McCullough, R. D., Chain growth mechanism for regioregular nickel-initiated cross-coupling polymerizations. *Macromolecules* **2004,** *37* (10), 3526-3528.
42. Suzuki, A., Recent advances in the cross-coupling reactions of organoboron derivatives with organic electrophiles, 1995–1998. *Journal of Organometallic Chemistry* **1999,** *576* (1), 147-168.
43. Hu, L.; Yang, Y.; Xu, J.; Liang, J.; Guo, T.; Zhang, B.; Yang, W.; Cao, Y., Blue light-emitting polymers containing fluorene-based benzothiophene-S,S-dioxide derivatives. *Journal of Materials Chemistry C* **2016,** *4* (6), 1305-1312.
44. Larsen, M. A.; Hartwig, J. F., Iridium-catalyzed C–H borylation of heteroarenes: scope, regioselectivity, application to late-stage functionalization, and mechanism. *J. Am. Chem. Soc.* **2014,** *136* (11), 4287-4299.
45. Paul, S.; Chotana, G. A.; Holmes, D.; Reichle, R. C.; Maleczka, R. E.; Smith, M. R., Ir-Catalyzed functionalization of 2-substituted indoles at the 7-position: nitrogen-directed aromatic borylation. *J. Am. Chem. Soc.* **2006,** *128* (49), 15552-15553.
46. Asakura, H.; Shishido, T.; Tanaka, T., In situ time-resolved XAFS study of the reaction mechanism of bromobenzene homocoupling mediated by [Ni(cod)(bpy)]. *The Journal of Physical Chemistry A* **2012,** *116* (16), 4029-4034.
47. Watanabe, M.; Tsuchiya, K.; Shinnai, T.; Kijima, M., Liquid crystalline polythiophene bearing phenylnaphthalene side-chain. *Macromolecules* **2012,** *45* (4), 1825-1832.
48. Wakim, S.; Blouin, N.; Gingras, E.; Tao, Y.; Leclerc, M., Poly(2,7-carbazole) derivatives as semiconductors for organic thin-film transistors. *Macromolecular Rapid Communications* **2007,** *28* (17), 1798-1803.
49. Tang, C. W.; VanSlyke, S. A., Organic electroluminescent diodes. *Applied Physics Letters* **1987,** *51* (12), 913-915.
50. Liu, M. S.; Luo, J.; Jen, A. K. Y., Efficient green-light-emitting diodes from silole-containing copolymers. *Chemistry of Materials* **2003,** *15* (18), 3496-3500.

51. Kamtekar, K. T.; Monkman, A. P.; Bryce, M. R., Recent advances in white organic light-emitting materials and devices (WOLEDs). *Advanced Materials* **2010,** *22* (5), 572-582.
52. Volyniuk, D.; Cherpak, V.; Stakhira, P.; Minaev, B.; Baryshnikov, G.; Chapran, M.; Tomkeviciene, A.; Keruckas, J.; Grazulevicius, J. V., Highly efficient blue organic light-emitting diodes based on intermolecular triplet–singlet energy transfer. *The Journal of Physical Chemistry C* **2013,** *117* (44), 22538-22544.
53. Cai, M.; Xiao, T.; Hellerich, E.; Chen, Y.; Shinar, R.; Shinar, J., High-efficiency solution-processed small molecule electrophosphorescent organic light-emitting diodes. *Advanced Materials* **2011,** *23* (31), 3590-3596.
54. Chen, F.-C.; Yang, Y.; Thompson, M. E.; Kido, J., High-performance polymer light-emitting diodes doped with a red phosphorescent iridium complex. *Applied Physics Letters* **2002,** *80* (13), 2308-2310.
55. Intemann, J. J.; Mike, J. F.; Cai, M.; Bose, S.; Xiao, T.; Mauldin, T. C.; Roggers, R. A.; Shinar, J.; Shinar, R.; Jeffries-El, M., Synthesis and characterization of poly(9,9-dialkylfluorenevinylene benzobisoxazoles): new solution-processable electron-accepting conjugated polymers. *Macromolecules* **2011,** *44* (2), 248-255.
56. Hellerich, E. S.; Intemann, J. J.; Cai, M.; Liu, R.; Ewan, M. D.; Tlach, B. C.; Jeffries-El, M.; Shinar, R.; Shinar, J., Fluorescent polymer guest:small molecule host solution-processed OLEDs. *Journal of Materials Chemistry C* **2013,** *1* (34), 5191-5199.
57. Rothe, C.; Chiang, C.-J.; Jankus, V.; Abdullah, K.; Zeng, X.; Jitchati, R.; Batsanov, A. S.; Bryce, M. R.; Monkman, A. P., Ionic iridium(III) complexes with bulky side groups for use in light emitting cells: reduction of concentration quenching. *Advanced Functional Materials* **2009,** *19* (13), 2038-2044.
58. Minaev, B.; Baryshnikov, G.; Agren, H., Principles of phosphorescent organic light emitting devices. *Phys. Chem. Chem. Phys.* **2014,** *16* (5), 1719-1758.
59. Li, H.; Zhang, C.; Li, D.; Duan, Y., Simulation of transform for external quantum efficiency and power efficiency of electroluminescent devices. *Journal of Luminescence*, 2007; Vol. 122, pp 626-628.
60. Croce, R.; van Amerongen, H., Natural strategies for photosynthetic light harvesting. *Nat. Chem. Biol.* **2014,** *10* (7), 492-501.
61. Baik, S.; Kim, D. W.; Park, Y.; Lee, T.-J.; Ho Bhang, S.; Pang, C., A wet-tolerant adhesive patch inspired by protuberances in suction cups of octopi. *Nature* **2017,** *546* (7658), 396-400.
62. d'Ischia, M.; Wakamatsu, K.; Cicoira, F.; Di Mauro, E.; Garcia-Borron, J. C.; Commo, S.; Galván, I.; Ghanem, G.; Kenzo, K.; Meredith, P.; Pezzella, A.; Santato, C.; Sarna, T.; Simon, J. D.; Zecca, L.; Zucca, F. A.; Napolitano, A.; Ito, S., Melanins and melanogenesis: from pigment cells to human health and technological applications. *Pigment Cell & Melanoma Research* **2015,** *28* (5), 520-544.
63. d'Ischia, M.; Napolitano, A.; Pezzella, A.; Meredith, P.; Sarna, T., Chemical and structural diversity in eumelanins – unexplored bio-optoelectronic materials. *Angewandte Chemie (International ed. in English)* **2009,** *48* (22), 3914-3921.
64. d'Ischia, M.; Napolitano, A.; Pezzella, A.; Land, E. J.; Ramsden, C. A.; Riley, P. A., 5,6-Dihydroxyindoles and indole-5,6-diones. In *Adv. Heterocycl. Chem.*, Alan, R. K., Ed. Academic Press: 2005; Vol. Volume 89, pp 1-63.
65. Meredith, P.; Sarna, T., The physical and chemical properties of eumelanin. *Pigment Cell Res.* **2006,** *19* (6), 572-594.
66. Nofsinger, J. B.; Forest, S. E.; Eibest, L. M.; Gold, K. A.; Simon, J. D., Probing the building blocks of eumelanins using scanning electron microscopy. *Pigment Cell Res.* **2000,** *13* (3), 179-184.
67. Ito, S., Reexamination of the structure of eumelanin. *Biochimica et Biophysica Acta (BBA) - General Subjects* **1986,** *883* (1), 155-161.

68. Wolbarsht, M. L.; Walsh, A. W.; George, G., Melanin, a unique biological absorber. *Appl. Opt.* **1981,** *20* (13), 2184-2186.
69. Riesz, J.; Gilmore, J.; Meredith, P., Quantitative scattering of melanin solutions. *Biophys. J.* **2006,** *90* (11), 4137-4144.
70. Vitkin, I. A.; Woolsey, J.; Wilson, B. C.; Anderson, R. R., Optical and thermal characterization of natural (Sepia officinalis) melanin. *Photochem. Photobiol.* **1994,** *59* (4), 455-462.
71. Meredith, P.; Riesz, J., Radiative relaxation quantum yields for synthetic eumelanin. *Photochem. Photobiol.* **2004,** *79* (2), 211-216.
72. McGinness, J.; Corry, P.; Proctor, P., Amorphous semiconductor switching in melanins. *Science* **1974,** *183* (4127), 853-855.
73. Jastrzebska, M. M.; Isotalo, H.; Paloheimo, J.; Stubb, H., Electrical conductivity of synthetic DOPA-melanin polymer for different hydration states and temperatures. *J. Biomater. Sci. Polym. Ed.* **1996,** *7* (7), 577-586.
74. Mostert, A. B.; Powell, B. J.; Pratt, F. L.; Hanson, G. R.; Sarna, T.; Gentle, I. R.; Meredith, P., Role of semiconductivity and ion transport in the electrical conduction of melanin. *Proceedings of the National Academy of Sciences* **2012,** *109* (23), 8943-8947.

CHAPTER II

EUMELANIN-INSPIRED CORE DERIVED FROM VANILLIN AS A BUILDING BLOCK FOR NOVEL ORGANIC SEMICONDCUTORS

2.1. INTRODUCTION

Organic semiconductors (OSCs) have created much interest in the scientific community over the last three decades due to the promise of low cost, light weight and a large area electronic devices.[1-3] Such materials have potential to generate ubiquitous photovoltaic power, transparent displays, efficient and inexpensive solid state lighting, flexible and rugged electronics.[4-6] Currently, more research is progressing to design and prodcuce new OSCs, with improved properties for efficient electronic devices. With three billions years of evolution, mother-nature has gifted great materials and methods to solve many issues in our lives. Therefore, it would be advantageous to develop materials inspired by nature. In terms of chemical and functional diversity, nature is a great source of new building blocks for bio-inspired OSCs. One such inspiration is the heterogeneous macromolecule, Melanin. Melanin is a natural pigment found in most of the organisms including humans, and it is the primary determinant of the skin tone in humans. It is also found in hair, eyes, inner ears and brain of humans.[7] Melanin acts as natural photo-protector against the harmful effects of UV radiation.[8-10] There are three basic types of melanin where eumelanin (black-brown variety)

is the most common. Scientists have already isolated natural eumelanin,a black-brown insoluble bio macromolecule, from the ink sac of cuttlefish *Sepia.* It has been determined that eumelanin is formed by the oxidative polymeization of two monomers, 5,6 –dihydroxyindole (DHI) and 5,6-dihydroxyindole carboxylic acid (DHICA). Optical, electronic, physical, metal chelating and structural properties of natural and synthetic eumelanin has been studied extensively.[9, 11] With the ground breaking work by McGinness and Proctor on the electrical switching of eumelanin, it was established that eumelanin was an amorphous organic semiconductor.[12] In 2012, Meredith and coworkers proved that eumelanin is an electronic-ionic conductor rather than an amorphous organic semiconductor.[13] Eumelanin shows broadband, monotonic light absorption propeties ranging from near UV through the near IR range. [14] The material has electrical conductivity up to 10^{-5} S cm^{-1} and good charge mobility as high as 2.1 x 10^{-3} cm^2 V^{-1} s^{-1}. [9, 11] Therefore, it seems that the eumelanin indole moiety can be utilized as a building block to synthesize new organic semiconductors. In order to develop well-defined, soluble eumelanin-inspired materials, a eumelanin-inspired core, namely methyl 4,7-dibromo-5,6-dimethoxy-1-methyl-1H-indole-2-carboxylate (DBI) was synthesized[15] as a new building block for organic semiconductors. Most organic compounds are derived from petroleum-based starting materials. Due to the increasing demand on oil, it would be advantageous to seek alternative sources for building blocks to develop new organic semiconductors. Thus, vanillin (extract of vanilla bean) was used to synthesize the eumelanin-inspired indole core.[16] This core was designed to functionalize at 4,7-positions of the central indolic benzene ring via transition metal catalyzed, cross-coupling reactions. To demonstrate the utility of the eumelanin-inspired core as a building block for OSCs, a model conjugated polymer was synthesized via a Sonogashira cross coupling reaction. The synthesis of eumelanin-inspired molecules and their physical, optical and electronic properties are discussed in this chapter.

2.2. SYNTHESIS AND DISCUSSION

The synthesis of eumelanin-inspired core was first attempted as shown in **Scheme 2.1.**

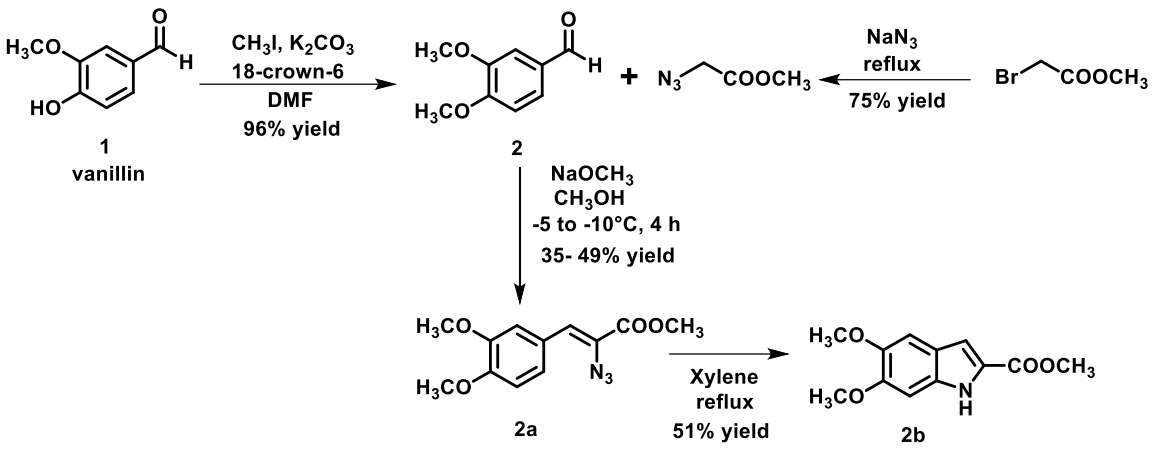

Scheme 2.1. Synthesis of eumelanin-inspired core.

Vanillin (**1**) was methylated with iodomethane in the presence of K_2CO_3 to obtain 3,4-dimethoxybenzaldehyde (**2)** in 96% yield. Methyl 2-azidoacetate was synthesized from 2-bromoacetate and sodium azide under refluxing conditions. 3,4-Dimethoxybenzaldehyde (**2)** was reacted with methyl 2-azidoacetate in MeOH, followed by the addition of sodium methoxide maintaining a temperature range of -5 °C to -10 °C. This process afforded methyl (Z)-2-azido-3-(3,4-dimethoxyphenyl)acrylate (**2a).** compound **2a** was cyclized to indole compound **2b** using xylene via Hemetsberger indole synthesis[17] under reflux conditions.

This route led to the desired indole core **2b**, but there were some limitations encountered with this route. First, maintaining the reaction temperature at -5 °C to -10 °C for 4 h was troublesome without a chiller. Second, the cyclization reaction occurred on both sides of the benzene ring forming more than one cyclized product which was hard to purify. With the alternate route shown in **Scheme 2.2,** an eumelanin-inspired core was successfully synthesized.

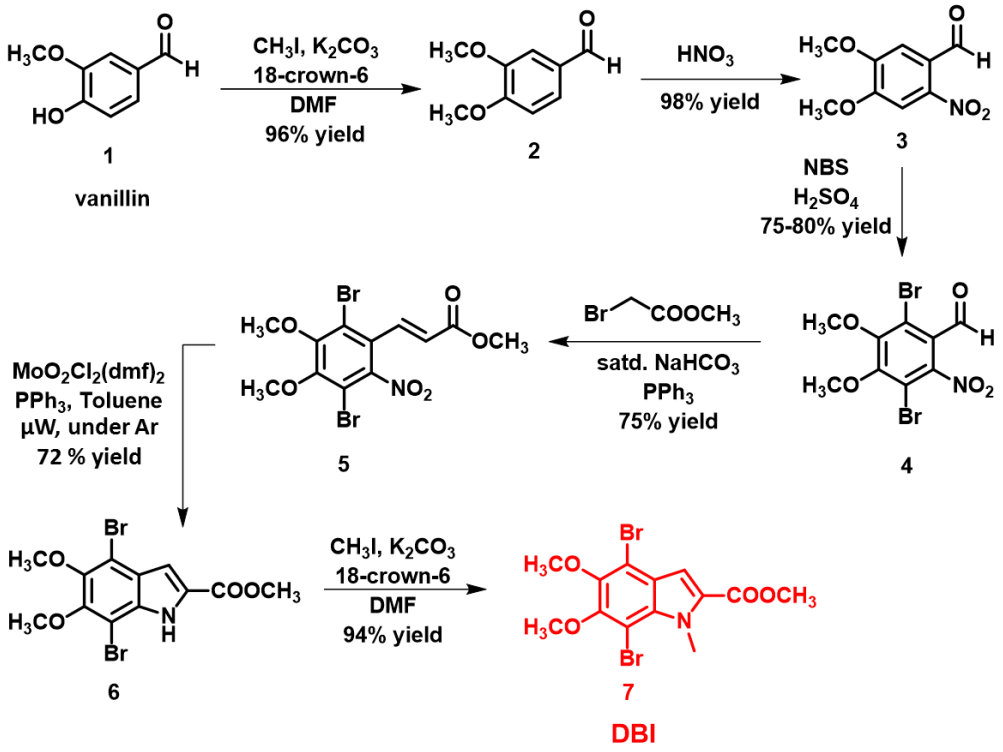

Scheme 2.2. Synthesis of Eumelanin-inspired core starting from vanillin.

The synthetic procedure to obtain the eumelanin-inspired core (**7**), [methyl 4,7-dibromo-5,6-dimethoxy-*N*-methyl-*1H*-indole-2-carboxylate (DBI)] was initiated with vanillin which was also used for the first route. Vanillin (**1**) was methylated to give 3,4-dimethoxybenzaldehyde (**2**) in the presence of K_2CO_3 in dry DMF. Then **2** which was nitrated with nitric acid to obtain 6-nitroveretraldehyde (**3)**. Bromination of **3** with *N*-bromosuccinimide produced **4.** A modified procedure was used to synthesize the olefin **5** by using methyl bromoacetate in the aqueous sodium bicarbonate, followed by Cadogan synthesis with molybdenum catalyst to afford dibromoindole (**6**). Compound **6** was *N*-methylated to avoid unwanted by-products during the cross coupling reactions. DBI (**7**) was synthesized with bromine atoms at the 4- and 7- positions of the indole moiety so it could serve as a universal partner for metal-catalyzed coupling reactions. This approach allowed for the functionalization at the 4- and 7- positions with phenylene ethynylene substituents using Sonogashira cross-coupling conditions. Eumelanin-inspired model polymer was synthesized

by incorporating the DBI with a phenylene diethynylene unit. The synthesis of phenylene diethynylene monomer is shown in the **Scheme 2.3.**

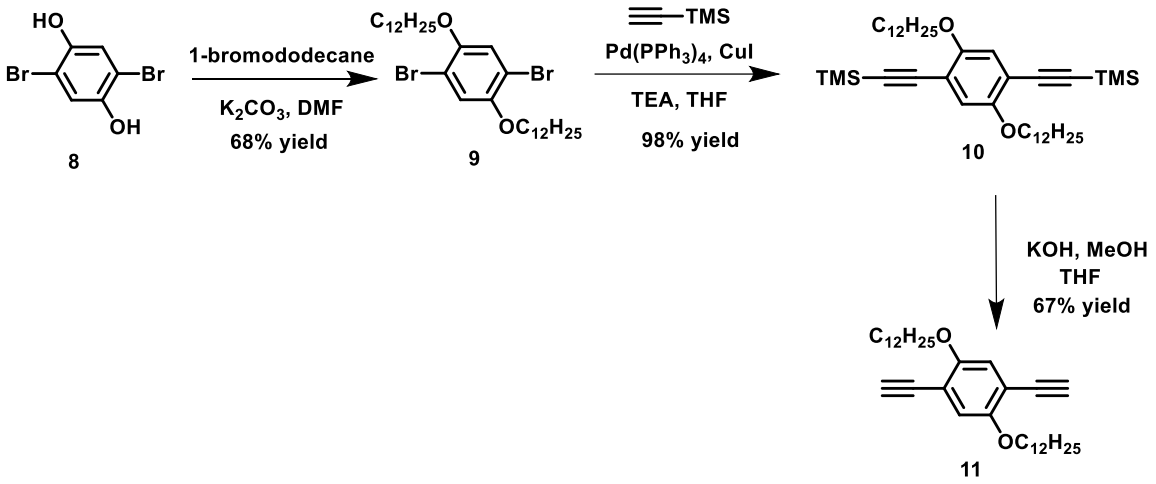

Scheme 2.3. The synthesis of phenylene diethynylene monomer

First, 2,5-Dibromobenzene-1,4-diol (**8**) was converted in to 1,4-dibromo-2,5-bis(dodedecyloxy)benzene (**9**) using 1-bromododecane in a Williamson synthesis. These long chain alkyl groups are important to increase the polymer solubility in common organic solvents. Compound **10** was prepared using compound **9** and ethynyltrimethylsilane in the presence of $Pd(PPh_3)_4$ and CuI. Finally, compound **11**, the phenylene diethynylene molecule was obtained by removing the TMS protecting groups, when compound **10** was treated with KOH in methanol.

The ethynyl group was chosen because of its ability to alter optoelectronic properties by extended effective π-conjugation length. The polymerization of **7** and 1,4-bis(dodecyloxy)-2,5-diethynylbenzene (**11**), was accomplished by Sonogashira cross coupling reaction using $Pd(PPh_3)_4$, CuI, triethylamine (Et_3N) and THF which resulted in a red polymer in 36% yield. The polymer was soluble in various solvents including THF, chloroform, toluene and chlorobenzene. The polymer solutions were light green in color. The structure of the polymer was confirmed by ^1H NMR spectroscopy. Gel permeation chromatography showed a number average molecular weight (M_n) of 13.6 kDa and PDI = 1.88.

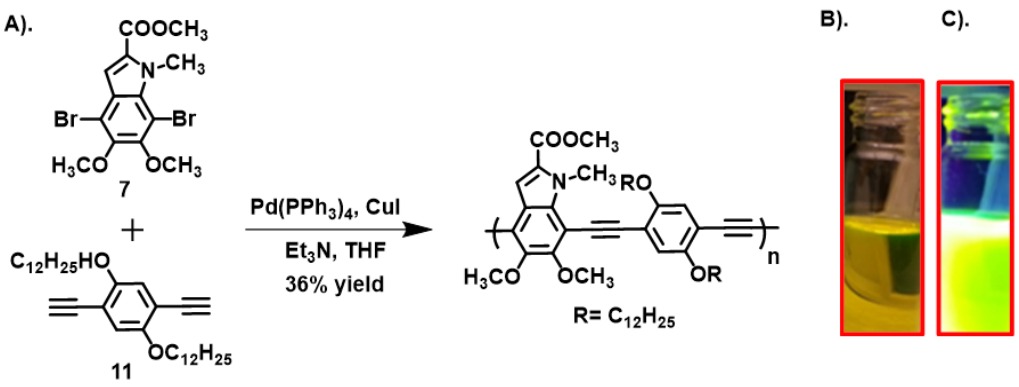

Scheme 2.4. A). Synthesis of eumelanin-inspired polymer B). Polymer in chloroform under visible light and C) Polymer solution under UV light at 365 nm.

The photophysical characteristics of the polymer, both in dilute solutions and in thin films, were examined using UV-vis absorption and fluorescence spectroscopy. The spectra are shown in **Figure 2.1.** The polymer exhibited an absorption maximum at 485 nm in $CHCl_3$ and a red-shifted absorption maximum of 526 nm for polymer thin films. This bathochromic shift is due to the π-π stacking of the polymer chains in the solid state which increases the conjugation length.

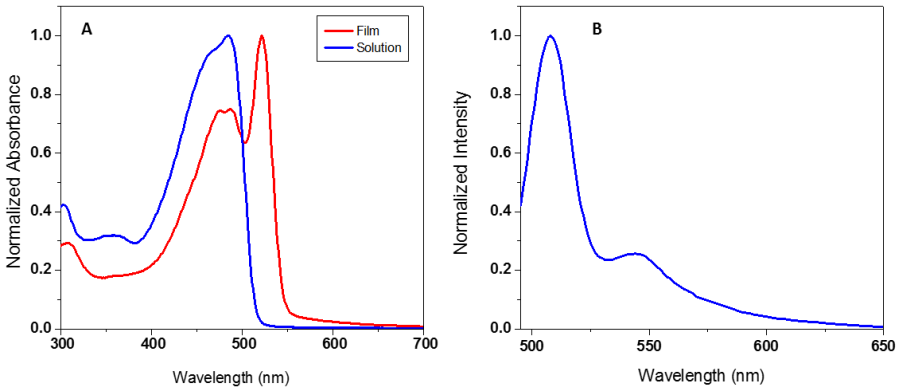

Figure 2.1. A). Absorption spectra of the polymer in $CHCl_3$ and in thin film B). Fluorescence spectrum of polymer dissolved in $CHCl_3$

Polymer dissolved in $CHCl_3$, exhibited green fluorescence with an emission maximum at 508 nm, and photoluminescence quantum yield of the polymer in dilute chloroform was 0.60 with reference to the standard quinine sulfate.

The electrochemical properties of the polymer were investigated by cyclic voltammetry. The cyclic voltommogram of the polymer in chloroform solution, drop-casted on glassy carbon electrode, is shown in **Figure 2.2.** The HOMO-LUMO levels of the polymer were -5.47 eV and -3.44 eV, respectively. The band gap of the polymer was 2.03 eV, which confirms that this polymer has semiconducting properties.

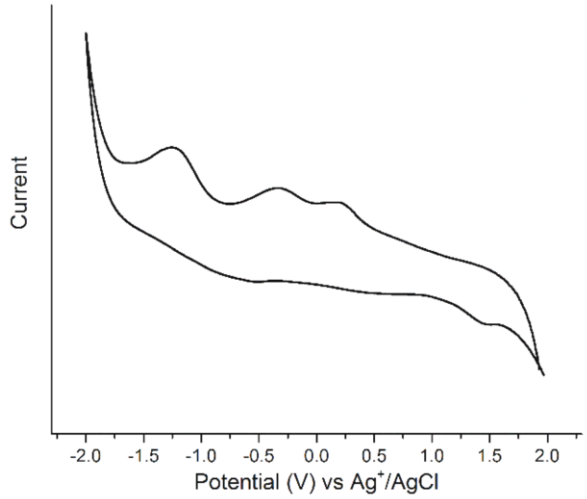

Figure 2.2. The cyclic voltammogram of the polymer.

The morphology of the polymer thin film was characterized by AFM as shown **Figure 2.3.** The polymer thin film appeared to be composed of packed, small grains varying in size, shape and averaging 20 nm in diameter. Further quantitative analysis showed a surface RMS roughness of 1.8 nm for the polymer thin films.

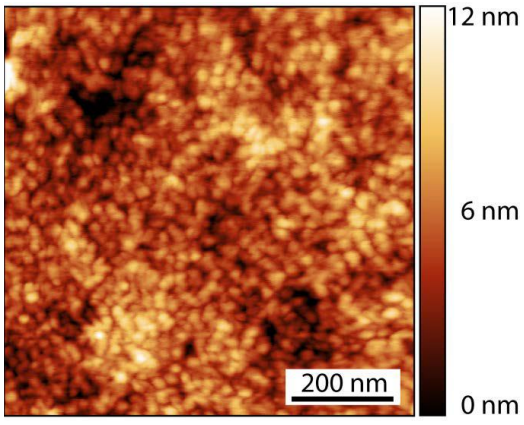

Figure 2.3. The 800 × 800 nm AFM topography image of the polymer thin film on Si wafer.

2.3. SUMMARY AND OUTLOOK

An eumelanin-inspired indole core (DBI) was synthesized starting from the vanillin. This novel core demonstrated that it can serve as a building block for the development of eumelanin-inspired organic semiconductors. Poly(indoylenephenyleneethynylene), a model polymer, was prepared by the Sonogashira cross coupling of this eumelanin-inspired core with phenylenediethynylene unit The resulting polymer formed absorption maximum at 485 nm and a red shifted emission maximum at 508 nm which is responsible for green fluorescence. The bandgap of the polymer was 2.03 eV which indicated that the polymer behaves as an organic semiconductor with promising characteristics for optoelectronic devices. Further optimization is needed to improve the yield and the molecular weight of the polymer. The polymer might be used as the emissive material in organic light emitting diodes and in certain electronic devices in the future.

2.4. EXPERIMENTAL SECTION

2.4.1. General methods and materials

Anhydrous *N*,*N*-dimethylformamide (DMF) and tetrahydrofuran (THF) were obtained from solvent purification system under ultra-pure argon. All other commercial reagents were used as received. Unless otherwise specified, all reactions were run in oven-dried glassware. Reactions were monitored by thin layer chromatography on silica G TLC plates (Sorbent Technologies No. 1634126). Purifications were performed by column chromatography on silica gel (Sorbent Technologies, 40-63 μm particle size) or neutral alumina (Sorbent Technologies, 32-63 μm particle size). Saturated aqueous solutions of NaCl, NH_4Cl and $NaHCO_3$ were used in work-up procedures. ^{1}H- and ^{13}C-NMR spectra were measured on a Bruker Avance 400 MHz instrument. Elemental analyses were performed by Atlantic Microlab, Inc., Norcross, GA 30071. Cyclic voltammetry was performed on a CH-instrument, 6017E model, with 0.1 M tetrabutylammonium hexafluorophosphate as supporting electrolyte in dry acetonitrile using a glassy carbon as the working electrode, platinum wire as the counter electrode and Ag/AgCl as the reference electrode

with a scan rate of 100 mV/sec. The HOMO and LUMO energy values were calculated from the onset of the first oxidation and reduction potentials from the equations E_{HOMO} (eV) = - [E_{ox}^{onset} - $E_{1/2}$ (Fc/Fc^+) + 4.8] and E_{LUMO} (eV) = - [E_{red}^{onset} - $E_{1/2}$ (Fc/Fc^+) + 4.8], where $E_{1/2}$ (Fc/Fc^+) was the cell correction. Gel permeation chromatography was performed using a Waters 1515 pump with a Waters 2414 refractive index detector with THF as solvent at 30 ℃ and with flow rate 1.0 mL/min. Polystyrene standards were used for calibration. UV-vis spectra were recorded on a Cary 5000 VIS-NIR spectrophotometer. Fluorescence spectra were recorded on a Cary Eclipse fluorescence spectrophotometer. Fluorescence and UV-vis measurements were taken in $CHCl_3$. Polymer film was prepared by drop-casting a polymer solution dissolved in $CHCl_3$. Optical bandgap was calculated from wavelength corresponding to the energy absorption onset from the intersection of the leading edge tangent with the *x*-axis. The polymer thin film for AFM was prepared by spin-coating from a 20 mg/mL solution in chloroform onto a clean Si wafer at 1000 rpm. The AFM measurements are carried out in an NT-MDT NTEGRA Prima AFM under a semi-contact mode using a silicon tip (spring force constant = 1.2 – 6.4 N/m). Quantum yield measurements were performed in dilute $CHCl_3$ solutions with absorbance ranging from 0.01 to 0.04. Quinine sulfate was used as the reference. The excitation wavelength of 313 nm was used to obtain the fluorescence spectra for each solution ranging from 320 to 600 nm. The fluorescence intensity (area of the fluorescence spectrum) was then calculated and recorded (**Table 2.1.**). Quantum yields were calculated[18] using the following equation: $\phi_s = \phi(A_r F_s / A_s F_r)(n_s^2 / n_r^2)$. ϕ_r is 0.51, A_s *and* A_r are absorbances of the sample and reference solutions, respectively at the same excitation wavelength, F_s *and* F_r are the corresponding relative integrated fluorescence intensities, n is the refractive index [$CHCl_3$ (n_s = 1.445) and 1 N H_2SO_4 (n_r = 1.339) were used].

Table 2.1. Quantum yield experimental data

Sample	Absorbance	Fluorescence intensity	Emission maximum (nm)
Standard	0.01	14578	455
	0.02	22858	
	0.03	32544	
	0.04	46907	
Polymer solution	0.01	19194	508
	0.02	23513	
	0.03	29978	
	0.04	37315	

2.4.2. Synthesis procedures

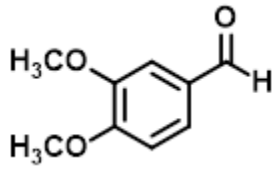

2

3,4-Dimethoxybenzaldehyde (2): To a stirred solution of vanillin **1** , (10.0 g, 65.7 mmol) in DMF (50 mL) was added potassium carbonate (13.68 g, 99.0 mmol), CH_3I (14.0 g, 99.0 mmol) and a crystal of 18-crown-6 and the solution was stirred at room temperature for overnight. The crude reaction mixture was poured into ice-cold water to form off-white solid (10.4 g, 96%). This product was taken as such to next step without any purification. mp 39-42 °C.

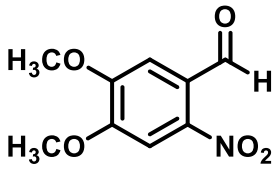

3

4,5-Dimethoxy-2-nitrobenzaldehyde (3): To a 500 mL Erlenmeyer flask with a magnetic stirrer, was added 50 mL nitric acid. To this mixture crushed **2** (10 g, 60.2 mmol) was added in small portions over a period of 15 min. The internal temperature was checked and maintained in the range

of 18-22 °C. After 15 min of stirring, the reaction mixture was poured in an aluminum foil covered beaker containing 500 mL of ice cold water. After stirring for 15 min in the dark, the solid was filtered and dried to yield **3** (11.34 g, 89%). This compound was taken to next step without any purification.[19] mp 130-133 °C.

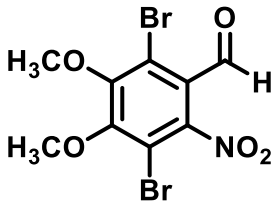

4

2,5-Dibromo-3,4-dimethoxy-6-nitrobenzaldehyde (4): To 250 ml 3-necked round bottom flask containing compound **3** (10.0g, 47.2 mmol) was added concentrated sulfuric acid (40 mL). To this system was added NBS (25.3g, 142.0 mmol) in portions over a period of 30 min. Then, the reaction vessel was stoppered using a septum and completely covered with aluminum foil to exclude light. After stirring the reaction mixture for 16 h at room temperature the reaction mixture was poured over 200 mL of ice cold water. The resulting precipitate was stirred for 15 min and filtered. The solid was washed again with water twice. This solid was transferred to a beaker containing 150 mL of ice cold water, and the mixture was stirred for 10 min and finally filtered to give the orange colored crude **4** in 84% yield. The crude product was taken to the next step without purification.[20] mp 152-155 °C.

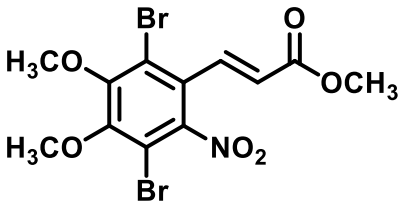

5

Methyl-3-(2,5-dibromo-3,4-dimethoxy-6-nitrophenyl)acrylate (5): To a Erlenmeyer flask, was added triphenylphosphine (3.5g, 13.5 mmol), methyl bromoacetate (1.3 mL, 13.5 mmol) and saturated aqueous solution of $NaHCO_3$ (15mL). The mixture was stirred for 1 h at room

temperature. Then compound **4** (5.0g, 13.5 mmol) was added and the resulting mixture was stirred at room temperature for 3 h. The reaction mixture was extracted with EtOAc (3 × 50 mL). The organic layer was washed with water, saturated NaCl, dried (Na_2SO_4), and concentrated under vacuum to give a thick brown liquid. The compound was purified using a silica gel column and eluted with hexanes/ EtOAc (95:5). Evaporation of the solvent yielded product **5** (4.31 g, 78%) as a pale yellow solid.[21] mp 76-78°C. ^{1}H NMR (400 MHz, $CDCl_3$) δ 7.57 (d, J = 16.3 Hz, 1H), 6.14 (d, J = 16.2 Hz, 1H), 3.96 (d, J = 8.6 Hz, 6H), 3.80 (s, 3H). ^{13}C NMR (101 MHz, $CDCl_3$) δ 165.36, 152.56, 151.82, 147.06, 137.26, 125.83, 125.62, 119.80, 109.64, 61.40, 61.15, 52.18. *Anal*. Calcd for $C_{12}H_{11}Br_2NO_6$: C, 33.91; H, 2.61; N, 3.30. Found: C, 34.17; H, 2.55; N, 3.29.

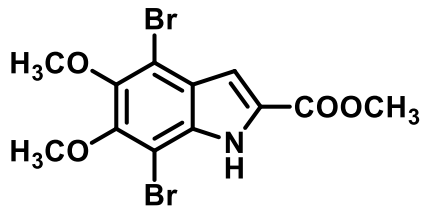

6

Methyl 4,7-dibromo-5,6-dimethoxy-1*H*-indole-2-carboxylate (6): To a 35 mL microwave reactor vessel, was added compound **5** (2.0 g, 4.7 mmol) along with triphenylphosphine (2.6 g, 9.9 mmol) and $MoO_2Cl_2(dmf)_2$ (8.3 mg, 5 mol%). The $MoO_2Cl_2(dmf)_2$ was prepared according to the reported procedure.[22] To this mixture, was added 5 mL of dry THF and the vessel was sealed and kept in the microwave reactor for 8 min under the following conditions: fixed power, 80 W; maximum temperature, 150 °C. After the reaction was over, the solvent was evaporated and column purification was done with hexanes/EtOAc/Et_3N (93:6.9:0.1) to obtained off white solid **6** (1.33 g, 72%). mp 165-167 °C. ^{1}H NMR (400 MHz, $CDCl_3$) δ 8.96 (s, 1H), 7.28 (d, *J* = 2.4 Hz, 1H), 3.99 – 3.89 (m, 9H). ^{13}C NMR (101 MHz, $CDCl_3$) δ 161.47, 150.24, 146.97, 132.36, 128.16, 124.74, 110.07, 109.41, 98.84, 61.60, 61.41, 52.31. *Anal*. Calcd for $C_{12}H_{11}Br_2NO_4$: C, 36.67; H, 2.82; N, 3.56. Found: C, 36.79; H, 2.85; N, 3.56.

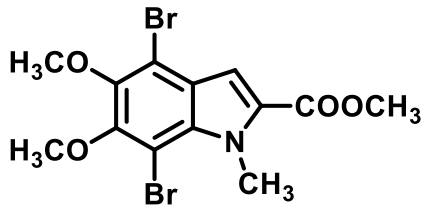

7

Methyl 4,7-dibromo-5,6-dimethoxy-1-methyl-1*H*-indole-2-carboxylate (7): To a stirred solution of compound **6** (4.6 g, 11.7 mmol) in DMF (40 mL), was added potassium carbonate (4.0 g, 29.4 mmol), CH_3I (4.1 g, 29.4 mmol) and a crystal of 18-crown-6 and stirred it at room temperature for 2 h. The crude reaction mixture was poured into ice-cold water to give the white solid **7** (3.93 g, 95 %). mp 136-137.5 °C ^{1}H NMR (300 MHz, $CDCl_3$) δ 7.29 (s, 1H), 4.46 (s, 3H), 3.91 (d, *J* = 0.8 Hz, 9H). ^{13}C NMR (101 MHz, $CDCl_3$) δ 161.97, 150.55, 146.81, 133.22, 130.14, 125.33, 111.77, 109.59, 100.12, 61.51, 61.42, 52.14, 35.06. Elemental Anal. Calcd for $C_{13}H_{13}Br_2NO_4$: C, 38.36; H, 3.22; N, 3.44. Found: C, 38.48; H, 3.16; N, 3.43.

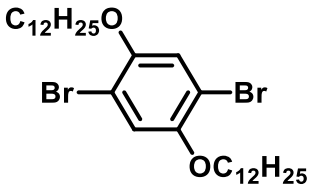

9

1,4-dibromo-2,5-bis(dodedecyloxy)benzene (9): A mixture of 2,5-Dibromobenzene-1,4-diol (**8**) (2.0 g, 7.5 mmol) and K_2CO_3 (2.0 g, 15 mmol) in 15 mL of dry DMF was stirred at room temperature for 1 h. Then 1-bromodecane (3.94 g, 15,8 mmol) was added dropwise to the reaction mixture which was heated to 80 °C for 12 h. The reaction misture was cooled to room temperature and added to a beaker containing 80 mL of ice cold water. The mixture was stirred for 20 min, and the resulting solid was filtered. The solid was purified using column chromatography using hexanes/EtOAc (99:1) to yield white color solid (3.08g , 68 %). ^{1}H NMR (400 MHz, $CDCl_3$) δ 7.08 (s, 2H), 3.94 (t, *J* = 6.5 Hz, 4H), 1.86 – 1.74 (m, 4H), 1.56 – 1.41 (m, 4H), 1.41 – 1.23 (m,

32H), 0.92 – 0.84 (m, 6H). ^{13}C NMR (101 MHz, $CDCl_3$) δ 150.08, 118.47, 111.14, 70.32, 31.93, 29.67, 29.65, 29.59, 29.56, 29.36, 29.31, 29.13, 25.94, 22.71, 14.13.

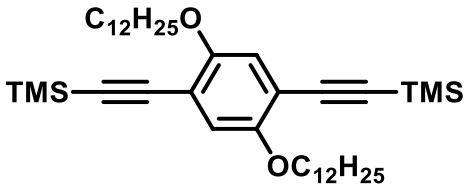

10

2,5-Bis(dodecyloxy)-1,4-phenylene)bis(ethyne-2,1-diyl)bis(trimethylsilane) (10): Dry THF (5 mL) was added to **9** (1.0 g, 1.6 mmol), and to this was added a mixture of CuI, $Pd(PPh_3)_4$ and triethylamine taken inside a glove box followed by the addition of ethynyltrimethylsilane (580 μL , 4.2 mmol) and heated to 40 °C for 12 h. Solvent was evaporated and the resulting crude was purified using column chromatography using hexanes/EtOAc (96:4) to yield white color solid **10** (1.00 g, 98%).^{1}H NMR (400 MHz, $CDCl_3$) δ 6.88 (s, 2H), 3.94 (t, *J* = 6.4 Hz, 4H), 1.78 (dt, *J* = 14.7, 6.5 Hz, 4H), 1.48 (q, *J* = 7.2 Hz, 4H), 1.28 (d, *J* = 17.1 Hz, 32H), 0.92 – 0.84 (m, 6H), 0.25 (s, 18H). ^{13}C NMR (101 MHz, $CDCl_3$) δ 154.05, 117.23, 113.97, 101.11, 100.11, 69.49, 31.97, 29.72, 29.68, 29.48, 29.40, 26.07, 22.74, 14.16.

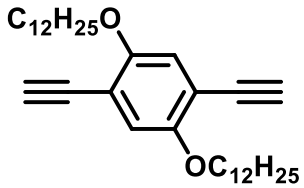

11

1,4-bis(dodecyloxy)-2,5-diethynylbenzene (11): The compound **10** (0.97 g, 1.5 mmol) was placed in a flask along with 20 mL of methanol and 75 mL of THF. The solution was stirred at room temperature for 16 h. To 200 mL of diethyl ether in separatory flask was added to the reaction mixture followed by 100 mL of brine solution. Another 2 × 50 mL extraction was done with EtOAc, the organic layers were combined dried with anhydrous Na_2SO_4 and the solvent was evaporated to yield yellow solid **11** (0.74 g, 99%). ^{1}H NMR (400 MHz, $CDCl_3$) δ 6.95 (s, 2H), 3.97

(t, *J* = 6.6 Hz, 4H), 3.32 (s, 2H), 1.85 – 1.73 (m, 4H), 1.50 – 1.40 (m, 4H), 1.34 – 1.24 (m, 32H), 0.92 – 0.83 (m, 6H). ^{13}C NMR (101 MHz, $CDCl_3$) δ 153.98, 117.73, 113.24, 82.39, 79.79, 69.66, 31.93, 29.67, 29.65, 29.59, 29.57, 29.36, 29.33, 29.13, 25.90, 22.70, 14.13.

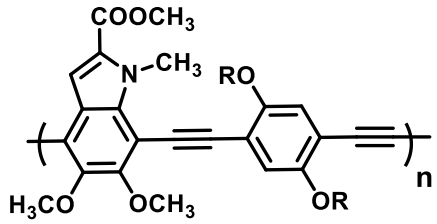

R= $C_{12}H_{25}$

Polymer synthesis: To a 10 mL reaction vial was added compound **7** (50 mg, 0.122 mmol) and compound **11** was placed inside a glove box and $Pd(PPh_3)_4$ (3.5 mg, 0.003 mmol), and CuI (0.6 mg, 0.003 mmol) were added, followed by 1 mL of Et_3N and 1 mL of THF. The vial was sealed inside the glove box and brought outside and heated to 80 °C for 48 hours. Then the reaction mixture was allowed to cool. The polymer was precipitated in beaker containing 40 mL of methanol. The resulting precipitate was filtered through a Soxhlet thimble, and the product was subjected to methanol, hexane and chloroform extractions. The solvent was evaporated to yield a red polymer in 36 % yield. ^{1}H NMR (400 MHz, Chloroform-*d*) δ 7.48-7.56 (broad, aryl and indole protons), δ 7.05-7.11 (broad, aryl and indole protons), δ 4.58-4.62 (broad, -N-CH_3), 4.06-4.11 (broad, -OCH_3), δ 3.91-3.94 (broad, -OCH_3), δ 1.85-1.96 (broad, -CH_2), δ 1.54 (broad, -CH_2), δ 1.24-1.36 (broad, -CH_2), δ 0.85-0.88 (broad, CH_3).

2.4.3. NMR spectra

^{1}H NMR of **5**

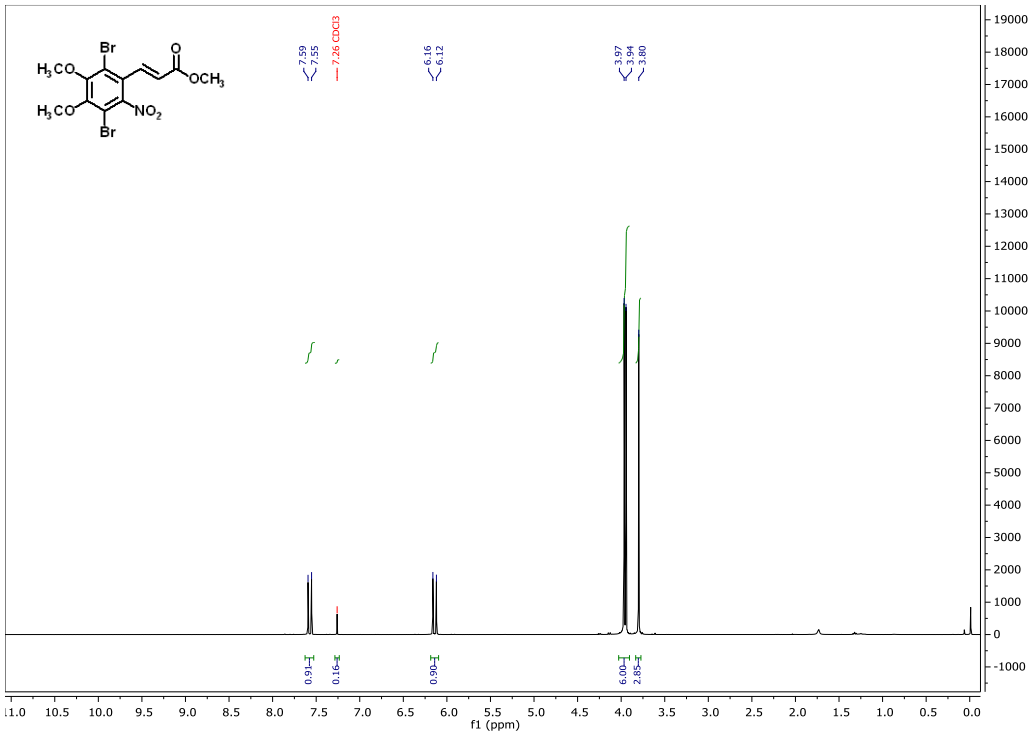

^{13}C of NMR **5**

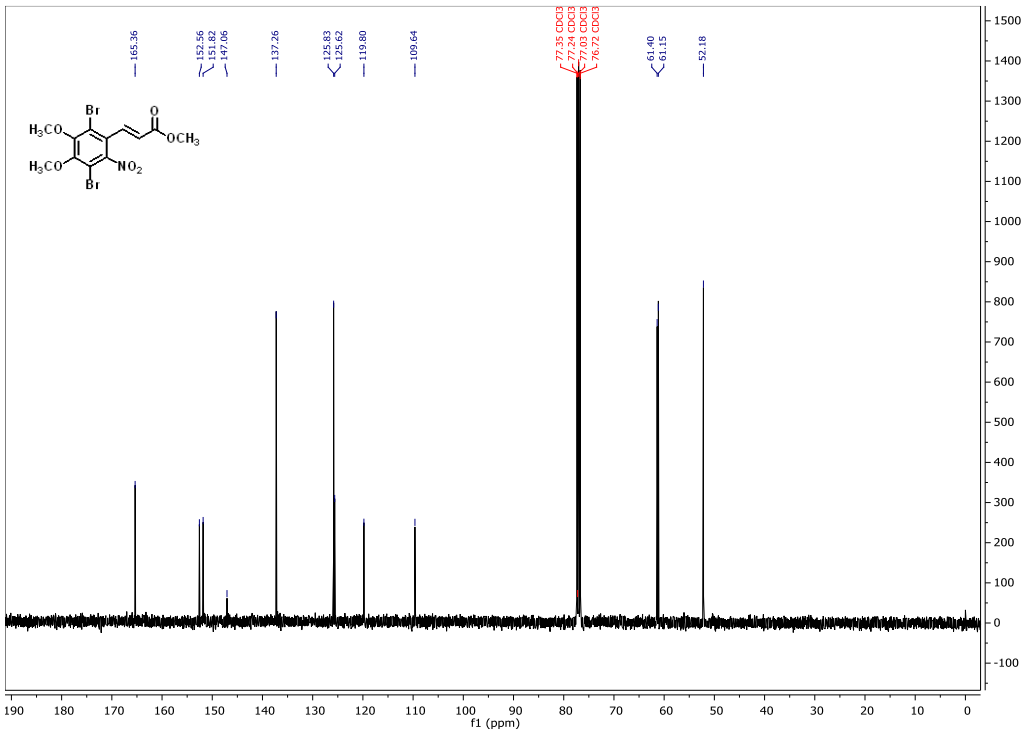

^{1}H NMR of **6**

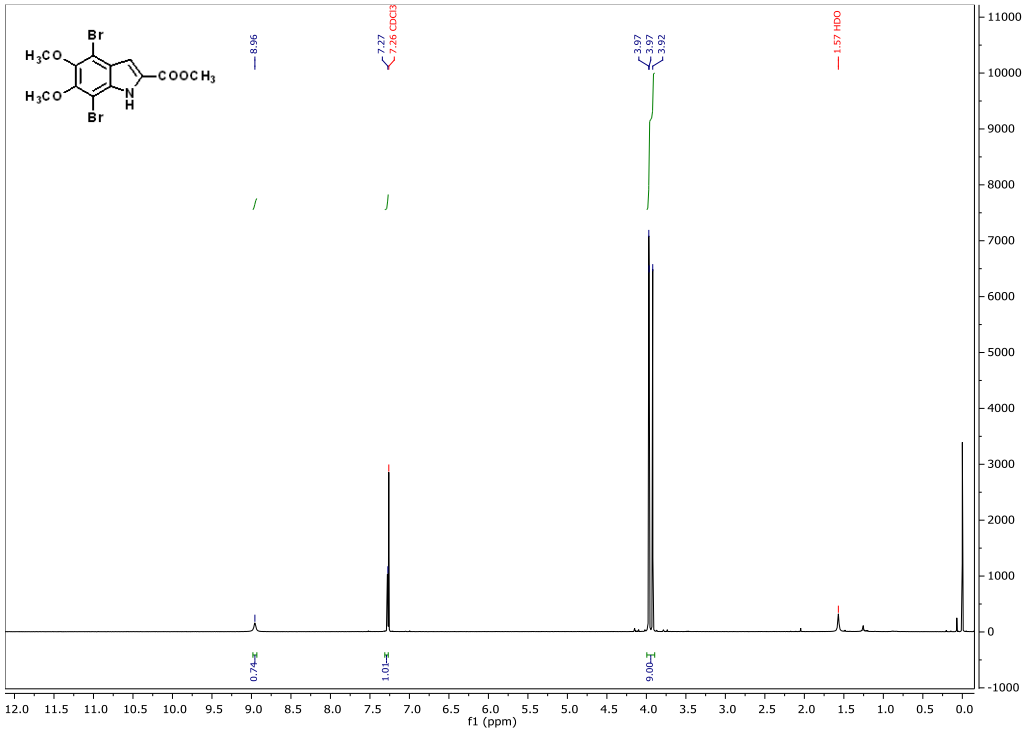

^{13}C of NMR **6**

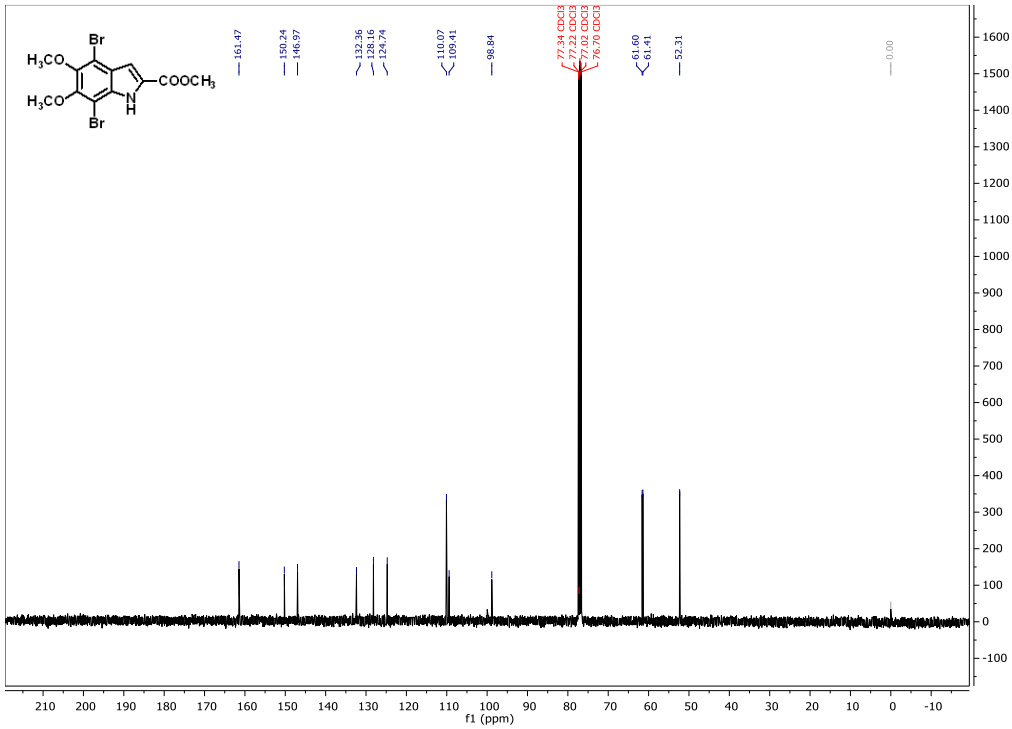

^{1}H NMR of **7**

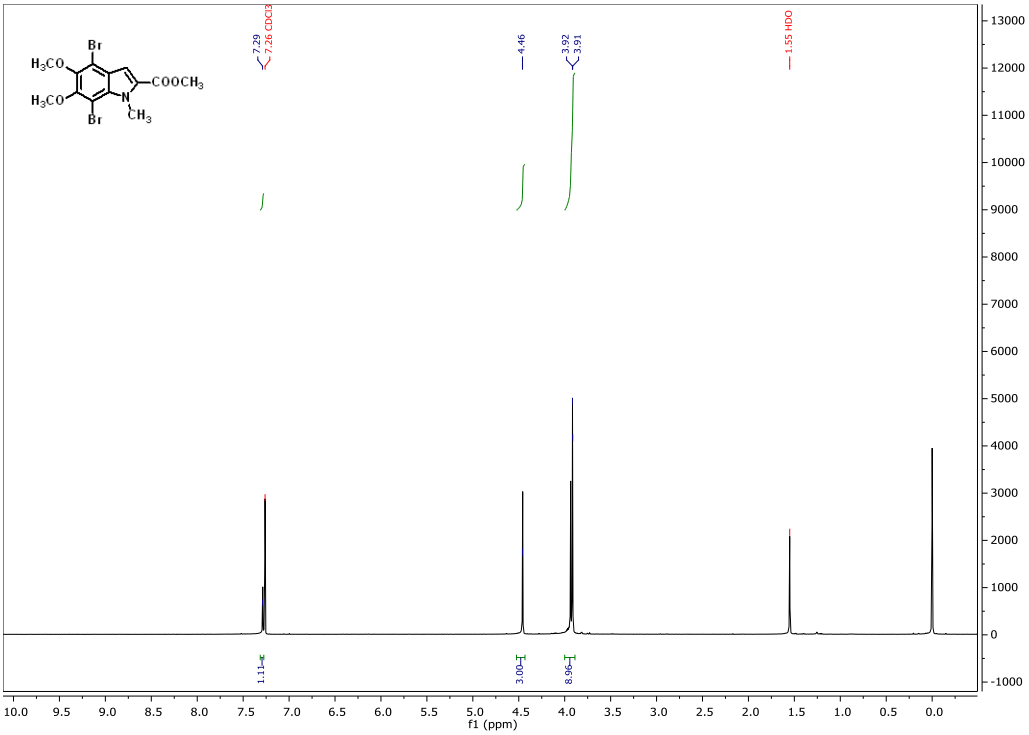

^{13}C of NMR **7**

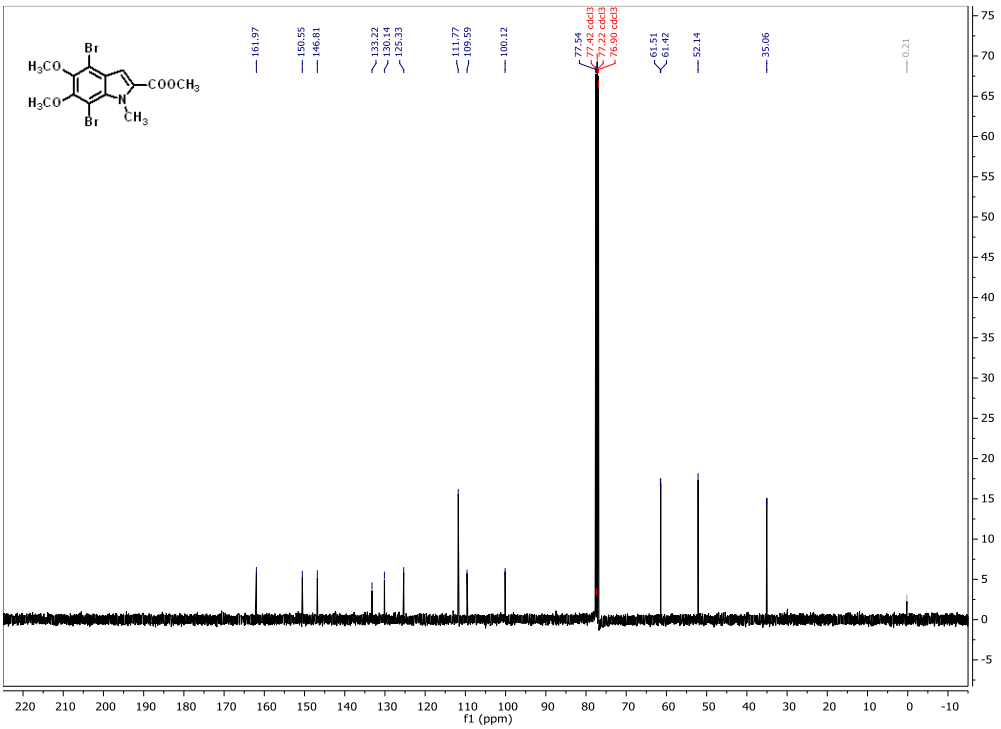

^{1}H NMR of **9**

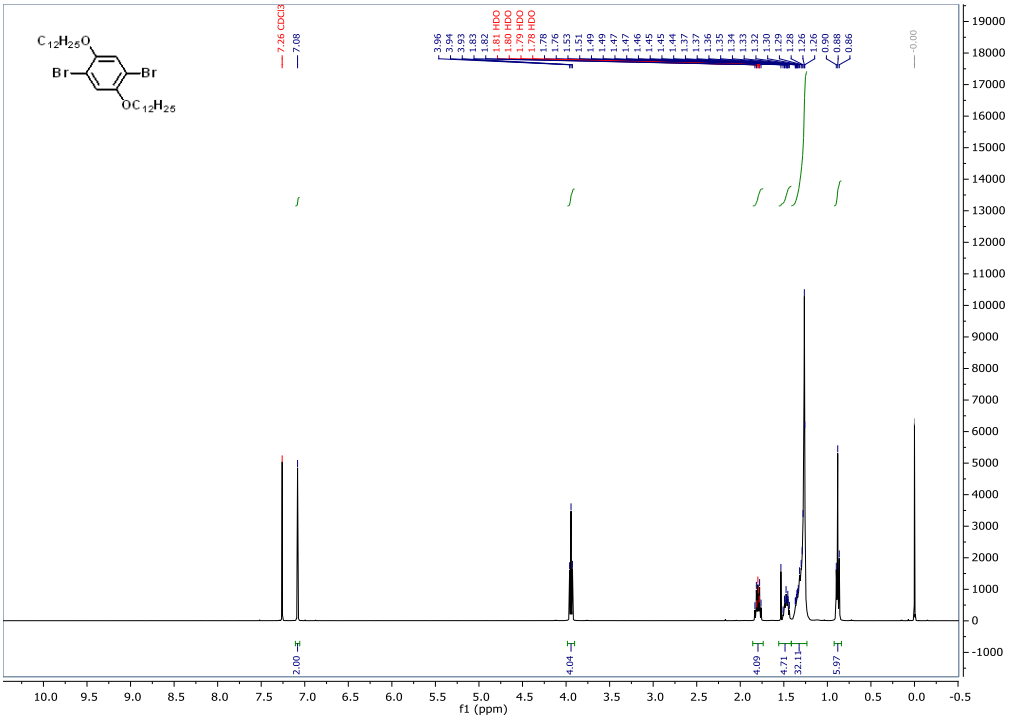

^{13}C of NMR **9**

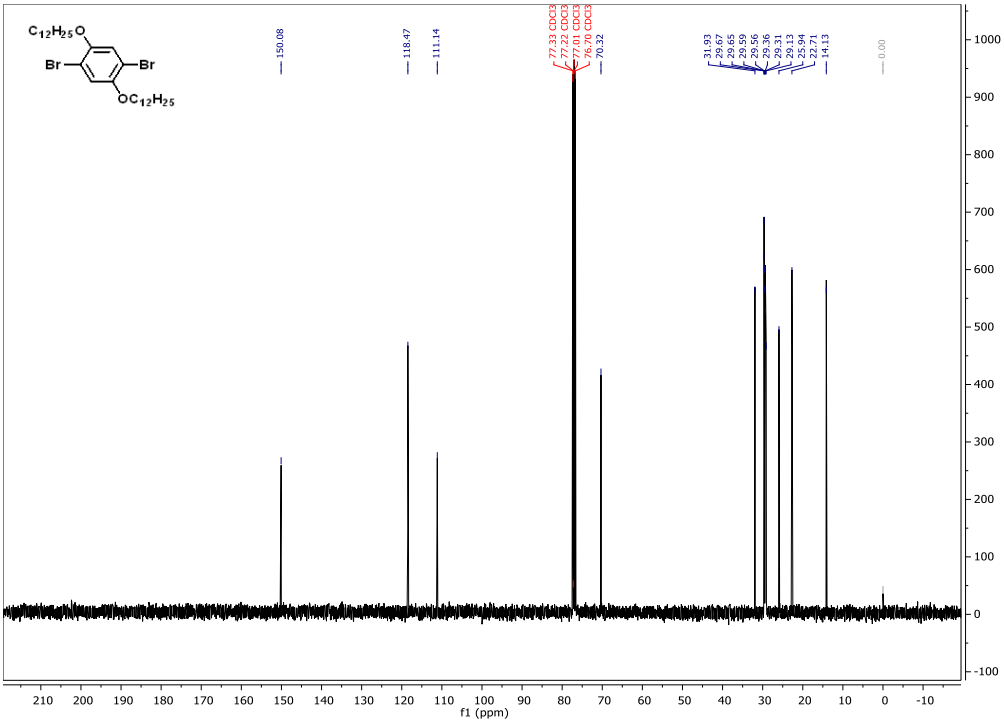

^{1}H NMR of **10**

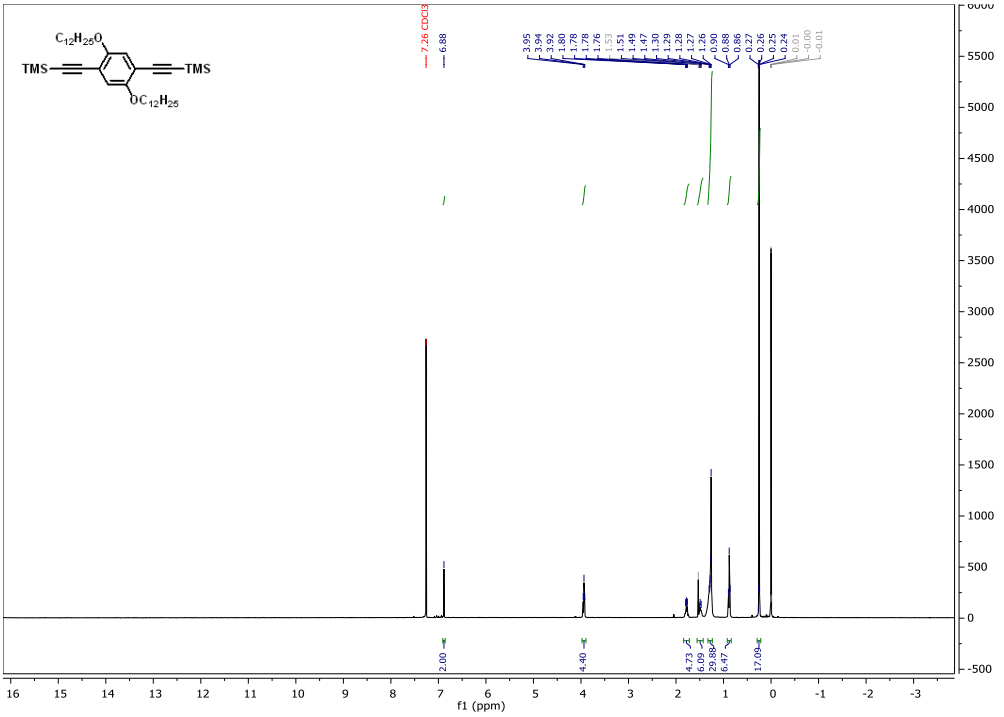

^{13}C NMR of **10**

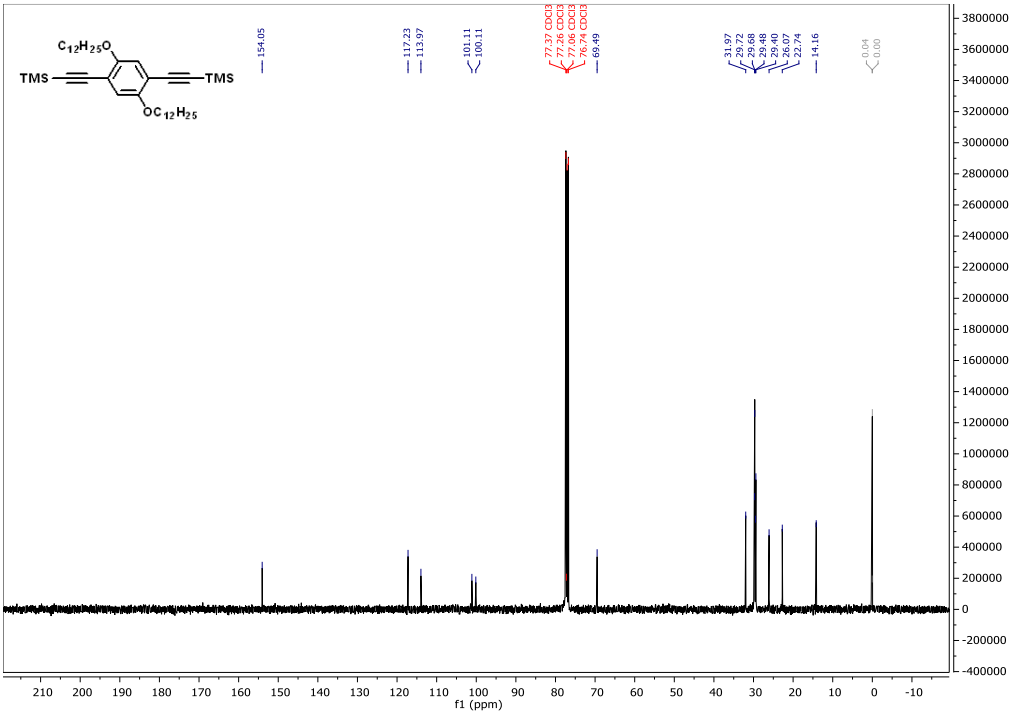

^{1}H NMR of **11**

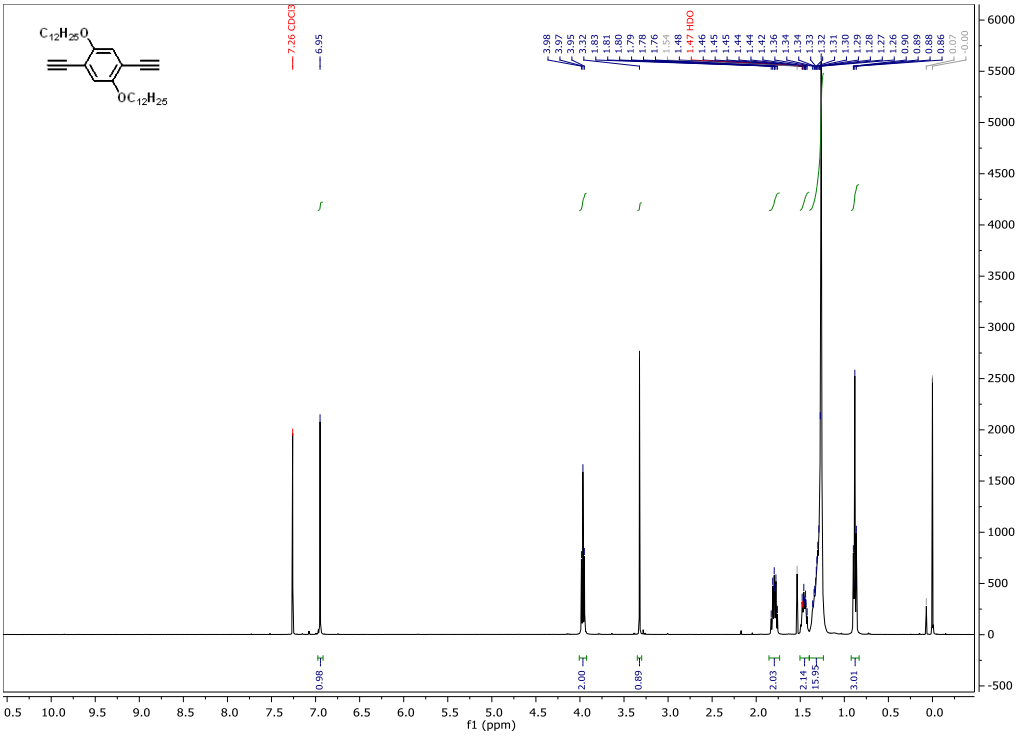

^{13}C NMR of **11**

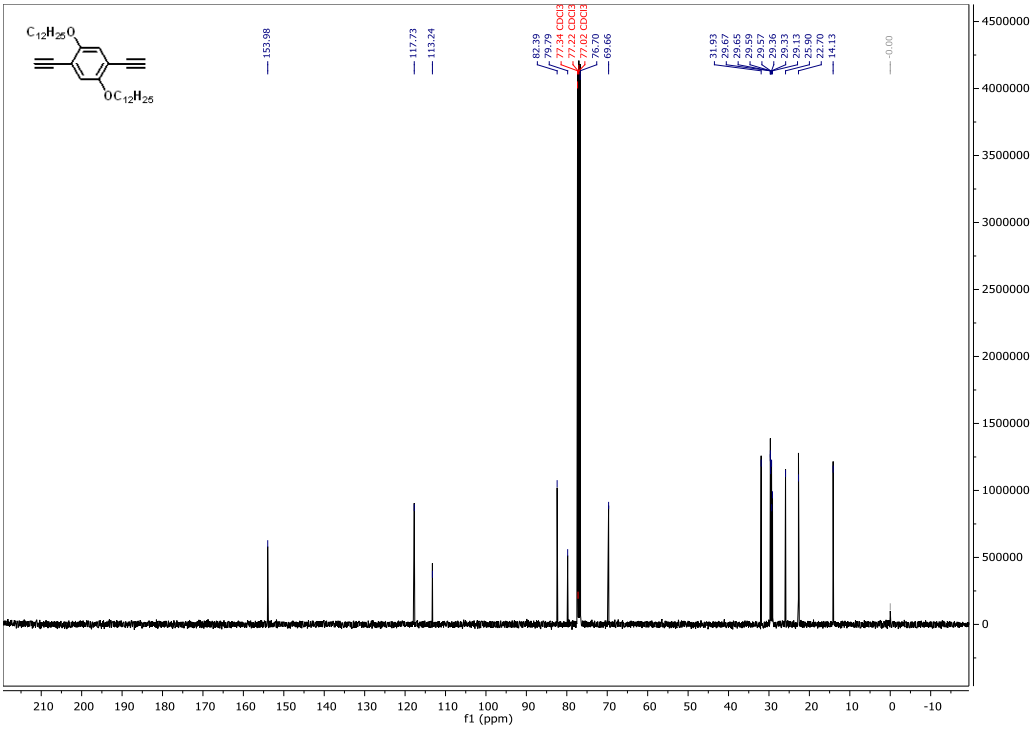

^{1}H NMR polymer

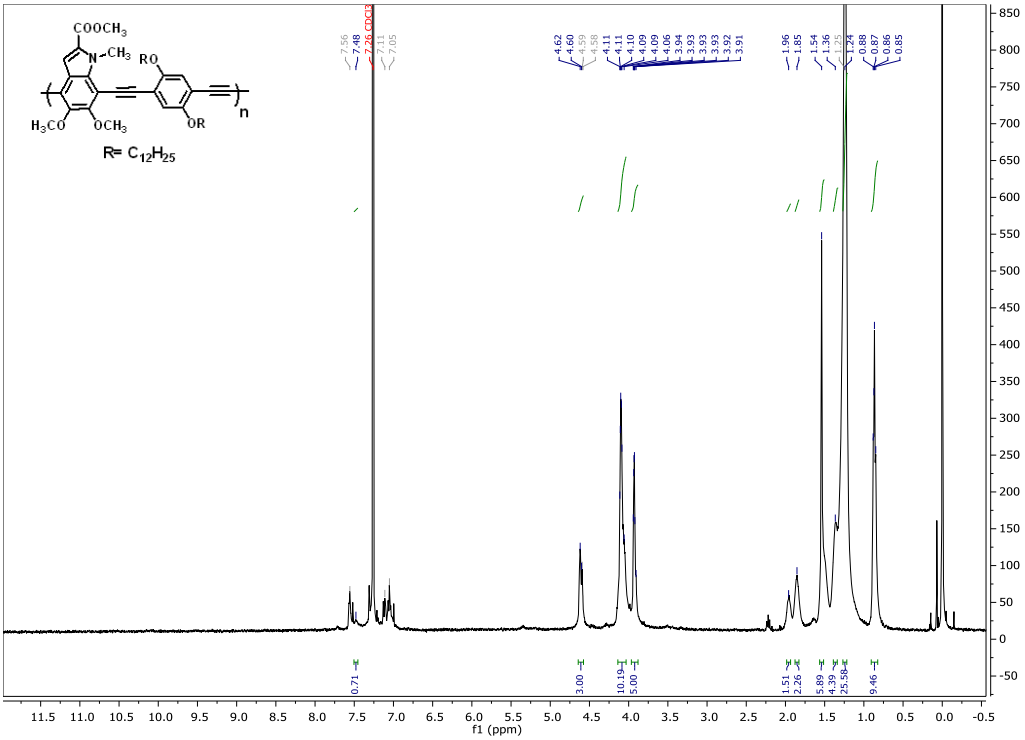

2.5. REFERENCES

1. Myers, J. D.; Xue, J., Organic semiconductors and their applications in photovoltaic devices. *Polymer Reviews* **2012,** *52* (1), 1-37.
2. Zhan, X.; Zhu, D., Conjugated polymers for high-efficiency organic photovoltaics. *Polymer Chemistry* **2010,** *1* (4), 409-419.
3. Grimsdale, A. C.; Leok Chan, K.; Martin, R. E.; Jokisz, P. G.; Holmes, A. B., Synthesis of light-emitting conjugated polymers for applications in electroluminescent devices. *Chem. Rev.* **2009,** *109* (3), 897-1091.
4. Forrest, S. R., The path to ubiquitous and low-cost organic electronic appliances on plastic. *Nature* **2004,** *428* (6986), 911-918.
5. Shirota, Y., Organic materials for electronic and optoelectronic devices. *Journal of Materials Chemistry* **2000,** *10* (1), 1-25.
6. Xue, J.; Perspectives on organic photovoltaics. *Polymer Reviews* **2010,** *50* (4), 411-419.
7. Pezzella, A.; Wünsche, J., Eumelanin: an old natural pigment and a new material for organic electronics – chemical, physical, and structural properties in relation to potential applications. In *Organic Electronics*, Wiley-VCH Verlag GmbH & Co. KGaA: 2013; pp 113-137.
8. Meredith, P.; Riesz, J., Radiative relaxation quantum yields for synthetic eumelanin¶. *Photochem. Photobiol.* **2004,** *79* (2), 211-216.
9. Meredith, P.; Sarna, T., The physical and chemical properties of eumelanin. *Pigment Cell Res.* **2006,** *19* (6), 572-594.
10. Brenner, M.; Hearing, V. J., The protective role of melanin against UV damage in human skin. *Photochem. Photobiol.* **2008,** *84* (3), 539-549.

11. d'Ischia, M.; Napolitano, A.; Pezzella, A.; Meredith, P.; Sarna, T., Chemical and structural diversity in eumelanins – unexplored bio-optoelectronic materials. *Angewandte Chemie (International Ed. in English)* **2009,** *48* (22), 3914-3921.
12. McGinness, J.; Corry, P.; Proctor, P., Amorphous semiconductor switching in melanins. *Science* **1974,** *183* (4127), 853-855.
13. Mostert, A. B.; Powell, B. J.; Pratt, F. L.; Hanson, G. R.; Sarna, T.; Gentle, I. R.; Meredith, P., Role of semiconductivity and ion transport in the electrical conduction of melanin. *Proceedings of the National Academy of Sciences* **2012,** *109* (23), 8943-8947.
14. D'Ischia, M.; Crescenzi, O.; Pezzella, A.; Arzillo, M.; Panzella, L.; Napolitano, A.; Barone, V., Structural effects on the electronic absorption properties of 5,6-dihydroxyindole oligomers: The potential of an integrated experimental and DFT approach to model eumelanin optical properties†. *Photochem. Photobiol.* **2008,** *84* (3), 600-607.
15. Selvaraju, S.; Niradha Sachinthani, K. A.; Hopson, R. A.; McFarland, F. M.; Guo, S.; Rheingold, A. L.; Nelson, T. L., Eumelanin-inspired core derived from vanillin: a new building block for organic semiconductors. *Chemical Communications* **2015,** *51* (14), 2957-2959.
16. Hocking, M. B., Vanillin: synthetic flavoring from spent sulfite liquor. *J. Chem. Educ.* **1997,** *74* (9), 1055.
17. Lehmann, F.; Holm, M.; Laufer, S., Rapid and easy access to indoles via microwave-assisted Hemetsberger–Knittel synthesis. *Tetrahedron Letters* **2009,** *50* (15), 1708-1709.
18. Crosby, G. A.; Demas, J. N., Measurement of photoluminescence quantum yields. Review. *The Journal of Physical Chemistry* **1971,** *75* (8), 991-1024.
19. Fetscher, C. A., *Org. Synth.* **1953,** *33*, 65.
20. Huleatt, P. B.; Lau, J.; Chua, S.; Tan, Y. L.; Duong, H. A.; Chai, C. L. L., Concise, efficient and practical assembly of bromo-5,6-dimethoxyindole building blocks. *Tetrahedron Letters* **2011,** *52* (12), 1339-1342.
21. Creencia, E. C.; Kosaka, M.; Muramatsu, T.; Kobayashi, M.; Iizuka, T.; Horaguchi, T., Microwave-assisted Cadogan reaction for the synthesis of 2-aryl-2H-indazoles, 2-aryl-1H-benzimidazoles, 2-carbonylindoles, carbazole, and phenazine. *Journal of Heterocyclic Chemistry* **2009,** *46* (6), 1309-1317.
22. Arnaiz, F. J.; Aguado, R.; Sanz-Aparicio, J.; Martinez-Ripoll, M., Addition compounds of dichlorodioxomolybdenum(VI) from hydrochloric acid solutions of molybdenum trioxide. Crystal structure of dichlorodioxodiaquamolybdenum(VI) bis(2,5,8-trioxanonane). *Polyhedron* **1994,** *13* (19), 2745-2749.

CHAPTER III

SYNTHESIS AND CHARACTERIZATION OF BLUE EMITTIMG EUMELANIN-INSPIRED POLYARYLENES FOR ORGANIC LIGHT EMITTING DIODES

3.1. INTRODUCTION

Conjugated polymers (CPs) have attracted much interest in the scientific community over the last three decades due to the promise of low cost, lightweight and large area electronic devices.[1-2] They have potential to create ubiquitous photovoltaic power in organic solar cells, transparent displays, efficient and inexpensive solid state lighting with organic light emitting diodes and other flexible and rugged electronics with organic field effect transistors.[3-6] Fluorene and carbazole containing materials are well-known as blue light emitters and show promising results in emissive layers of organic light emitting diodes (OLEDs).[7-14] Among the three color emitters which are red, green and blue in OLEDs, there is a great demand on blue emitting materials due to lower device stability, efficiency and color purity.[15-18] Although, the indole core has been used in blue emitting materials,[19-23] to our knowledge, there are no examples showing utilization of the indole moiety through its 4- and 7- positions in the blue emitting copolymers. An indole core is unique due to its existence as a parent substance in a large number of important biological compounds that occur in

nature.[24-26] It is a building block in the naturally occurring heterogeneous macromolecule, Melanin.[27-28] Eumelanin is the major form of melanin, a pigment responsible for black brown color in mammals including human.[29-30] It is the primary determinant of the skin tone of human and also found in human hair, eyes, inner ears and brain. It is known as a biosynthesized molecule which consists of 5,6-dihydroxyindole (DHI) and 5,6-dihydroxyindole-2-carboxylic acid (DHICA) units.[31-33] The optical, electronic, physical, metal chelating and structural properties of the natural and synthetic eumelanin have been studied extensively.[30, 32-35]

In chapter 2, the synthesis was discussed of an eumelanin-inspired core (DBI) similar to the building blocks of natural eumelanin, as well as the incorporation of the core with phenylenediethynylene to obtain poly(indoylenephenyleneethynylene) polymer.[36] Our group also demonstrated the incorporation of our eumelanin-inspired core into conjugated polymers by coupling it with the phenylene groups via different carbon-carbon bond linkages.[37] These poly(indoylenearyleneethynylene)s and poly(indoylenearylenevinylene)s showed good optical, electronic and physical properties. In this chapter, the synthesis, optical, physical and electrochemical properties of novel blue emitting, eumelanin-inspired polyarylenes are presented.

3.2. SYNTHESIS AND DISCUSSION

First, the feasibility of incorporating DBI with other arylene groups were tested by synthesizing two conjugated small molecules, Fl-DBI-Fl (**12**) and Th-DBI-Th (**13**) via Suzuki and Stille cross coupling conditions as shown in **Scheme 3.1.** 9,9-Dicotylfluorene-2-boronic acid pinacol ester was reacted with DBI via Suzuki coupling to yield **12** (70%). Stille coupling of 2-(tributylstannyl)thiophene with DBI resulted **13** (80%).

To optical properties of **12** and **13** were evaluated, namely the UV/Vis absorption and fluorescence spectroscopy in dilute chloroform. The absorption and emission spectra of the molecules are shown in **Figure 3.1.**

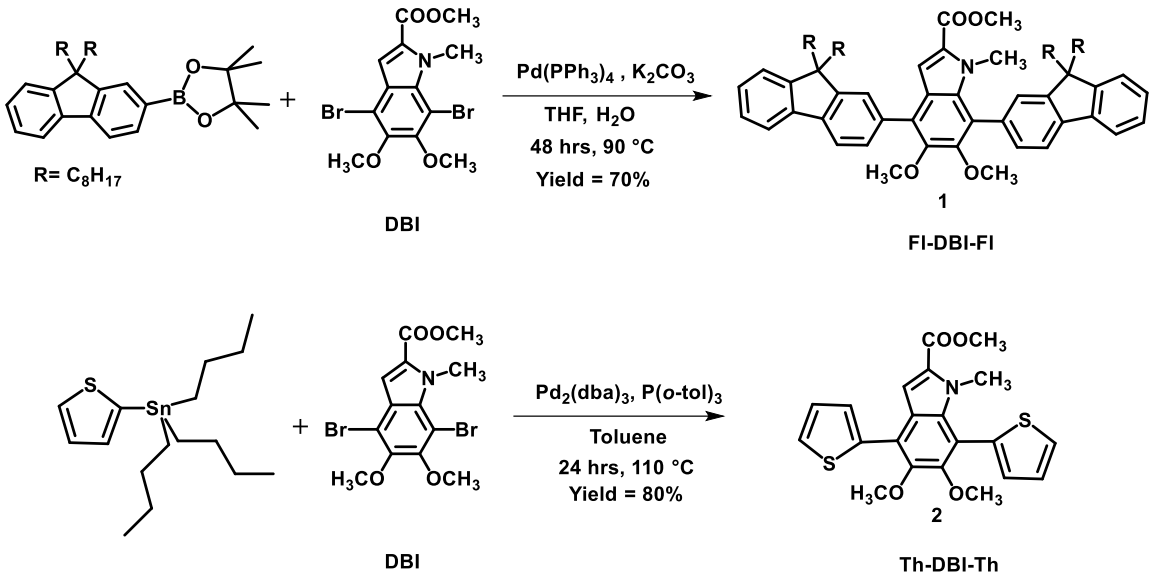

Scheme 3.1. The synthesis of eumelanin-inspired small molecules.

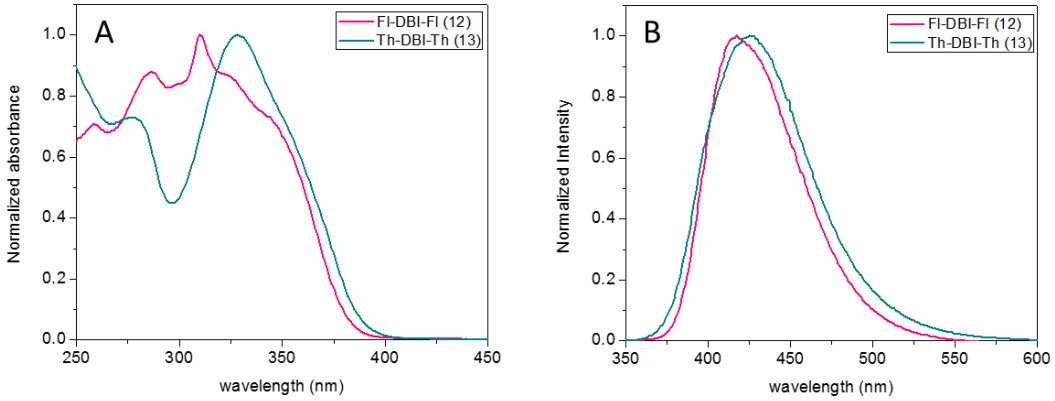

Figure 3.1. A). The UV/Vis absorption spectra of two compounds in $CHCl_3$ B). Fluorescence spectra of two compound in $CHCl_3$.

The absorption of **12** and **13** lay in the range of 250 nm-400 nm, having maxima at 310 nm and 328 nm respectively. The emission was in the blue region and showed an emission maximum at 417 nm for **12** and at 425 nm for **13**. Due to these interesting blue emitting properties of the small molecules, we were motivated to synthesize eumelanin-inspired polyarylenes. Fluorene and carbazole containing compounds have been highly used as blue emitters in the organic light

emitting diodes. Therefore, eumelanin-inspired fluorene and carbazole containing copolymers were designed and synthesized via Pd^0 catalyzed Suzuki coupling conditions.

Side chain variations can have an effect on the optical properties of the conjugated polymers.[38-39] In order to investigate the effect on optoelectronic properties caused by the different alkyl chains of the polymers, two poly(indoylene-*co*-fluorene) (PIF) polymers were synthesized. In this synthesis, 9,9-dioctylfluorene-2,7-diboronic acid bis(1,3-propanediol) ester and 9,9-dihexylfluorene-2,7-diboronic acid bis(1,3-propanediol) ester were used as fluorene monomers. The synthesis is shown in **Scheme 3.2.**

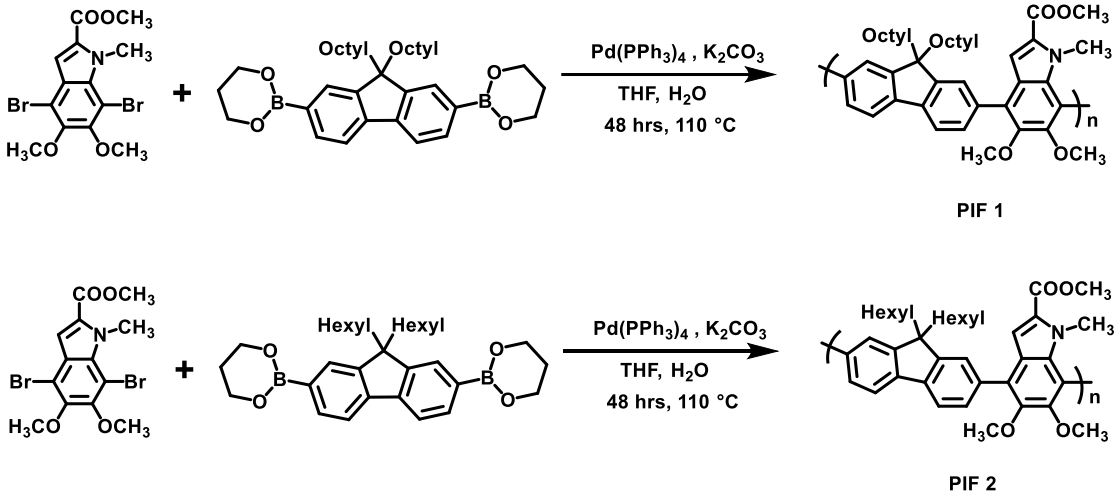

Scheme 3.2. The synthesis of poly(indoylene-*co*-fluorene)s.

Two polymer were synthesized using $Pd(PPh_3)_4$ as the catalyst and K_2CO_3 as the base in 1:1 ratio of THF:DI water as the solvent. The structures of the two polymers were confirmed with ^1H NMR. PIF polymers were isolated in 78-82% yields after reprecipitation in the methanol. The number average and weight average molecular weights and polydispersity indices (PDIs) of the polymers (**Table 3.1**) were determined using gel permeation chromatography with reference to polystyrene standards. Two copolymers had similar molecular weights and PDIs. Thermal properties of the polymers were determined with differential scanning calorimetry (DSC) and thermogravimetric analysis (TGA) methods, and data are shown in **Table 3.1.**

Table 3.1. The structural and thermal properties of PIF polymers

Polymer	M_n[a] (kDa)	M_w[a] (kDa)	PDI[a]	Yield (%)	T_d[b] (°C)	T_g[c] (°C)
PIF 1	18.8	37.5	1.99	78	-56	431
PIF 2	20.9	51.0	2.43	82	-56	434

[a] The number-average molecular weight and the PDI were measured by GPC using polystyrene standards. [b] By TGA under N_2. [c] Data from DSC, second scan reported, heating rate 3 °C min^{-1} under N_2

In DSC thermograms (**Figure 3.2**.) the derivative of reversible heat flow as a function of temperature, showed distinct peaks at -56 ˚C for both PIF 1 and PIF 2 polymers. These peaks are for the glass transition temperatures (T_g) of the polymers. Crystallization and melting transitions were not observed in the scanning temperature range, which suggested that polymers were amorphous in nature. The TGA plot showed that both polymers exhibit good thermal stabilities under N_2, indicating 5% decomposition at 431 °C for PIF 1 and 434 °C for PIF 2. The rigid backbone of these polymers may attribute to the higher thermal stabilities.

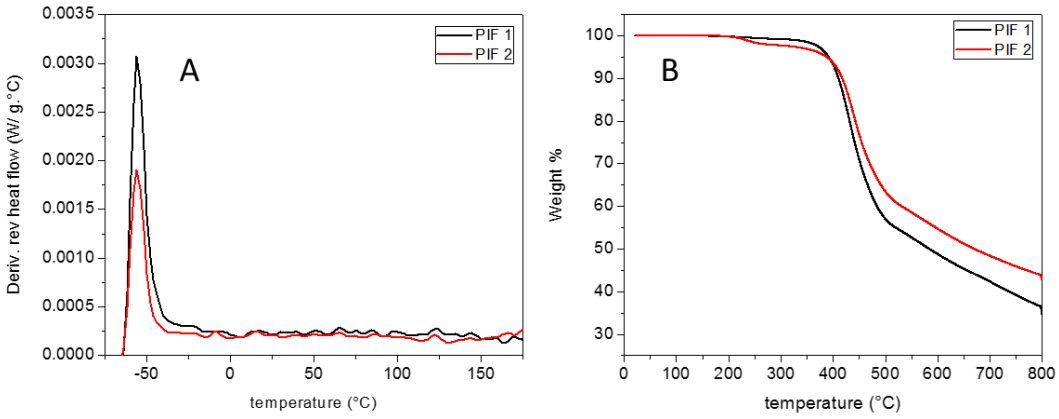

Figure 3.2. A). Differential scanning calorimetry (DSC) scans of polymers: a plot showing derivative of reversible heat flow as a function of temperature B). Thermogravimetric analysis of polymers.

Optical properties of the polymers were measured and listed in **Table 3.2.** Both PIF 1 and PIF 2 polymers showed similar optical properties. UV-Vis absorption and fluorescence spectra of the two polymers are shown in **Figure 3.3.** The absorbance spectra of PIF 1 and PIF 2 in chloroform solution overlapped and have maximum absorbance at 360 °C.

Table 3.2. The optical and electronic properties of PIF polymers.

Polymer	λ_{abs} sol[a] (nm)	λ_{abs} film[a] (nm)	λ_{ems} sol[a] (nm)	E_g^{opt} (eV)[b]	E_{ox} (V)[c]	HOMO (eV)[d]	LUMO (eV)[e]
PIF 1	360	361	416	3.10	1.30	-5.71	-2.61
PIF 2	360	361	415	2.96	1.30	-5.71	-2.75

[a] Measured in dilute chloroform. [b] Measured from the tangent drawn at the onset of absorption. [c] Measured from the onset of the oxidation wave.[d] Calculated from the onset of the first oxidation from the equations E_{HOMO} (eV) = -[E_{ox}onset - $E_{1/2}$ (Fc/Fc^+) + 4.8] where $E_{1/2}$ (Fc/Fc^+) was the cell correction.[e] Calculated from the equation LUMO = (E_g^{opt} - HOMO).

Although the maximum absorbance of the two polymers in the solid state is exactly same, the absorption spectrum of PIF 2 polymer in the solid state (thin films) showed red-shifted broadening when comparing to the PIF 1 polymer. This could be contribute to better polymer stacking for PIF 2 in the solid state. The fluorescence spectra of the two polymers in $CHCl_3$ is also overlapped. These results indicate that straight chain alkyl groups on the fluorene block have very little effect on the optical properties of these polymers.

The optical bandgaps were calculated from the absorption in thin films. Wavelengths corresponding to the energy of absorption were measured at the intersection of the leading edge tangent with the *x*-axis. The absoption onsets of PIF 1 and PIF 2 were around 400 nm and 418 nm, respectively. Thus the optical band gaps (E_g^{opt}) are 3.10 eV and 2.96 eV. The electronic properties were measured by cyclic voltammetry on thin films of the polymers, and the results are summarized in **Table 3.2.**

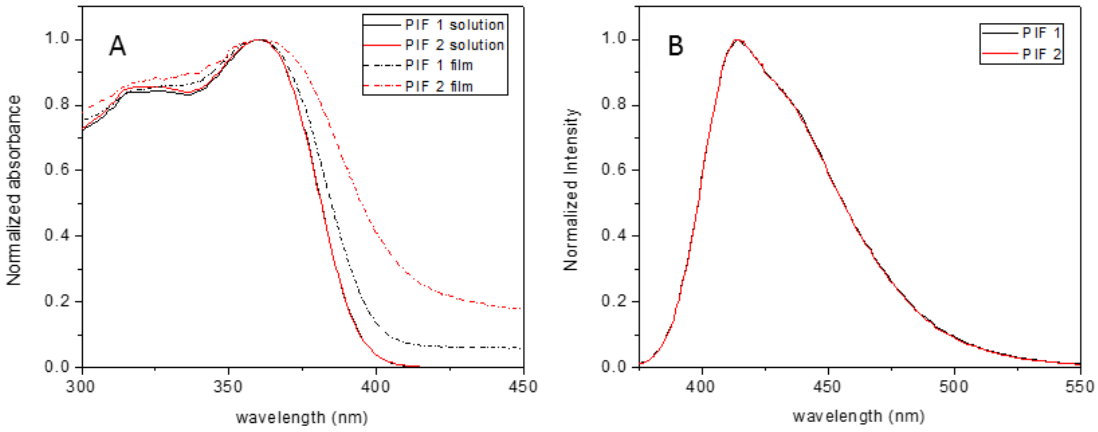

Figure 3.3. A). The UV/Vis absorption spectra of polymers PIF1 and PIF2 in $CHCl_3$ (solid lines) and in thin film (dashed lines) B). Fluorescence spectra of the two polymers in $CHCl_3$.

The HOMO energy values were calculated from the onset of the first oxidation from the equation HOMO (eV) = - [E_{ox}onset - $E_{1/2}$ (Fc/Fc^+) + 4.8] where $E_{1/2}$ (Fc/Fc^+) was the cell correction with respect to the standard compound ferrocene (Fc). As the onset oxidation potentials of PIF 1 and PIF 2 both occurred at 1.30 V against $Ag/AgCl_2$ (as shown in **Figure 3.4**), the HOMO levels of both PIF 1 and PIF 2 were -5.71 eV. Both polymers showed irreversible oxidation potentials, and no any reduction waves could be seen. Therefore, the LUMO energy values were calculated to be -2.61 eV and -2.75 eV from the equation LUMO = (E_g^{opt} − HOMO).

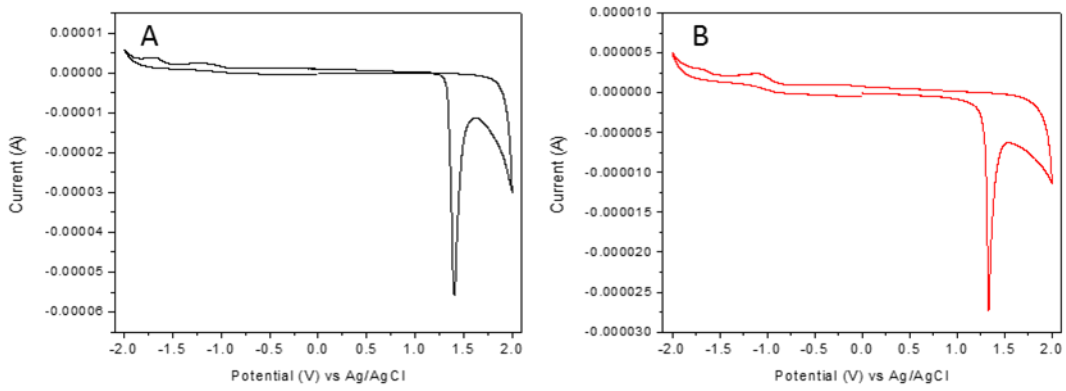

Figure 3.4. The cyclic voltammograms of A). PIF 1 B). PIF 2.

Next, the effects of different aryl groups such as fluorene and carbazole on the optoelectronic properties of the polymers were investigated. Thus we attempted the synthesis of the functionalized carbazole monomer **15** from commercially available 3,6-dibromocarbazole shown in **Scheme 3.3.**

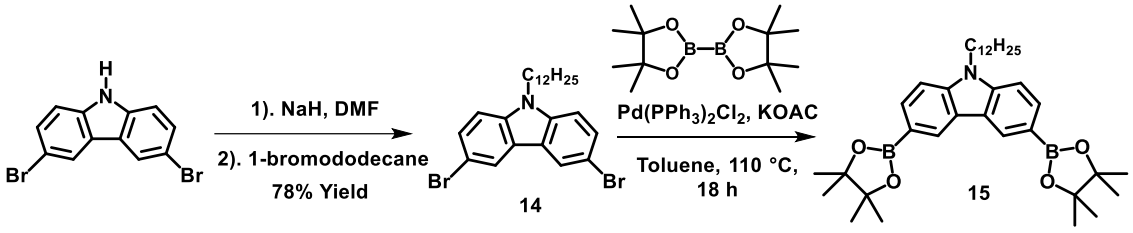

Scheme 3.3. The attempted synthesis of carbazole monomer (**15**).

In order to incorporate solubilizing groups on the carbazole monomer, 3,6-dibromocarbazole was alkylated to obtain compound **14** (78%). Compound **14** underwent Pd catalyzed borylation with bis(pinacolato diborane) [$(Bpin)_2$] as the boron source. This reaction was not complete even after 18 h and formed the desired product **15**, an undesired Bpin/Br functionalized product **Y** (**Scheme 3.4)** and some unidentified impurities. Based on the ^{1}H NMR analysis of the crude reaction mixture, the ratio between the remained starting material (SM), **15** and **Y** were 1:2:1. To optimize the reaction, several conditions were varied including various catalyst such as palladium catalysts ($Pd(PPh_3)_2Cl_2$, $Pd(PPh_3)_4$ and $Pd(dppf)Cl_2$), solvents (toluene, DMF and dioxane), temperatures (80, 90 and 110 °C) and reaction times which are shown in **Table 3.3.** All reactions resulted in the desired product, product **Y** and minor impurities.

The attempted isolation of the desired product by column chromatography was challenging. The compound was not stable during column chromatography even with the silica basified with trimethylamine. The alternate route for the diborylation involved lithium halogen exchange with n-BuLi, and quenching with excess of 2-isopropoxy-4,4,5,5-tetramethyl-1,3,2-dioxabrolane. Unfortunately, the process formed undesired Bpin/H functionalized product in addition to same products formed by the Pd catalyzed borylation reaction.

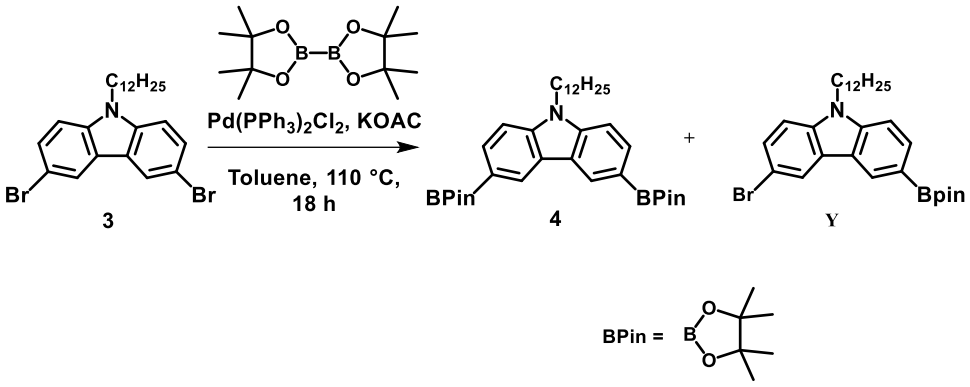

Scheme 3.4. The borylation reaction of 3,6-dibromo-9-dodecylcarbazole.

Table 3.3. Different conditions used to optimize the borylation reaction of carbazole and product ratios.

run	Catalyst (mol %)	Base (equiv.)	Solvent	Temp. (°C)	Time (h)	Product ratio
1.	$Pd(PPh_3)_2Cl_2$ (5)	KOAc (5)	toluene	110	18	SM: 15: Y = 1:2:1
2.	$Pd(PPh_3)_2Cl_2$ (5)	KOAc (7)	toluene	110	18	15 : Y = 3:2
3.	$Pd(PPh_3)_2Cl_2$ (5)	KOAc (10)	toluene	110	18	15 : Y = 3:2
4.[40]	$Pd(PPh_3)_4$	KOAc (8)	DMF	80	16	15 : Y = 2:1
5.	$Pd(dppf)Cl_2$)	KOAc (8)	dioxane	90	24	15 : Y = 2:1

Hence, the commercially available 9-(heptadecan-9-yl)-2,7-bis(4,4,5,5-tetramethyl-1,3,2-dioxaborolan-2-yl)-9H-carbazole was used to synthesize poly(indoylene-*co*-carbazole) (PIC) via a Pd-catalyzed Suzuki polymerization reaction shown in **Scheme 3.5.** After reprecipitation in methanol, PIC was isolated in 64%.

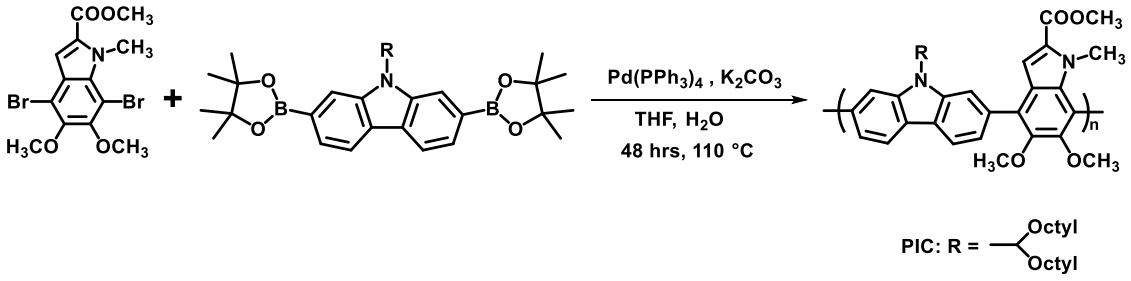

Scheme 3.5. The synthesis of PIC polymer

To investigate the effect of aryl groups on eumelanin-inspired polyarylenes, the physical, optical and electronic properties of PIF 1 and PIC were compared. The structures of the two polymers were confirmed with ^{1}H NMR, ^{13}C NMR, HMQC, HMBC and FTIR. In FTIR, the characteristic peak for the ester carbonyl group at 1710 cm^{-1} confirmed the incoporation of the eumelanin-inspired core in both polymers. PIF 1 and PIC were soluble in chloroform, THF and chlorobenzene. The number average molecular weight (M_n) and polydispersity index (PDI) are shown in the **Table 3.4**. Both polymers had similar M_n values and PDIs. The effect of the molecular weight on the optical, physical and electronic properties of the polymers are negligible.

Table 3.4. Structural and thermal properties of PIF 1 and PIC polymers.

Polymer	M_n[a] (kDa)	M_w[a] (kDa)	PDI[a]	Yield (%)	T_d[b] (°C)	T_g[c] (°C)
PIF 1	18.8	37.5	1.99	78	-51	431
PIC	11.0	40.4	3.65	64	-51	427

[a] The number-average molecular weight and the PDI were measured by GPC using polystyrene standards. [b] By TGA under N_2 [c] Data from DSC, second scan reported, heating rate 3 °C min^{-1} under N_2.

The thermal properties and stabilities of the two polymers were determined by DSC and TGA, and thermograms can be found in the **Figure 3.5.**

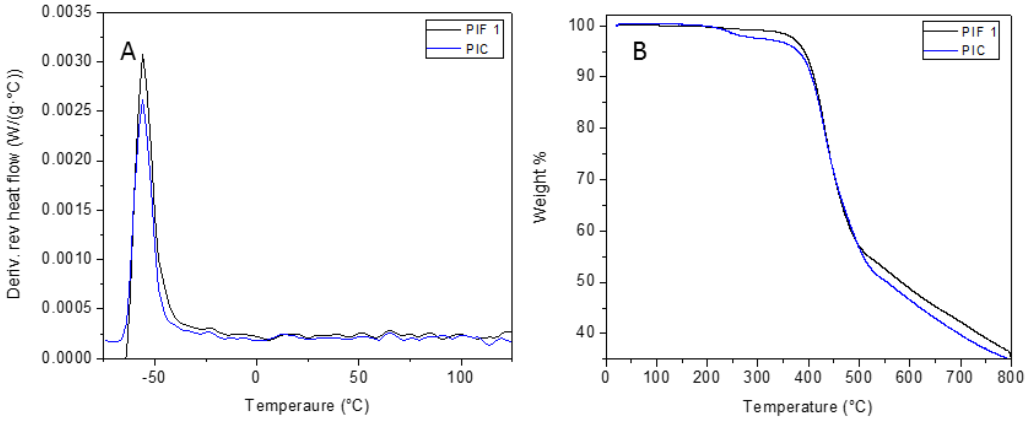

Figure 3.5. A). Differential scanning calorimetry (DSC) scans of PIF 1 and PIC: a plot showing derivative of reversible heat flow as a function of temperature B). Thermogravimetric analysis of the polymer.

The glass transition temperature (T_g) of PIC and PIF 1 were -56 °C, and there was no crystallization or melting transitions observed in the scanning range. This suggested that PIC was also an amorphous polymer. The TGA plot showed that both polymers exhibited good thermal stabilities under N_2, indicating 5% decomposition at 431 °C for PIF 1 and 427 °C for PIC. As in the PIF polymers, the rigid backbone of the PIC polymer may attribute to its higher thermal stability.

The photophysical properties of PIF 1 and PIC were evaluated using UV-Vis absorption and fluorescence spectroscopy in solutions and in thin films. The absorption and fluorescence spectra of the polymers are shown in **Figure 3.6.**, and the results are summarized in **Table 3.5.**

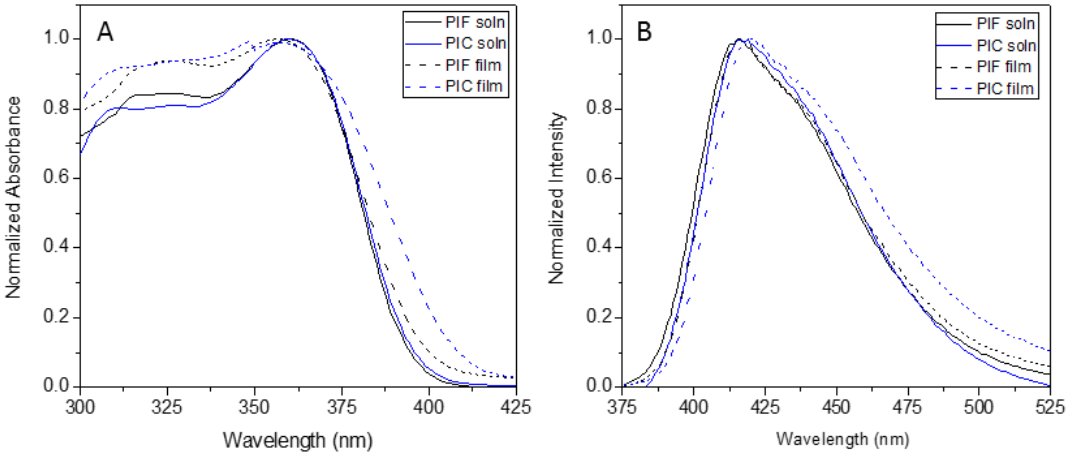

Figure 3.6. A). Absorption spectra of PIF 1 and PIC polymers in solution ($CHCl_3$, solid lines) and in thin film (cast from $CHCl_3$, dashed lines) B). Fluorescence spectra of polymers in solution ($CHCl_3$, solid lines) and in thin film (cast from $CHCl_3$, dashed lines). Polymers were excited at 360 nm for both solution and film.

Both polymers in solution and in thin films showed light absorption from the visible to the medium UV region. This absorption was attributed to a strong featureless $\pi - \pi^*$ transition with a maximum of 360-361 nm. It can be seen that the absorption spectrum of each polymer in solution was almost identical to their absorption in film, implying the limited π stacking of polymer chains in the solid state due to non-coplanarity of the polyarylenes.

When comparing the absorption spectra of two polymers in both solution and in film, there was no significant difference. This is a common trend for copolymers having fluorene and carbazole units attached to the same arylene group.[7] This similar absorption may be due to the similar structures of the polymers except for the N atom present in the carbazole unit of PIC polymer. The fluorescence spectra of both PIF 1 and PIC polymers in $CHCl_3$ and in the solid state, upon excitation of 360 nm, emit in the deep blue range at a maximum of 417- 418 nm. The emission of polymers in solution and in thin films show a similar trend. The fluorescence quantum yields of PIF 1 and PIC in dilute chloroform were calculated to be 60% and 39% respectively with reference to the standard, quinine sulfate. It is lower for PIC possibly due to the heteroatom effect in PIC that favors the non-radiative pathways.[40]

Table 3.5. Optical and electronic properties of PIF 1 and PIC polymers.

Polymer	Media	λ_{abs}[a] (nm)	λ_{ems}[a] (nm)	φ[b]	E_g^{opt} (eV)[c]	E_{ox} (V)[d]	HOMO (eV)[e]	LUMO (eV)[f]
PIF	$CHCl_3$	361	416	0.60				
	Film	360	416		3.10	1.30	-5.71	-2.61
PIC	$CHCl_3$	361	417	0.39				
	Film	360	418		3.02	1.20	-5.61	-2.59

[a] Measured in dilute chloroform. [b] Quantum yields measured in dilute chloroform solutions relative to quinine sulfate [c] Measured from the tangent drawn at the onset of absorption. [d] Measured from the onset of the oxidation wave. [e] Calculated from the onset of the first oxidation using the equations E_{HOMO} (eV) = -[E_{ox}onset - $E_{1/2}$ (Fc/Fc^+) + 4.8] where $E_{1/2}$ (Fc/Fc^+) was the cell correction. [f] Calculated from the equation LUMO = (E_g^{opt} - HOMO).

The optical bandgaps were calculated from the absorption plots of the thin films. Wavelengths corresponding to the energy absorption were measured at the intersection of the leading edge tangent with the *x*-axis. The absoption onsets of PIF 1 and PIC are around 400 nm and 410 nm; thus the optical band gaps (E_g^{opt}) were 3.10 eV and 3.02 eV.

The electronic properties were measured by cyclic voltammetry on thin films of these polymers, and the results are summarized in **Table 3.5.** The HOMO energy values were calculated from the onset of the first oxidation from the equations HOMO (eV) = - [E_{ox}^{onset} - $E_{1/2}$ (Fc/Fc^+) + 4.8] where $E_{1/2}$ (Fc/Fc^+) was the cell correction. As the onset oxidation potential of PIC occurs at 1.20 V vs Ag/$AgCl_2$ (**Figure 3.7.**), the HOMO level of PIC was calculated to be -5.61 eV. As in PIF 1, PIC showed irreversible oxidation potentials and no reduction wave. Therefore, the LUMO energy value was calculated to be -2.59 eV from the equation of LUMO = (E_g^{opt} − HOMO).

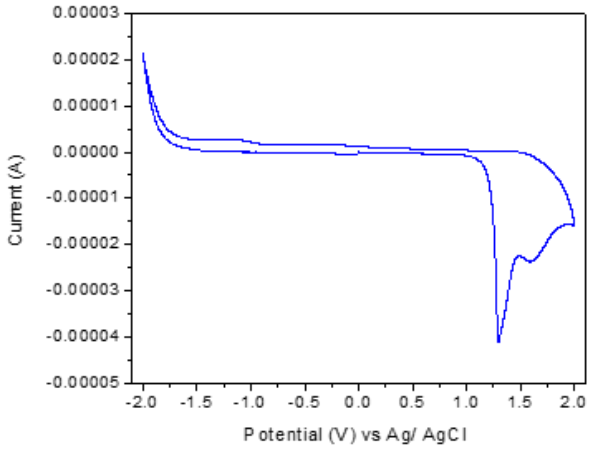

Figure 3.7. The Cyclic voltammogram of PIC polymer

3.3. SUMMARY AND OUTLOOK

Novel eumelanin-inspired polyarylenes were synthesized by coupling the eumelanin-inspired core (DBI) with well-known fluorene and carbazole arylene groups via Suzuki polymerization.

These polymers showed deep blue emitting properties and show promise as blue emitters in organic light emitting diodes. To investigate the side chain effect on the optical, physical and electronic properties of the polymers, two types of poly(indoylene-*co*-fluorene) polymers were synthesized. Polymers containing dioctyl and dihexyl side chains on fluorene monomers were compared. According to the results, there was no significant difference on the optical, physical and electronic properties of the polymers as a result of the different side chains. Poly(indoylene-*co*-carbazole)

(PIC) polymer was synthesized to study the effect of different aryl groups on the optical, physical and electronic properties of the polymers. PIC was compared with PIF 1 since both of these polymers had similar side chains. Both PIF 1 and PIC showed similar physical, optical and electronic properties but showed different fluorescence quantum yields. When compared to PIC (0.39), PIF 1 had greater quantum yield (0.60) which implied the fluorescence emission is more effective in PIF 1.

3.4 EXPERIMENTAL SECTION

3.4.1 Materials

9,9-Dioctylfluorene-2,7-diboronic acid bis(1,3-propanediol) ester, 9,9-dihexylfluorene-2,7-diboronic acid bis(1,3-propanediol) ester and 9,9-dicotylfluorene-2-boronic acid pinacol ester were purchased from Sigma Aldrich. 3,6-Dibromocarbazole and 2-(tributylstannyl)thiophene were purchased from Alfa Aesar and 9-(heptadecan-9-yl)-2,7-bis(4,4,5,5-tetramethyl-1,3,2-dioxaborolan-2-yl)-9*H*-carbazole was purchased from Ark Pharm. These compounds were used as received. Anhydrous tetrahydrofuran (THF) and chloroform ($CHCl_3$) were obtained a solvent purification system under ultrapure argon. Distilled water was degassed with argon while sonicating the flask. DBI was synthesized according to the previously reported procedure.[36] All the other commercial reagents were used as received**.**

3.4.2 Instrumentation

^1H, and ^{13}C NMR experiments were done to confirm the structures of the polymers. All spectra were acquired on a Varian Inova 400 MHz spectrometer using a OneNMR probe, with a nominal temperature setting of 25 °C. Chemical shifts were measured with respect to TMS (δ = 0 ppm). FTIR experiments were evaluated on a Nicolet iS50 FT-IR instrument using an ATR diamond. GPC was performed using a Waters 1515 isocratic pump with a Waters 2410 refractive index detector using THF as the solvent at 35 °C with a flow rate of 1.0 mL/min. Molecular weights of polymers were measured reference to polystyrene standards. UV–visible and fluorescence spectra

were recorded on a Cary 5000 UV–VIS NIR spectrophotometer and a Cary Eclipse fluorescence spectrophotometer, respectively. UV–visible and fluorescence measurements were obtained using polymer solutions in $CHCl_3$, and thin films were drop-casted from these solutions.

Cyclic voltammetry (CV) was performed on a BASI CV-50W Version 2.3 instrument with 0.1 M tetrabutylammonium hexafluorophosphate as the supporting electrolyte in dry acetonitrile using a glassy carbon working electrode, platinum wire as the counter electrode, and Ag/AgCl as the reference electrode with a scan rate of 100 mV s^{-1}. The CV experiment was performed by drop-casting a thin film of the polymer on the glassy carbon working electrode.

The TGA measurements were performed using a high-resolution thermogravimetric analyzer TA instrument Model Q-50, within the temperature interval of 30–800 °C, with a heating rate of 20 °C min^{-1} under a continuous nitrogen flow. DSC was performed using a TA Instruments Model Q-2000 from -80 °C to 300 °C at a heating rate of 3 °C min^{-1} in a modulated mode. The second thermal cycle (cooling cycle) was chosen to observe the thermal transitions in polymers. All DSC runs were performed under a nitrogen atmosphere.

Quantum yield measurements were performed for PIF 1 and PIC polymers in dilute $CHCl_3$ solutions with absorbance ranging from 0.01 to 0.04. Quinine sulfate was used as the reference. An excitation wavelength of 313 nm was used to obtain the fluorescence spectra for each solution ranging from 320 nm to 600 nm. The fluorescence intensity (area of the fluorescence spectrum) was then calculated and recorded. (**Table 3.6**) Quantum yields were calculated[41] using the following equation: $\phi_s = \phi(A_r F_s / A_s F_r)(n_s^2/n_r^2)$. ϕ_r is 0.51, A_s *and* A_r are absorbances of the sample and reference solutions, respectively. At the same excitation wavelength, F_s *and* F_r are the corresponding relative integrated fluorescence intensities, n is the refractive index [$CHCl_3$ (n_s = 1.445) and 1 N H_2SO_4 (n_r = 1.339) were used].

Table 3.6. Quantum yield experimental data

Sample	Absorbance	Fluorescence intensity	Emission maximum (nm)
Standard	0.012	40867	455
	0.016	45825	
	0.020	53308	
	0.033	50703	
PIF 1	0.012	41956	416
	0.016	47279	
	0.020	51773	
	0.033	56239	
Standard	0.012	40867	455
	0.016	40667	
	0.020	51850	
	0.033	78520	
PIC	0.012	26419	417
	0.016	28602	
	0.020	35697	
	0.033	49948	

3.4.3. Synthesis procedures

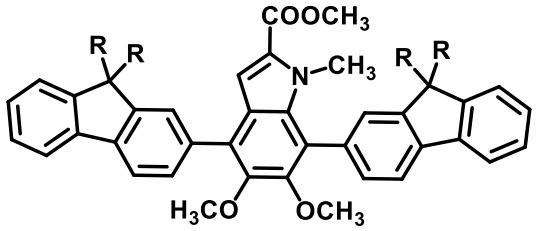

12

Methyl 4,7-bis(9,9-dioctyl-9*H*-fluoren-2-yl)-5,6-dimethoxy-1-methyl-1*H*-indole-2-carboxylate (12): In a 25-mL, oven-dried Schlenk flask were placed methyl 4,7-dibromo-5,6-dimethoxy-1-methyl-1*H*-indole-2-carboxylate (DBI) (350 mg, 0.86 mmol), 9,9-dioctylfluorene-2-

boronic acid pinacol ester (893 mg, 1.73 mmol) and K_2CO_3 (1.98 g , 14.33 mmol). The system was then kept under vacuum for 20 min followed purging with Ar for 15 min. Then, $Pd(PPh_3)_4$ (30 mg, 3 mol %) was added to the flask inside the glovebox, followed by dry THF (7 mL) and degassed water (7 mL). The reaction mixture was heated to reflux (90 °C) for 48 h under Ar atmosphere and then cooled to room temperature. Hydrochloric acid (6N, 30 mL) was added and stirred 15 min. The compound was extracted with chloroform (3 x 60 mL), washed with brine (2 x 50 mL) and dried with anhydrous Na_2SO_4. The solvent was evaporated and crude product was purified by silica column chromatography using the 10% ethyl acetate in hexanes as the eluent to give white solid. (620 mg, 70%). ^{1}H NMR (400 MHz, $CDCl_3$) δ 7.88 – 7.74 (m, 4H), 7.66 – 7.59 (m, 2H), 7.48 – 7.42 (m, 2H), 7.37 (q, *J* = 8.0, 6.7 Hz, 7H), 3.80 (s, 3H), 3.66 (d, *J* = 5.7 Hz, 6H), 3.54 (s, 3H), 2.03 (s, 8H), 1.28 – 0.96 (m, 48H), 0.86 – 0.70 (m, 12H). ^{13}C NMR (101 MHz, $CDCl_3$) δ 162.23, 151.05, 150.76, 150.64, 150.52, 150.31, 145.56, 140.99, 140.83, 140.73, 140.34, 134.73, 134.52, 133.69, 129.35, 129.06, 128.69, 128.13, 127.26, 127.06, 126.88, 126.79, 125.22, 124.95, 122.96, 122.85, 121.18, 119.80, 119.72, 119.42, 119.21, 111.00, 77.34, 77.22, 77.02, 76.70, 61.21, 61.06, 55.15, 51.42, 40.68, 40.58, 40.53, 34.84, 31.80, 30.16, 30.13, 30.06, 29.38, 29.33, 29.28, 29.23, 23.94, 23.86, 22.61, 22.59, 14.07.

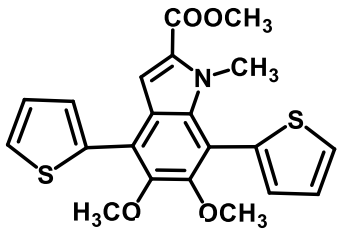

13

Methyl 5,6-dimethoxy-1-methyl-4,7-di(thiophen-2-yl)-1*H*-indole-2-carboxylate (13): In a 100-mL, oven-dried, 1-NRB was added methyl 4,7-dibromo-5,6-dimethoxy-1-methyl-1H-indole-2-carboxylate (DBI) (500 mg, 1.23 mmol), 2-(tributylstannyl)thiophene (1145 mg, 3.07 mmol), $Pd_2(dba)_3$ (34 mg, 3 mol %) and P(*o*-tol)$_3$ (67 mg , 0.22 mmol) inside the glovebox. The flask was equipped with a condenser with a septum on the top. Outside the glovebox, Toluene (20 mL) was

added to the reaction through the septum. The reaction mixture was heated to reflux (110 °C) for 24 h under Ar atmosphere then cooled to room temperature. DI water (60 mL) was added to the reaction mixture and the compound was extracted with ethyl acetate (3 x 60 mL), washed with brine (2 x 50 mL) and dried with anhydrous Na_2SO_4. The solvent was evaporated and the crude product was purified by silica column chromatography using the 4% ethyl acetate in hexanes as the eluent to give a white solid. (406 mg, 80%). ^{1}H NMR (400 MHz, $CDCl_3$) δ 7.49 (s, 4H), 7.21 (s, 1H), 7.17 (s, 1H), 7.11 (s, 1H), 3.83 (d, *J* = 21.7 Hz, 9H), 3.60 (s, 3H).^{13}C NMR (101 MHz, $CDCl_3$) δ 162.17, 151.92, 145.31, 136.08, 135.40, 134.81, 129.38, 129.30, 128.03, 126.82, 126.78, 126.74, 126.40, 122.17, 121.83, 113.09, 111.23, 77.33, 77.22, 77.02, 76.70, 61.80, 61.02, 51.62, 33.88.

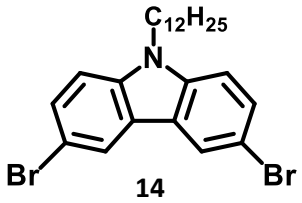

14

2,7-Dibromo-9-dodecyl-9*H*-carbazole (14): 2,7-dibromo-9*H*-carbazole (500 mg, 1.538 mmol) were measured in to 250 mL 3NRB and dry DMF (25.0 mL) was added with stirring until the solid dissolved. Then, the 3-NRB was kept in an ice bath. Sodium hydride was added in excess to the reaction solution and which was stirred for 30 minutes until no more bubbles released. 1-Bromododecane (0.41 mL, 1.692 mmol) was added dropwise to the reaction and stirred for 18h at rt. The reaction was worked up by adding excess DI water (200.0 mL) and extracting with ethyl acetate (3 x 50 mL). The ethyl acetate layer was washed with brine (2 x 50 mL) and dried with Na_2SO_4. The solvent was evaporated and the product was purified by silica column chromatography using hexanes as the eluent to give a white solid **14** (583 mg, 78 %). ^{1}H NMR (400 MHz, $CDCl_3$) δ 8.07 (s, 2H), 7.49 (s, 2H), 7.21 (s, 2H), 4.17 (s, 2H), 1.75 (s, 2H), 1.19 (d, *J* = 31.2 Hz, 20H), 0.80 (s, 3H). ^{13}C NMR (101 MHz, $CDCl_3$) δ 139.32, 129.00, 123.26, 111.92, 110.41, 77.33, 77.33, 77.02, 76.70, 43.37, 31.91, 29.58, 29.45, 29.33, 28.84, 27.22, 22.69, 14.14.

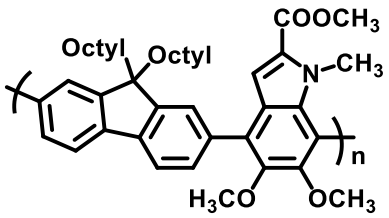

PIF 1

Poly(indoylene-*co*-dioctylfluorene) (PIF 1): To a 25-mL, oven-dried Schlenk flask was added methyl 4,7-dibromo-5,6-dimethoxy-1-methyl-1*H*-indole-2-carboxylate (DBI) (100 mg, 0.24 mmol), 9,9-dioctylfluorene-2,7-diboronic acid bis(1,3-propanediol) ester (141 mg, 0.24 mmol) and K_2CO_3 (566 mg , 4.09 mmol) which was then kept under vacuum for 20 min, followed by Ar purged for 15 min. Then $Pd(PPh_3)_4$ (14 mg, 5 mol %) was added added to the flask inside the glovebox. Then dry THF (4 mL) and degassed water (4 mL) were added to the flask. The reaction mixture was heated to reflux for 48 h under Ar atmosphere and then cooled to room temperature. Hydrochloric acid (6N, 15 mL) was added and the mixture was stirred 15 min. The polymer was extracted with chloroform (3 x 40 mL), washed with brine (2 x 50 mL) and dried with anhydrous Na_2SO_4. The solvent was evaporated and the solid was redissolved in THF (2 mL).The solution was poured dropwise into methanol (25 mL) to precipitate the polymer. The resulting precipitate was redissolved in chloroform (2 mL) and reprecipitated in methanol (25 mL). The off white polymer PIF 1 was collected and subjected to high vacuum. The final product of PIF 1 was collected (122 mg, 78%). ^{1}H NMR (400 MHz, Chloroform-*d*) δ 7.93 (s, 2H), 7.70 (s, 2H), 7.53 (s, 2H), 7.29 (d, *J* = 22.3 Hz, 2H), 3.83 (s, 3H), 3.71 (s, 6H), 3.55 (s, 3H), 2.09 (s, 4H), 1.13 (s, 23H), 0.82 (s, 11H). ^{13}C NMR (101 MHz, $CDCl_3$) δ 162.25, 150.67, 145.61, 140.64, 140.23, 134.78, 134.01, 133.72, 129.53, 129.13, 128.84, 128.69, 125.31, 125.03, 123.00, 121.18, 119.42, 77.32, 77.00, 61.25, 55.29, 51.46, 40.88, 34.91, 31.80, 30.17, 29.52, 29.47, 29.27, 24.05, 22.59, 14.05. M_n= 18.8 kDa and PDI = 1.99.

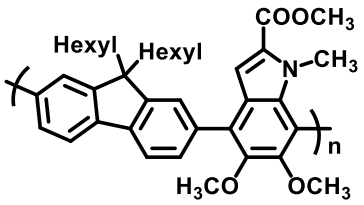

PIF 2

Poly(indoylene-*co*-dihexylfluorene) (PIF 2): PIF 2 was synthesized according to the same procedure as for PIF 1 using DBI (100 mg, 0.25 mmol), 9,9-Dihexylfluorene-2,7-diboronic acid bis(1,3-propanediol) ester (123.0 mg, 0.25 mmol), K_2CO_3 (566 mg , 4.09 mmol) and $Pd(PPh_3)_4$ (14 mg, 5 mol %) with THF (4 mL) and distilled water (4 mL). An off white precipitate of PIF 2 was resulted. (116 mg, 82%). ^{1}H NMR (400 MHz, $CDCl_3$) δ 7.93 (s, 1H), 7.70 (s, 2H), 7.54 (s, 2H), 7.30 (d, *J* = 7.5 Hz, 2H), 3.84 (s, 3H), 3.71 (s, 6H), 3.60 (s, 3H), 1.55 (s, 4H), 1.25 (s, 1H), 1.14 (s, 8H), 0.78 (s, 8H). M_n= 20.9 kDa and PDI = 2.43.

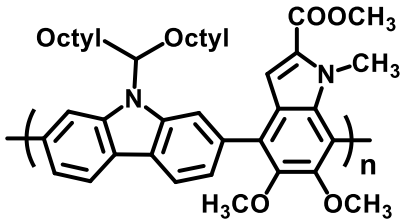

PIC

Poly(indoylenecarbazole) (PIC) : PIC was also synthesized according to the same procedure as for PIF 1 using DBI (49.5 mg, 0.14 mmol), 9-(Heptadecan-9-yl)-2,7-bis(4,4,5,5-tetramethyl-1,3,2-dioxaborolan-2-yl)-9H-carbazole (80.0 mg, 0.14 mmol), K_2CO_3 (280 mg , 2.28 mmol) and $Pd(PPh_3)_4$ (7 mg, 5 mol %) with THF (3.1 mL) and distilled water (3.1 mL). An off white precipitate of PIC was resulted. (57 mg, 64%) ^{1}H NMR (400 MHz, $CDCl_3$) δ 8.31 (s, 2H), 7.87 (d, *J* = 70.4 Hz, 2H), 7.59 (s, 1H), 7.38 (d, *J* = 8.7 Hz, 2H), 4.66 (s, 1H), 3.78 (d, *J* = 25.9 Hz, 6H), 3.51 (s, 3H), 2.40 (s, 2H), 1.97 (s, 2H), 1.15 (s, 20H), 0.81 (s, 6H).^{13}C NMR (101 MHz, $CDCl_3$) δ 162.18, 159.76, 150.71, 145.60, 142.07, 138.97, 134.85, 129.07, 128.44, 123.12, 121.67, 119.79, 111.15, 77.23, 77.11, 76.91, 76.80, 76.60, 61.34, 61.10, 51.33, 34.46, 33.76, 31.68, 31.65, 29.34, 29.11, 29.07, 26.94, 22.50, 13.95. M_n= 11.0 kDa and PDI = 3.65.

3.4.4. Spectra

^{1}H NMR of compound **12**

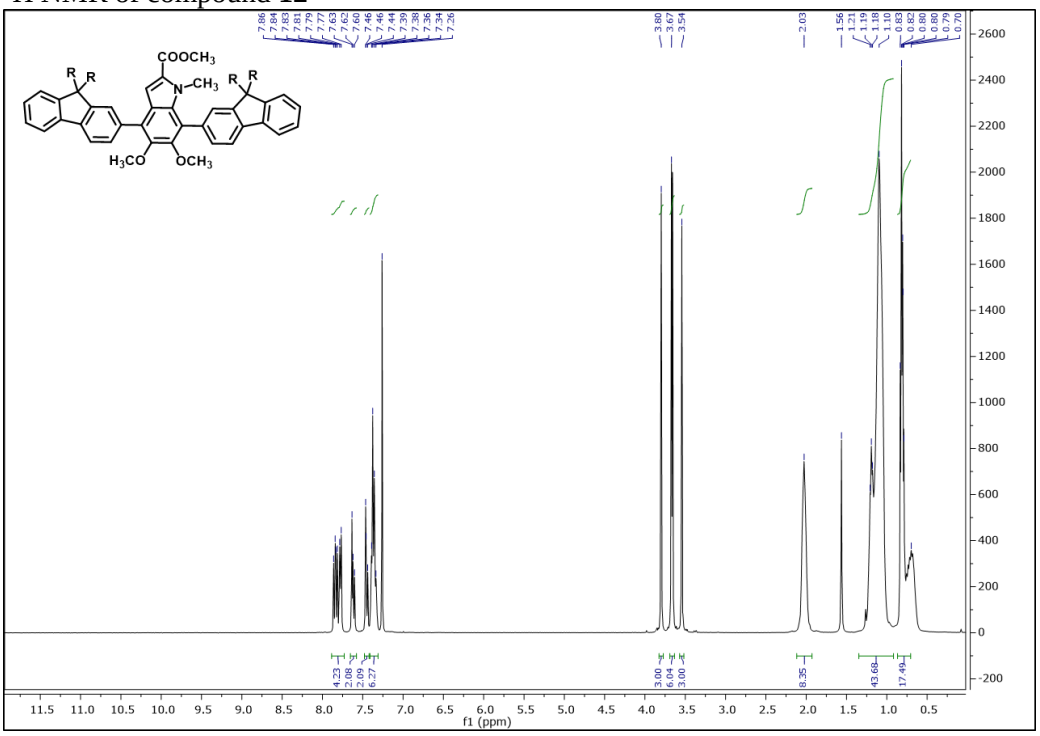

^{13}C NMR of compound **12**

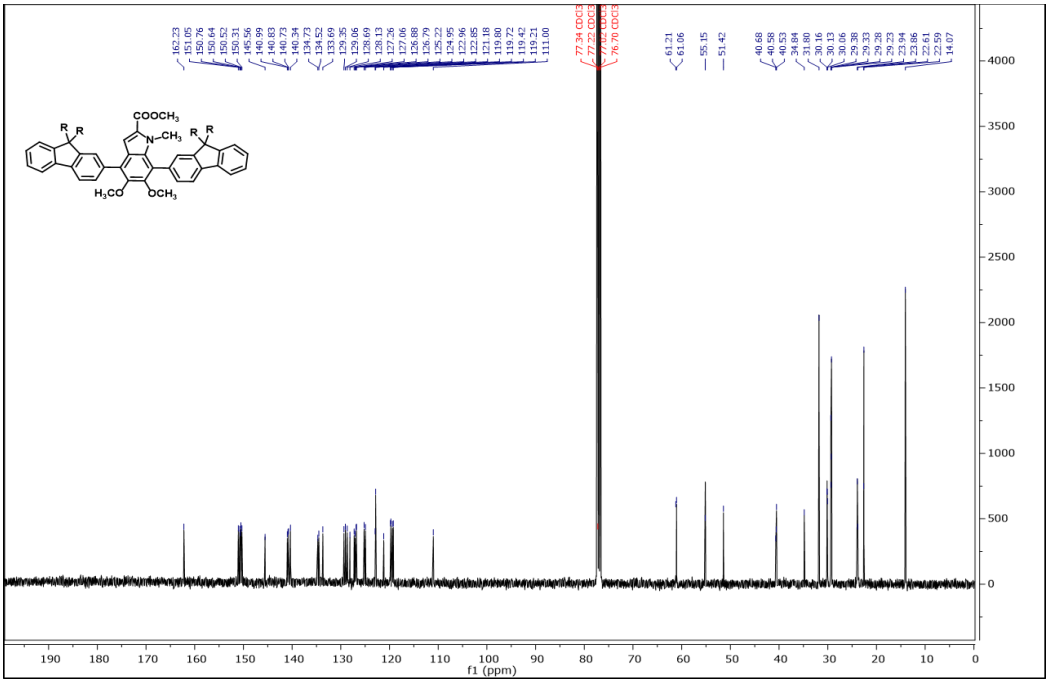

^{1}H NMR of compound **13**

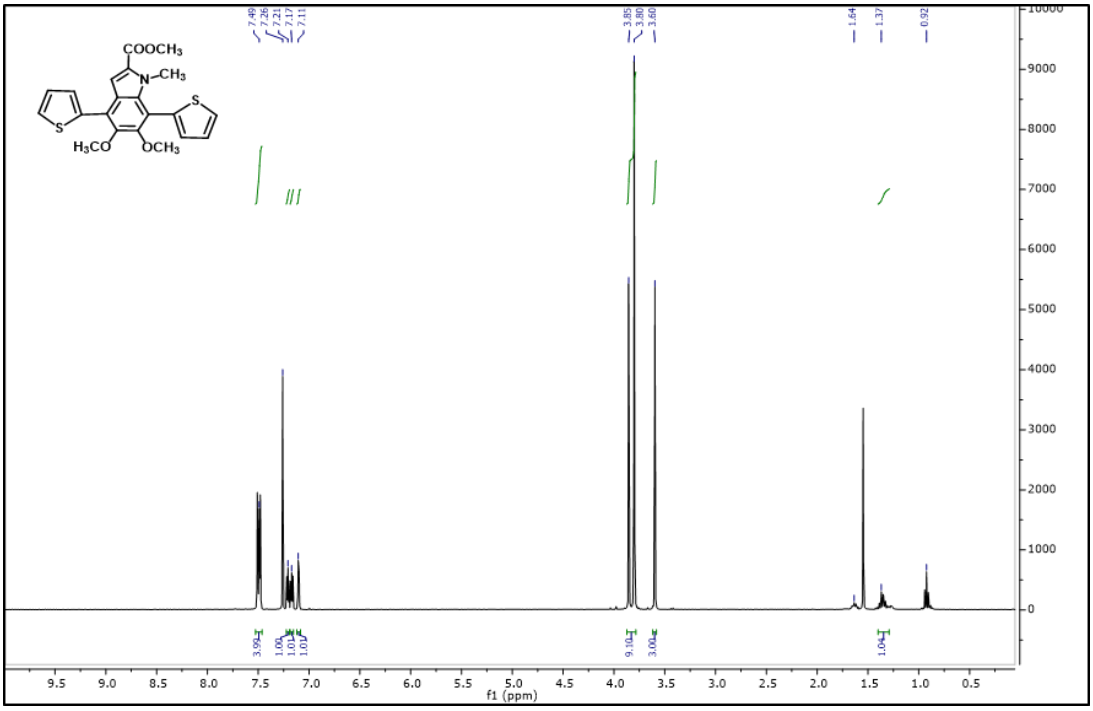

^{13}C NMR of compound **13**

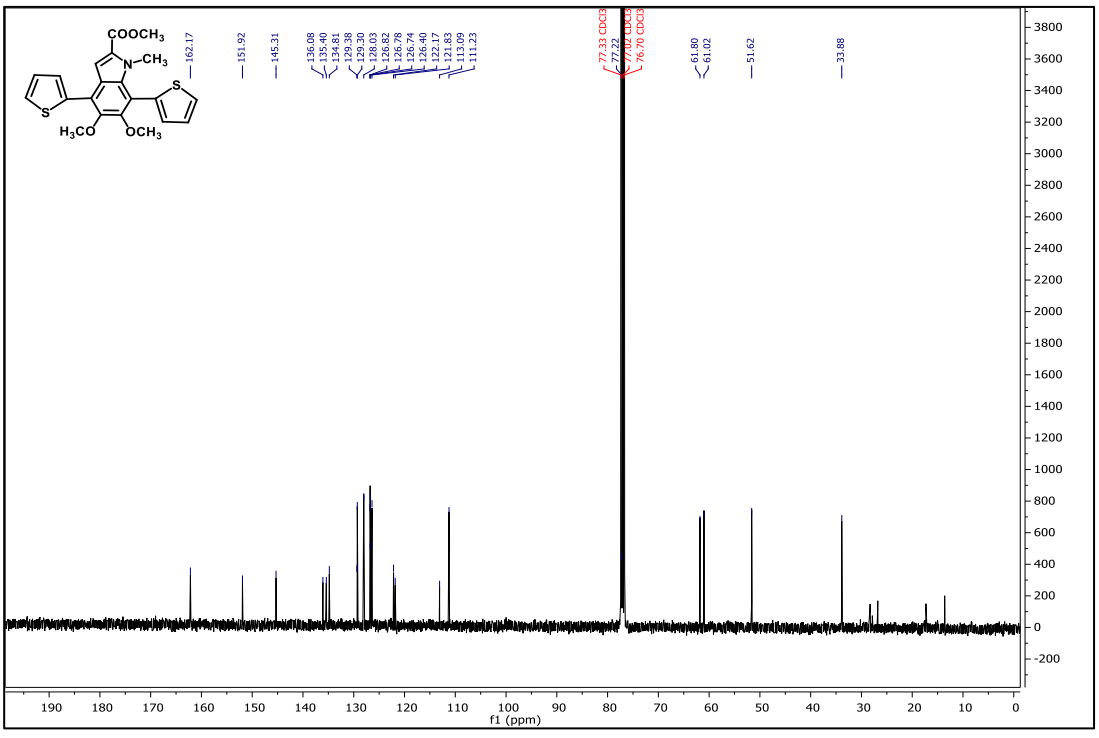

^{1}H NMR of compound **14**

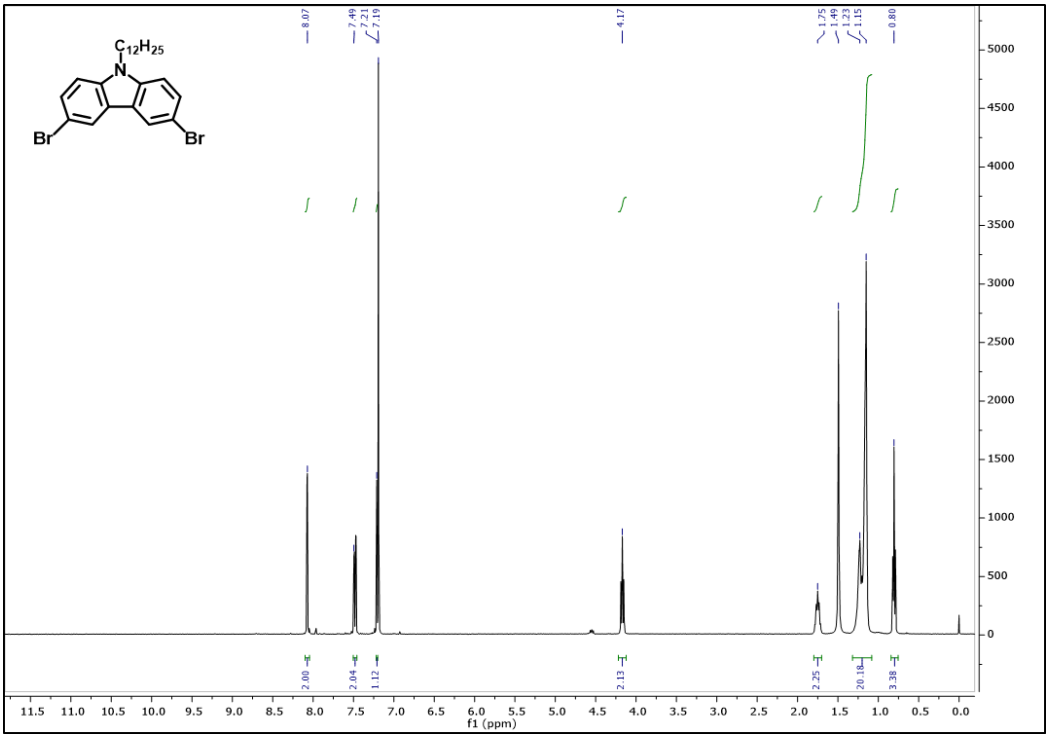

^{13}C NMR of compound **14**

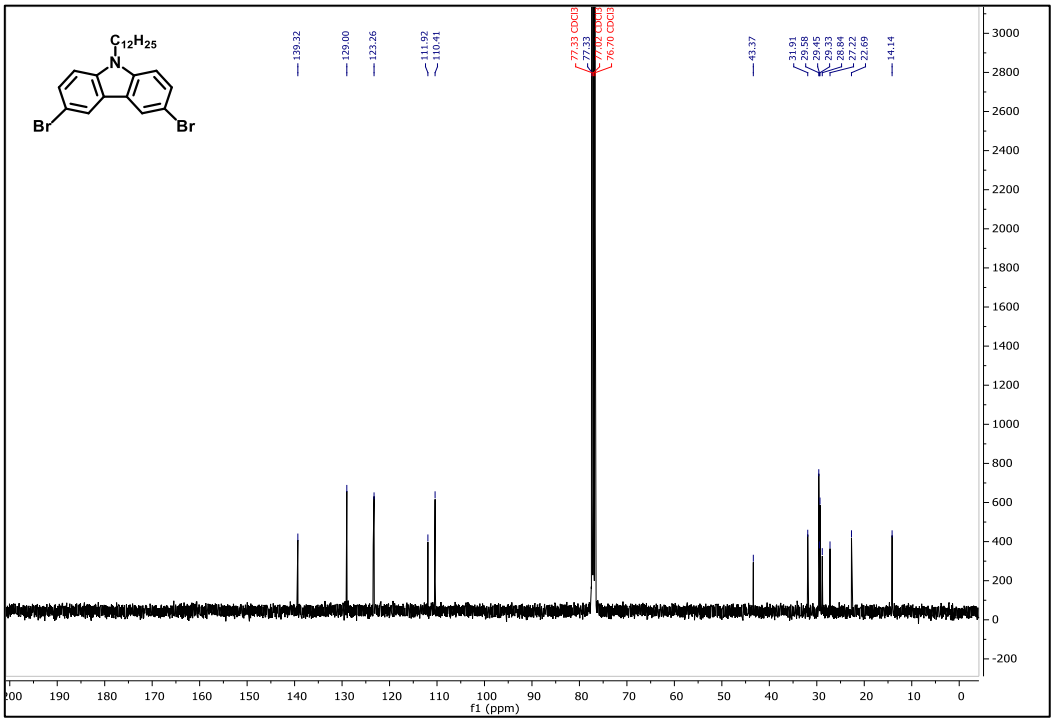

^{1}H NMR of PIF 1

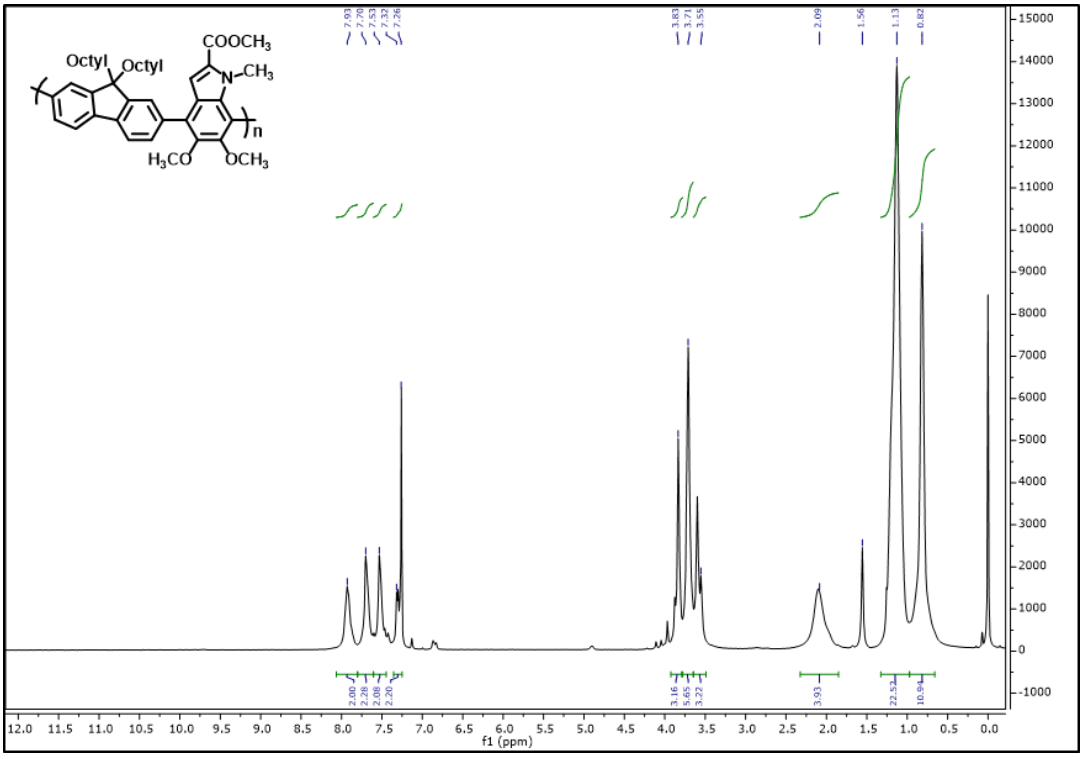

^{13}C NMR of PIF 1

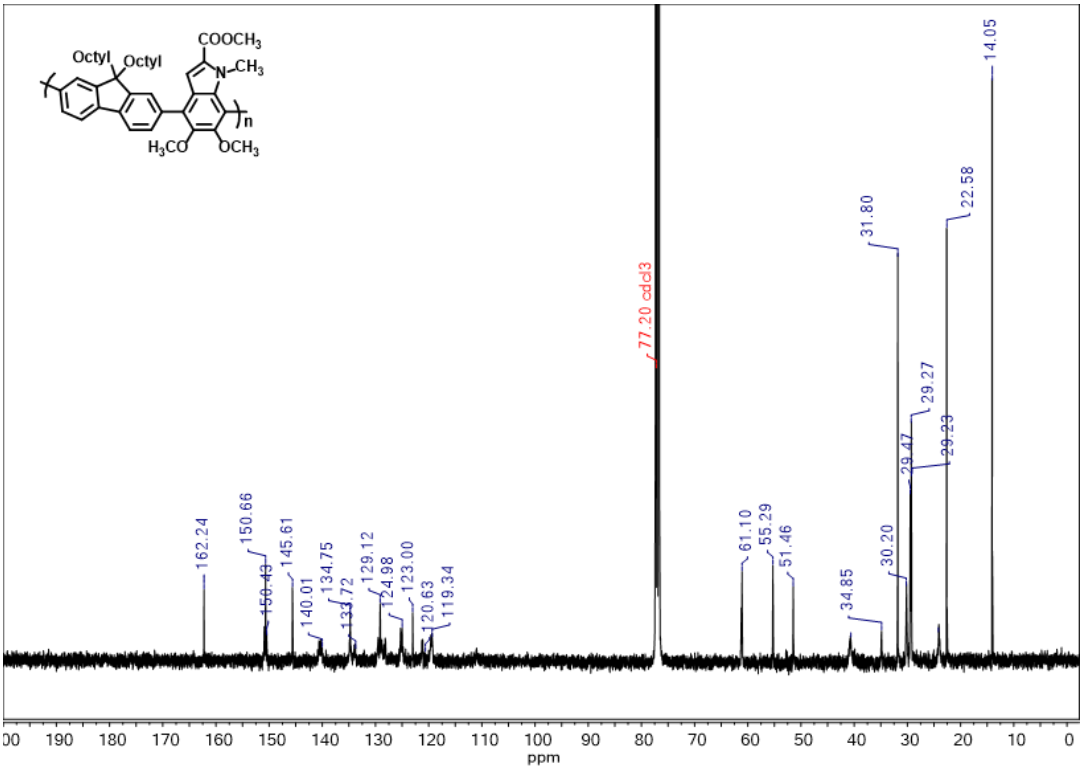

^{1}H NMR of PIF 2

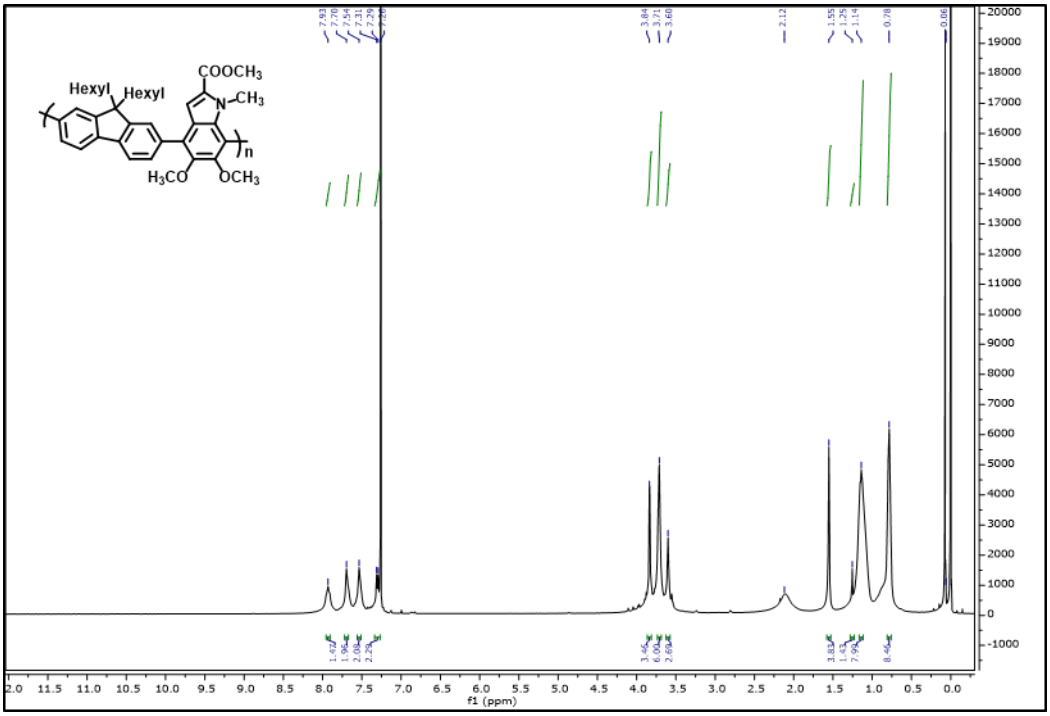

^{1}H NMR of PIC

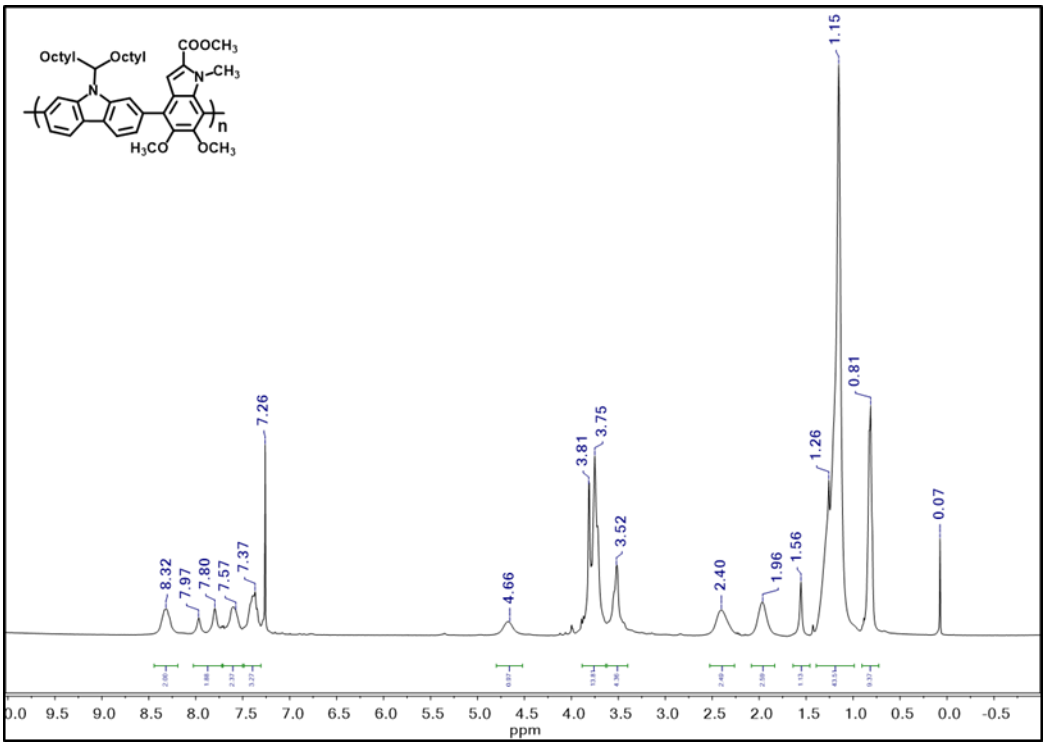

^{13}C NMR of PIC

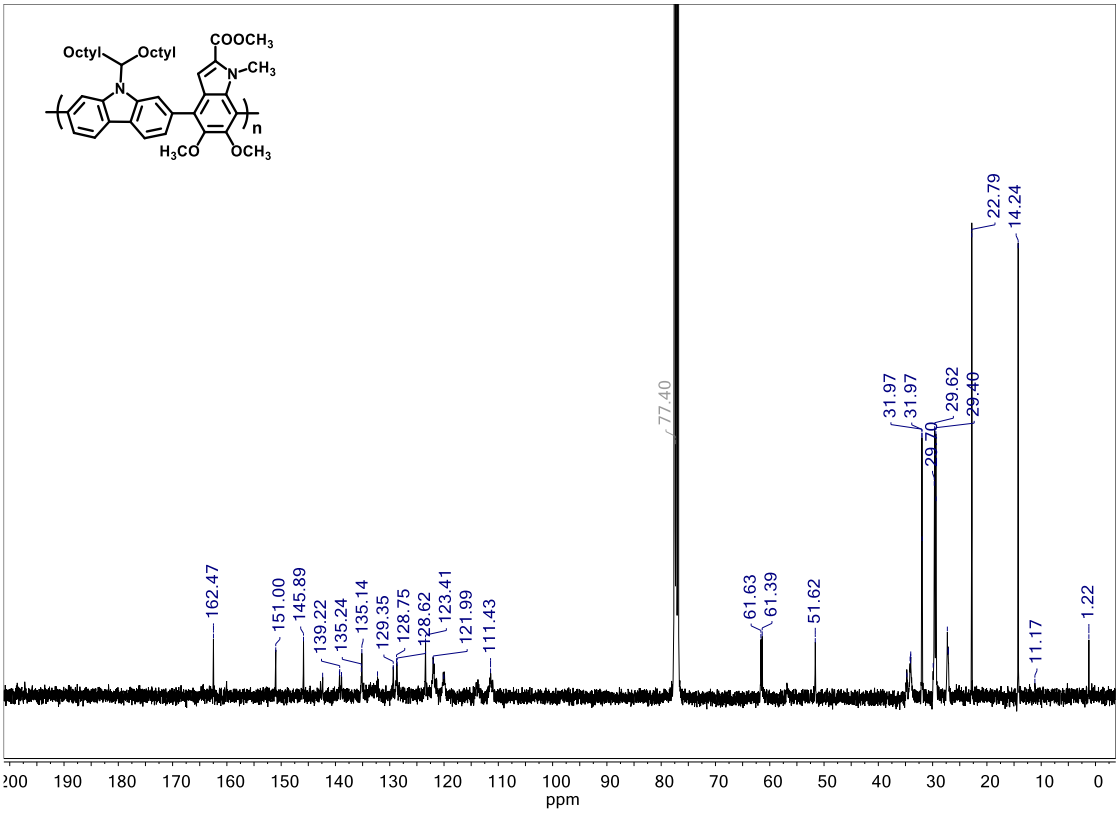

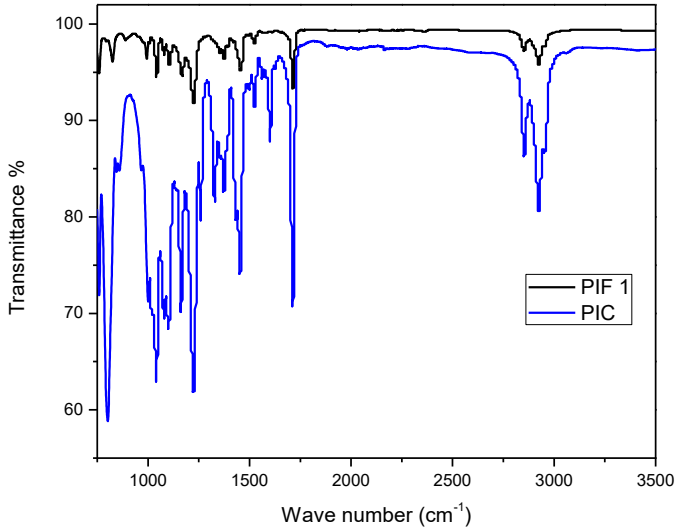

Figure 3.8. FTIR spectra of PIF 1 and PIC

3.5. REFERENCES

1. Forrest, S. R., The path to ubiquitous and low-cost organic electronic appliances on plastic. *Nature* **2004,** *428* (6986), 911-918.
2. Shirota, Y., Organic materials for electronic and optoelectronic devices. *Journal of Materials Chemistry* **2000,** *10* (1), 1-25.
3. Burroughes, J.; Bradley, D.; Brown, A.; Marks, R.; Mackay, K.; Friend, R.; Burns, P.; Holmes, A., Light-emitting diodes based on conjugated polymers. *Nature* **1990,** *347* (6293), 539-541.
4. AlSalhi, M. S.; Alam, J.; Dass, L. A.; Raja, M., Recent advances in conjugated polymers for light emitting devices. *International Journal of Molecular Sciences* **2011,** *12* (3), 2036-2054.
5. Facchetti, A., π-Conjugated polymers for organic electronics and photovoltaic cell applications. *Chemistry of Materials* **2011,** *23* (3), 733-758.
6. Moliton, A.; Hiorns, R. C., Review of electronic and optical properties of semiconducting π-conjugated polymers: applications in optoelectronics. *Polymer International* **2004,** *53* (10), 1397-1412.
7. Hu, L.; Yang, Y.; Xu, J.; Liang, J.; Guo, T.; Zhang, B.; Yang, W.; Cao, Y., Blue light-emitting polymers containing fluorene-based benzothiophene-S,S-dioxide derivatives. *Journal of Materials Chemistry C* **2016,** *4* (6), 1305-1312.
8. Liu, C.; Fu, Q.; Zou, Y.; Yang, C.; Ma, D.; Qin, J., Low turn-on voltage, high-power-efficiency, solution-processed deep-blue organic light-emitting diodes based on starburst oligofluorenes with diphenylamine end-capper to enhance the HOMO level. *Chemistry of Materials* **2014,** *26* (10), 3074-3083.
9. Sergent, A.; Zucchi, G.; Pansu, R. B.; Chaigneau, M.; Geffroy, B.; Tondelier, D.; Ephritikhine, M., Synthesis, characterization, morphological behaviour, and photo- and electroluminescence of highly blue-emitting fluorene-carbazole copolymers with alkyl side-chains of different lengths. *Journal of Materials Chemistry C* **2013,** *1* (19), 3207-3216.
10. Xu, J.; Yu, L.; Hu, L.; He, R.; Yang, W.; Peng, J.; Cao, Y., Color tuning in inverted blue light-emitting diodes based on a polyfluorene derivative by adjusting the thickness of the light-emitting layer. *Journal of Materials Chemistry C* **2015,** *3* (38), 9819-9826.
11. Kim, S. H.; Jang, J.; Lee, J. Y., High efficiency phosphorescent organic light-emitting diodes using carbazole-type triplet exciton blocking layer. *Applied Physics Letters* **2007,** *90* (22), 223505.
12. Lee, W.-Y.; Chen, C.-W.; Chueh, C.-C.; Yang, C.-C.; Chen, W.-C., Synthesis of new fluorene-indolocarbazole alternating copolymers for light-emitting diodes and field effect transistors. *Polym. J. (Tokyo, Jpn.)* **2008,** *40* (3), 249-255.
13. Svetlichnyi, V. M.; Alexandrova, E. L.; Miagkova, L. A.; Matushina, N. V.; Nekrasova, T. N.; Tameev, A. R.; Stepanenko, S. N.; Vannikov, A. V.; Kudryavtsev, V. V., Photophysical properties of indolo[3,2-b]carbazoles as a promising class of optoelectronic materials. *Semiconductors* **2010,** *44* (12), 1581-1587.
14. Cho, M. J.; Kim, S. J.; Yoon, S. H.; Shin, J.; Hong, T. R.; Kim, H. J.; Son, Y. H.; Kang, J. S.; Um, H. A.; Lee, T. W.; Bin, J.-K.; Lee, B. S.; Yang, J. H.; Chae, G. S.; Kwon, J. H.; Choi, D. H., New bipolar host materials for realizing blue phosphorescent organic light-emitting diodes with high efficiency at 1000 cd/m2. *ACS Applied Materials & Interfaces* **2014,** *6* (22), 19808-19815.
15. Wang, Z.; Liu, W.; Xu, C.; Ji, B.; Zheng, C.; Zhang, X., Excellent deep-blue emitting materials based on anthracene derivatives for non-doped organic light-emitting diodes. *Optical Materials* **2016,** *58*, 260-267.
16. Cook, J. H.; Santos, J.; Al-Attar, H. A.; Bryce, M. R.; Monkman, A. P., High brightness deep blue/violet fluorescent polymer light-emitting diodes (PLEDs). *Journal of Materials Chemistry C* **2015,** *3* (37), 9664-9669.

17. Jeong, S. H.; Lee, J. Y., Dibenzothiophene derivatives as host materials for high efficiency in deep blue phosphorescent organic light emitting diodes. *Journal of Materials Chemistry* **2011,** *21* (38), 14604-14609.
18. Wettach, H.; Jester, S. S.; Colsmann, A.; Lemmer, U.; Rehmann, N.; Meerholz, K.; Höger, S., Deep blue organic light-emitting diodes based on triphenylenes. *Synthetic Metals* **2010,** *160* (7), 691-700.
19. Hwu, J. R.; Hsu, Y. C.; Josephrajan, T.; Tsay, S.-C., Fine tuning of blue photoluminescence from indoles for device fabrication. *Journal of Materials Chemistry* **2009,** *19* (19), 3084-3090.
20. Lee, C. W.; Lee, J. Y., Above 30% External quantum efficiency in blue phosphorescent organic light-emitting diodes using pyrido[2,3-b]indole derivatives as host materials. *Advanced Materials* **2013,** *25* (38), 5450-5454.
21. Garrote Cañas, A. M.; Martsinovich, N.; Sergeeva, N. N., π-Conjugated indole dyads with strong blue emission made possible by stille cross-coupling and double fischer indole cyclisation. *ChemistrySelect* **2017,** *2* (8), 2433-2438.
22. Park, M. S.; Lee, J. Y., An indole derivative as a high triplet energy hole transport material for blue phosphorescent organic light-emitting diodes. *Thin Solid Films* **2013,** *548*, 603-607.
23. Kim, D. Y.; Kim, Y. S.; Lee, S. E.; Kim, Y. K.; Yoon, S. S., 9,10-Diphenylanthracene derivative substituted with indole moiety for blue organic light-emitting diodes. *Molecular Crystals and Liquid Crystals* **2017,** *644* (1), 197-204.
24. Sharma, V.; Kumar, P.; Pathak, D., Biological importance of the indole nucleus in recent years: A comprehensive review. *Journal of Heterocyclic Chemistry* **2010,** *47* (3), 491-502.
25. Zhang, M.-Z.; Chen, Q.; Yang, G.-F., A review on recent developments of indole-containing antiviral agents. *Eur. J. Med. Chem.* **2015,** *89*, 421-441.
26. Lee, Y.-J.; Han, Y.-R.; Park, W.; Nam, S.-H.; Oh, K.-B.; Lee, H.-S., Synthetic analogs of indole-containing natural products as inhibitors of sortase A and isocitrate lyase. *Bioorg. Med. Chem. Lett.* **2010,** *20* (23), 6882-6885.
27. Wolbarsht, M. L.; Walsh, A. W.; George, G., Melanin, a unique biological absorber. *Appl. Opt.* **1981,** *20* (13), 2184-2186.
28. Watt, A. A. R.; Bothma, J. P.; Meredith, P., The supramolecular structure of melanin. *Soft Matter* **2009,** *5* (19), 3754-3760.
29. Prota, G., CHAPTER 5 - EUMELANINS. In *Melanins and Melanogenesis*, Academic Press: San Diego, 1992; pp 88-118.
30. Pezzella, A.; Wünsche, J., Eumelanin: An Old Natural Pigment and a New Material for Organic Electronics – Chemical, Physical, and Structural Properties in Relation to Potential Applications. In *Organic Electronics*, Wiley-VCH Verlag GmbH & Co. KGaA: 2013; pp 113-137.
31. d'Ischia, M.; Napolitano, A.; Pezzella, A.; Land, E. J.; Ramsden, C. A.; Riley, P. A., 5,6-Dihydroxyindoles and Indole-5,6-diones. In *Adv. Heterocycl. Chem.*, Alan, R. K., Ed. Academic Press: 2005; Vol. Volume 89, pp 1-63.
32. Meredith, P.; Sarna, T., The physical and chemical properties of eumelanin. *Pigment Cell Res.* **2006,** *19* (6), 572-594.
33. d'Ischia, M.; Napolitano, A.; Pezzella, A.; Meredith, P.; Sarna, T., Chemical and structural diversity in eumelanins – unexplored bio-optoelectronic materials. *Angewandte Chemie (International ed. in English)* **2009,** *48* (22), 3914-3921.
34. D'Ischia, M.; Crescenzi, O.; Pezzella, A.; Arzillo, M.; Panzella, L.; Napolitano, A.; Barone, V., Structural effects on the electronic absorption properties of 5,6-dihydroxyindole oligomers: the potential of an integrated experimental and DFT approach to model eumelanin optical properties. *Photochem. Photobiol.* **2008,** *84* (3), 600-607.
35. Meredith, P.; Riesz, J., Radiative relaxation quantum yields for synthetic eumelanin. *Photochem. Photobiol.* **2004,** *79* (2), 211-216.

36. Selvaraju, S.; Niradha Sachinthani, K. A.; Hopson, R. A.; McFarland, F. M.; Guo, S.; Rheingold, A. L.; Nelson, T. L., Eumelanin-inspired core derived from vanillin: a new building block for organic semiconductors. *Chemical Communications* **2015,** *51* (14), 2957-2959.
37. Adhikari, S.; Hopson, R. A.; Sedai, B. R.; McFarland, F. M.; Guo, S.; Nelson, T. L., Synthesis and characterization of eumelanin-inspired poly(indoylenearylenevinylene)s and poly(indoylenearyleneethynylene)s. *Journal of Polymer Science Part A: Polymer Chemistry* **2017,** *55* (3), 457-463.
38. Tekin, E.; Egbe, D. A. M.; Kranenburg, J. M.; Ulbricht, C.; Rathgeber, S.; Birckner, E.; Rehmann, N.; Meerholz, K.; Schubert, U. S., Effect of side chain length variation on the optical properties of PPE-PPV hybrid polymers. *Chemistry of Materials* **2008,** *20* (8), 2727-2735.
39. Duan, C.; Willems, R. E. M.; van Franeker, J. J.; Bruijnaers, B. J.; Wienk, M. M.; Janssen, R. A. J., Effect of side chain length on the charge transport, morphology, and photovoltaic performance of conjugated polymers in bulk heterojunction solar cells. *Journal of Materials Chemistry A* **2016,** *4* (5), 1855-1866.
40. Yu, C.-Y.; Shih, T.-Y., Alternating copolymers containing fluorene and oxadiazole derivatives for fluorescent chemosensors. *Synthetic Metals* **2014,** *191*, 12-18.
41. Crosby, G. A.; Demas, J. N., Measurement of photoluminescence quantum yields. Review. *The Journal of Physical Chemistry* **1971,** *75* (8), 991-1024.

CHAPTER IV

ELECTROGENERATED-CHEMILUMINESCENCE AND ORGANIC LIGHT EMITTING DIODES OF DEEP BLUE EMITTING EUMELANIN-INSPIRED POLYARYLENES

4.1. INTRODUCTION

Organic light emitting diodes (OLEDs) have attracted significant attention due to their application in full-color flat-panel displays and the next generation energy saving solid state lightning.[1-5] In OLEDs, among the three primary color emitters are red, green and blue. There is a high demand for blue emitting materials due to the lower device stability, efficiency and color purity. According to the National Television System Committee (NTSC) standards, Commission Internationale de l'Eclairage (CIE) coordinates of the blue electroluminescence for the full color displays should be (0.14, 0.08).[4-6] Recently, OLEDs which emit from deep blue through the violet range of the spectrum have received much attention.[7-10] Deep blue light is necessary to achieve good color performance in white OLEDs for solid state lighting. It also provides greater color contrast and a wider color range in OLED displays. Although, many organic deep blue emitting materials have

been designed and synthesized, a need exists for new material with higher stability, efficiency and color purity to improve the performance of OLEDs.

Conjugated polymers having fluorenes and carbazoles are widely used in OLEDs due to their blue emitting properties.[7,11-14] Two novel eumelanin-inspired polyarylenes were synthesized by incorporating the eumelanin-inspired core with fluorene and carbazole units.With their characterization, these polymers showed interesting deep blue emitting properties. Their properties were further analyzed using a technique called electrogenerated chemiluminescence (ECL). In this technique, the oxidized and reduced (cationic and anionic) species are electrically generated on an electrode surface to form an excited state which will decay and lose the energy by emitting as light.[15-16] OLEDs were fabricated with eumelanin inspired polymers as the guest in two different host materials as the emissive layer. These devices emitted blue light as expected. The results of ECL analysis and the measurements of the blue OLEDs will be presented in this chapter.

4.2. ELECTRO-GENERATED CHEMILUMINESCENCE

4.2.1. Theory

ECL generally consists of a radical annihilation between a radical anion and a radical cation produced on an electrode surface to form an excited-state that emits light.[17-18] If this annihilation energy is sufficient to populate the singlet state, then the ECL generates an excited state via a singlet-singlet annihilation (S-route).[16] The excited state formed during ECL is the same as that in photoluminescence (PL). A proposed ECL generation mechanism for PIF 1 and PIC is shown below with P as the polymer [Eq. (1) – (4)]

$$\boldsymbol{P} + \boldsymbol{e}^{-} \rightarrow \boldsymbol{P}^{\cdot -} \qquad (1)$$

$$\boldsymbol{P} - \boldsymbol{e}^{-} \rightarrow \boldsymbol{P}^{\cdot +} \qquad (2)$$

$$P^{\cdot+} + P^{\cdot-} \rightarrow P^{*} \quad (3)$$

$$P^{*} \rightarrow P + h\nu \quad (4)$$

4.2.2. Results and Discussion

The ECL of PIF 1 and PIC polymers (**Scheme 4.1**) was studied to further understand their light emitting properties.

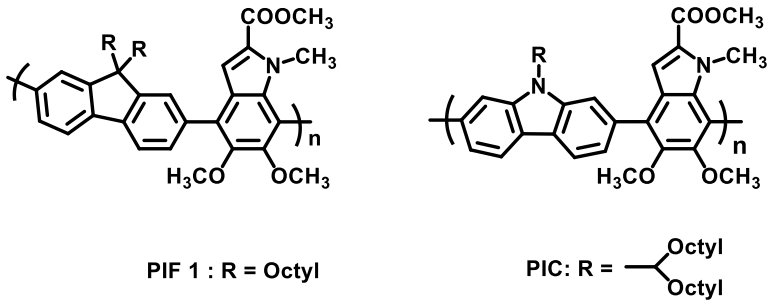

Figure 4.1. The structures of PIF 1 and PIC polymers

Since ECL generation required both the radical cation and the radical anion, ECL was only observed after the polymers were both reduced and oxidized. In **Figure 4.2**, the polymer thin films which were dropcasted from THF solutions on to the working electrode were first reduced by scanning to negative potentials (**1**) then oxidized by scanning to positive potentials (**2**). The oxidized species were relatively stable and therefore reacted with the reduced species after the ECL observed around 1.8 V vs. SCE (**3**) to produce an addition ECL emission around –1.2 V vs. SCE (**4**). PIF 1 showed a more intense ECL around -1.2 V vs. SCE compared to the PIC polymer.

As shown in **Figure 4.3**, the electrode potential was then stepped between 2 V and -2 V for 0.5 s to test ECL stability. During the first step, only one reagent species was formed, hence no ECL was observed. During the second step both oxidized and reduced species were present and they reacted to form an excited state that emitted blue light. The observed ECL intensity increased as more radical species were generated and it was relatively stable over the time.

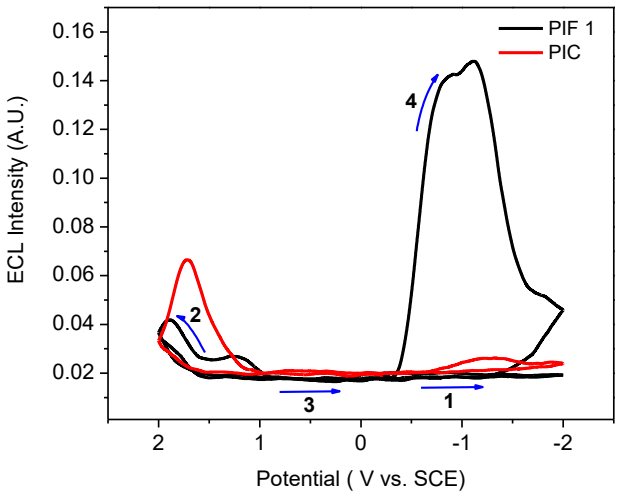

Figure 4.2. ECL spectra of 0.3 mg/mL of PIF 1 and PIC polymers dissolved in THF and drop casted on glassy carbon disk electrode. Potentials were scanned in the negative direction first and show two full cycles. Supporting electrolyte: 0.1 M $LiClO_4$ in acetonitrile.

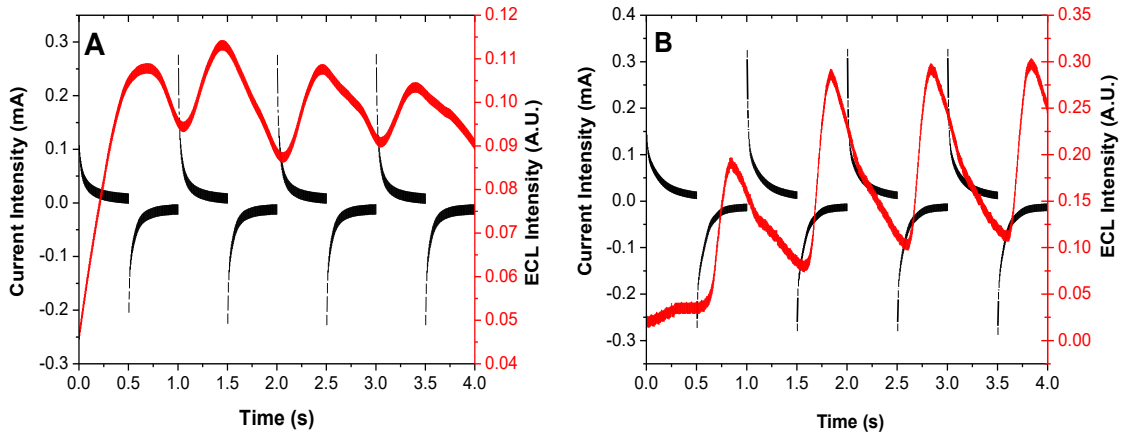

Figure 4.3. Current and ECL responses of 0.3 mg/mL (A) PIC and (B) PIF 1 polymers in acetonitrile with 0.1 M $LiClO_4$. Pulse width: 0.5 s at 650 V. Potential between 2 V and – 2 V. Both PIF and PIC polymers were dissolved in THF and drop casted on glassy carbon disk electrode.

ECL of these polymers in THF solutions was also investigated and spectra are shown in **Figure 4.4.** Both PIF 1 and PIC polymers emitted light after a complete cycle with both the oxidized and the reduced species, but the additional ECL around -1.2 V was not observed in both polymer solutions possibly due to the low stability of the generated species as well as mass transfer of these species in the electrolyte.

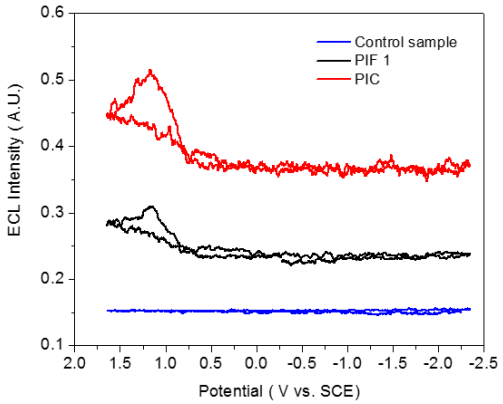

Figure 4.4. ECL spectra of 0.3 mg/mL of PIF 1 and PIC polymers dissolved in THF. Potentials were scanned in the negative direction first and show two full cycles. Supporting electrolyte: 0.1 M $TBAPF_6$ in THF.

Compared to the photoluminescence spectrum of PIF 1 (λ = 422 nm), the ECL spectrum showed a red-shifted emission (λ = 460 nm) (**Figure 4.5.**). The emission at a longer wavelength in the ECL spectrum could possibly be due to the formation of excimers after ion annihilation.[19] An excimer, which is an excited state dimer, is unstable in the ground state, and its emission usually resulted in structureless, broad peaks at longer wavelengths.[4]

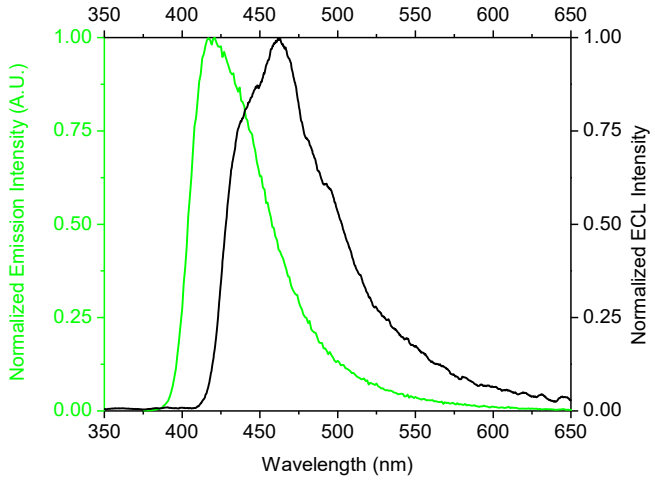

Figure 4.5. Emission spectra (green) and ECL spectra (black) of 0.3 mg/mL PIF 1 polymer recorded for 60 s by changing potential stepwise between 2 V and -2 V. Working electrode: Pt wire at a scan rate of 100 mV/s. Supporting electrolyte: 0.1 M $TBAPF_6$ in dichloromethane.

The ECL efficiency of PIF 1 (Φ_{ECL} = 6.1 %) and PIC (Φ_{ECL} = 0.4 %) was estimated using the following equation relative to the standard, 9,10 diphenylanthracene (DPA) having, a known efficiency (Φ_{ECL} = 8 %).[15] The spectral data of DPA are shown in **Figure 4.6.**

$$\emptyset_{ECL} = \frac{\frac{ECL\ Intensity}{Current\ intensity}(polymer\ sample)}{\frac{ECL\ intensity}{Current\ intensiy}(DPA\ sample)} \times 8\%\ (DPA\ \emptyset_{ECL})$$

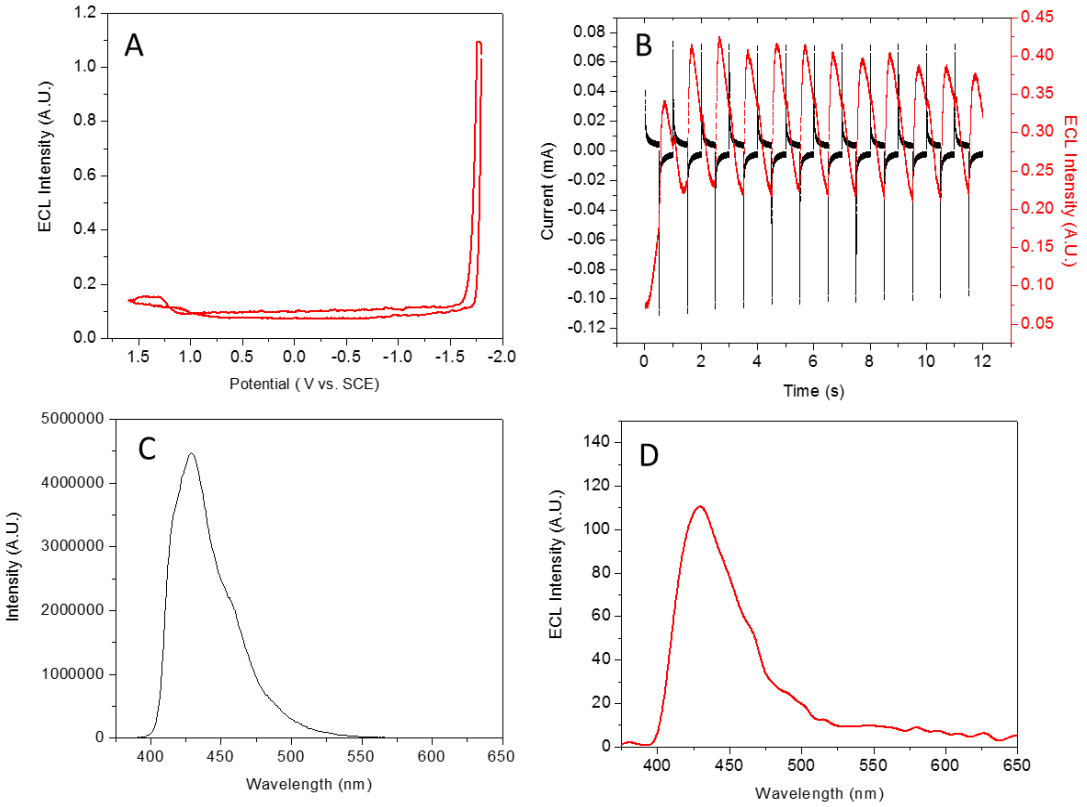

Figure 4.6. A). ECL spectrum of DPA B). Current and ECL response vs time graph C). Fluorescence spectrum D). ECL vs wavelength graph of 0.1 mM DPA in 0.1 M $TBAPF_6$ in acetonitrile

4.2.3. Experimental section

The PIF 1 and PIC polymers (0.3 mg/mL) were dissolved in THF or dichloromethane (DCM) and characterized electrochemically in solution or as a thin film drop casted on the working electrode. Electrochemical and ECL measurements were performed using a bipotentionstat CHI760C (CH

Instruments, Inc., Austin, TX) connected to a 1931C high performance low-power optical meter (Newport Corporation, Irvine, CA). The ECL signal was detected and amplified by a photomultiplier (PMT). A three electrode system was used and included a glassy carbon (GC) or a platinum (Pt) electrode as the working electrode, a graphite counter electrode, a silver wire as the reference electrode, 0.1 M lithium perchlorate ($LiClO_4$) or tetrabutylammonium hexafluorophosphate ($TBAPF_6$) as the supporting electrolyte and acetonitrile (ACN) as the solvent. The fluorescence spectra were measured using a fluoromax-3 (Jobin Yvon Horiba). The ECL signal was measured using a liquid nitrogen cooled digital CCD spectroscopy system (Acton Spec-10:100B Princeton Instruments, Trenton, NJ) coupled with an Acton SP2500 monochromator (Princeton Instruments, Trenton, NJ).

4.3. ORGANIC LIGTH EMITTING DIODE FABRICATION

4.3.1. Theory

OLEDs operate by the injection of electrons and holes from negative cathode and positive anode, respectively. These charges move forward to the electron transporting layer and a hole transporting layer. When these charges capture each other within the emissive layer, they recombine and form neutral bound excited state which is called exciton loses its energy as visible light which is emitted from the OLEDs.[20]

4.3.2. Results and Discussion

Since the ECL efficiency of PIC was very low compared to that of the PIF 1, only PIF 1 was used to fabricate OLEDs. The simple architecture of an OLED and the device structure of OLEDs fabricated with the PIF 1 polymer is shown in **Figure 4.7.**

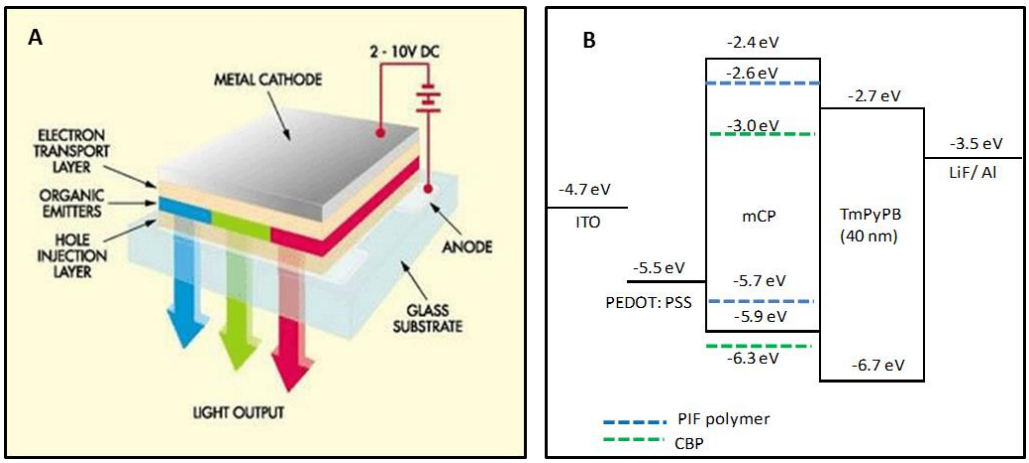

Figure 4.7. A). The simple architecture of OLED B). The device structure of OLEDs fabricated with PIF 1 polymer.

OLED devices with the structure: ITO/ PEDOT:PSS (60nm)/ (PIF + host)/ TmPyPB (40 nm)/ LiF (1 nm)/ Al (100 nm) was fabricated using different emissive layers. The organic compounds used in each layer are shown in **Figure 4.8.** Indium-tin oxide (ITO) coated on a glass substrate was used as the hole injection layer due to its relatively high work function and its transparent nature.[20] Poly(3,4-ethylenedioxythiophene)-poly(styrenesulfonate) (PEDOT:PSS) was used as the hole transporting layer due to its high work function, high transparency in the visible range (higher than 80%), good electrical conductivity and the ability to reduce the ITO surface roughness, while increasing its work function.[21] First, the neat PIF 1 was used as the emissive layer but showed very low performances. This may be due to the strong concentration quenching of the polymer in its solid state.[22-23] Therefore, PIF 1 polymer was blended with two host materials, 1,3-Bis(*N*-carbazolyl)benzene (mCP) and 4,4′-Bis(*N*-carbazolyl)-1,1′-biphenyl (CBP) to improve the efficiencies of the devices. 1,3,5-Tris(3-pyridyl-3-phenyl)benzene (TmPyPB) was used as the electron transporting layer and as well as the hole/exciton-blocking material with high electron mobility of 10^{-4}-10^{-3}cm^{2}V^{-1}s^{-1}. A very thin layer (1 nm) of LiF was deposited in between the TmpyPB and the Al cathode to act as a buffer layer to enhance the electron injection between the cathode and electron transporting layer. While increasing the number of electrons injected and transported in to the emissive layer, it decreases the number of holes that reach the cathode

Therefore, it is involved in the process of increasing the luminescence as well as decreasing the turn-on voltage.[24] Al metal was used as the cathode due to its lower work function.

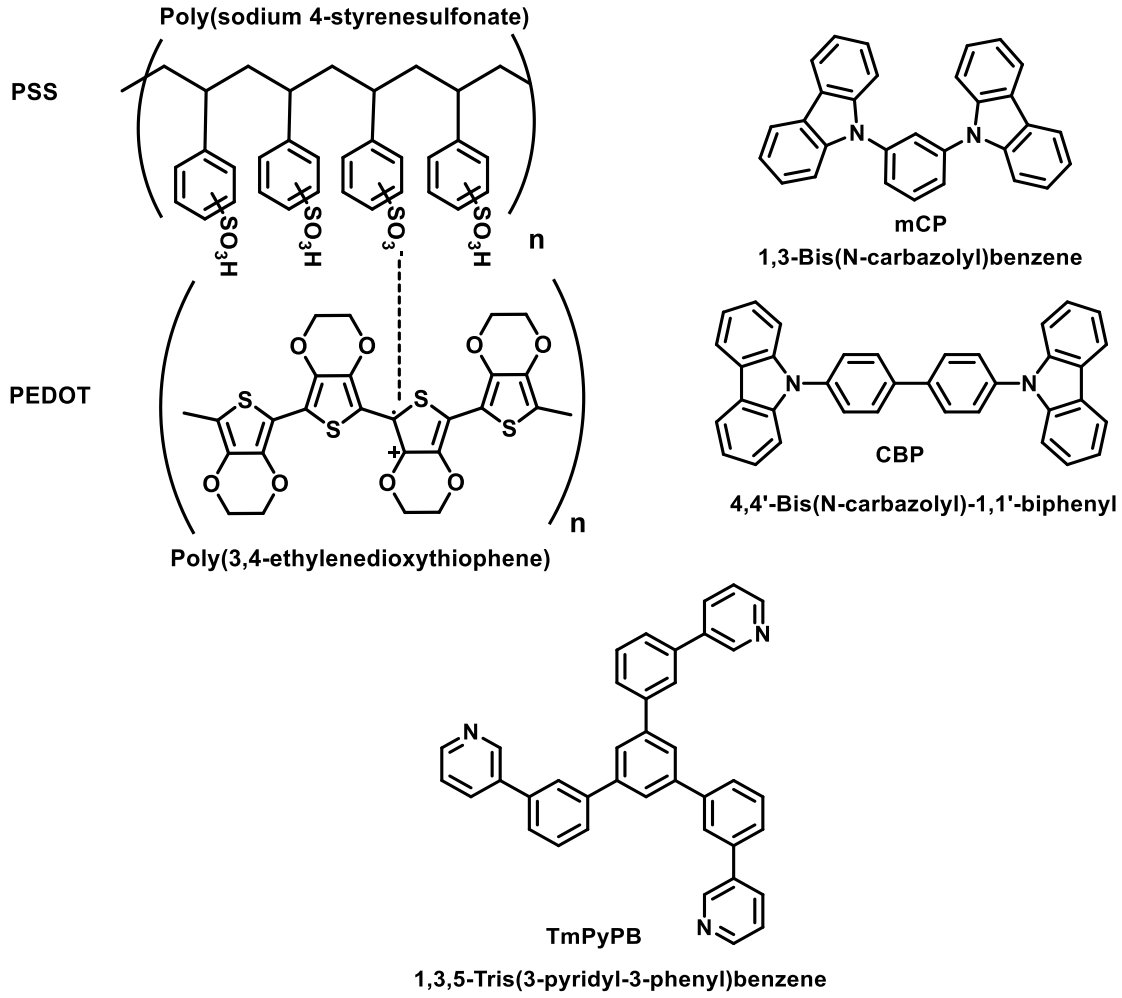

Figure 4.8. The organic compounds in each layer of OLEDs fabricated with PIF 1

Four devices were fabricated using PIF 1 blended with host materials as the emissive layers. The device performance data is shown in **Table 4.1.**

Table 4.1. The OLED device performance data for PIF 1 polymer.

Polymer	Weight % in host	Host	V_{on}[a] [V]	Current density [J, mA/ cm^2]	Brightness [Cd/m^2]	efficiency[Cd/A , (% EQE)[b]]	λ_{max}^{EL} [nm]
PIF	2.0	CBP	5.4	361	148	0.40 (0.79)	416
	5.0	CBP	5.2	324	137	0.50 (0.95)	418
	5.0	mCP	5.6	279	199	1.02 (1.09)	417
	100.0	-	8.8	94	141	0.30 (0.31)	418

According to the brightness verses voltage graph shown in **Figure 4.9**, the highest brightness (199 Cd/m^2) coccured with 5.0 wt % of PIF 1 in a mCP device. This brightness seems to be very low when compared with the brightness of normal green emitting OLEDs. Our resultant brightness is very good for deep blue emitting OLEDs which are limited greatly by their reduced photopic response factor.[25]

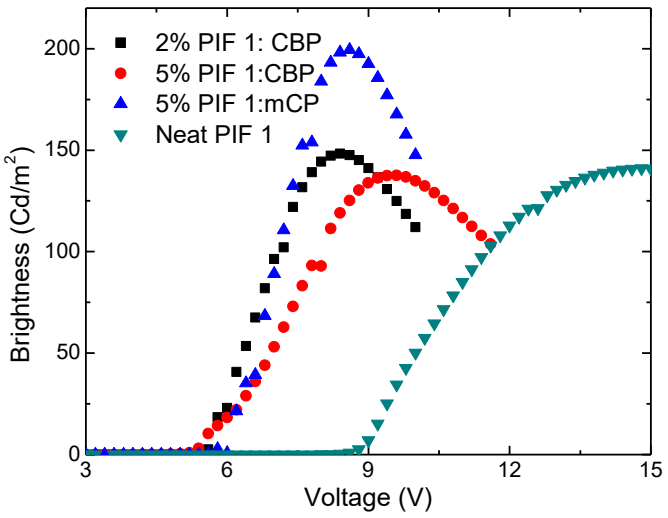

Figure 4.9. The brightness vs voltage of OLEDs for PIF 1.

The photopic response reflects the sensitivity of the human eye to bright visible light. The responsivity of the human eye varies greatly across the visible spectrum, and it is much weaker in

the blue region compared to green. Higher brightness is achieved in the device with mCP as the host and it is most likely due to the efficient charge transfer between the polymer and mCP when compared to devices with CBP as the host. The turn-on voltage is the voltage where the brightness is 1 Cd/m^2 and it is 5.4 V, for the device showing maximum brightness. This value is within the range of deep blue emitting polymer LEDs. [26-27] The maximum current density recorded is 361 J, mA/ cm^2 (**Figure 4.10**). Both brightness and current density were lower for the device fabricated with the neat polymer due to concentration quenching.

The luminous efficiency and the external quantum efficiency of the devices were determined and are shown in graphs in **Figure 4.11.** The highest luminous efficiency of 1.02 Cd/A was for the device with 5 wt% polymer + mCP as the emissive layer. External quantum efficiency (EQE %) is the percentage ratio between the numbers of photons emitted and the numbers of electrons injected. The maximum EQE was 1.1% for the device with mCP as the host.

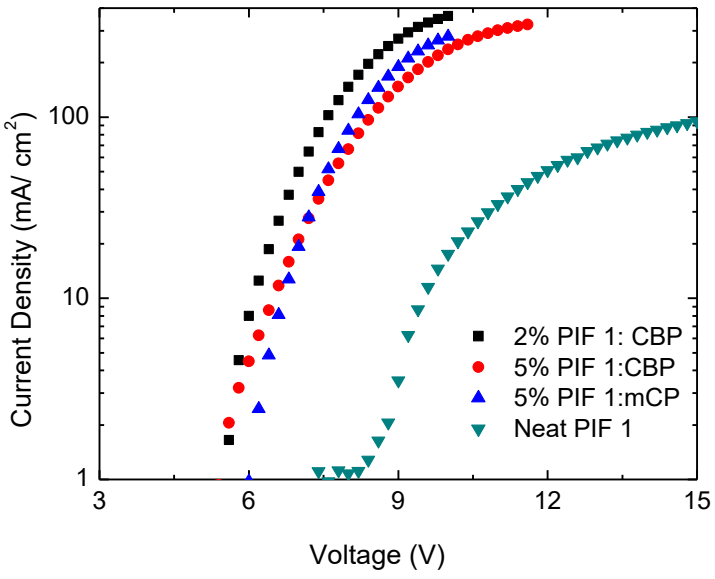

Figure 4.10. The current density vs voltage of OLEDs for PIF 1.

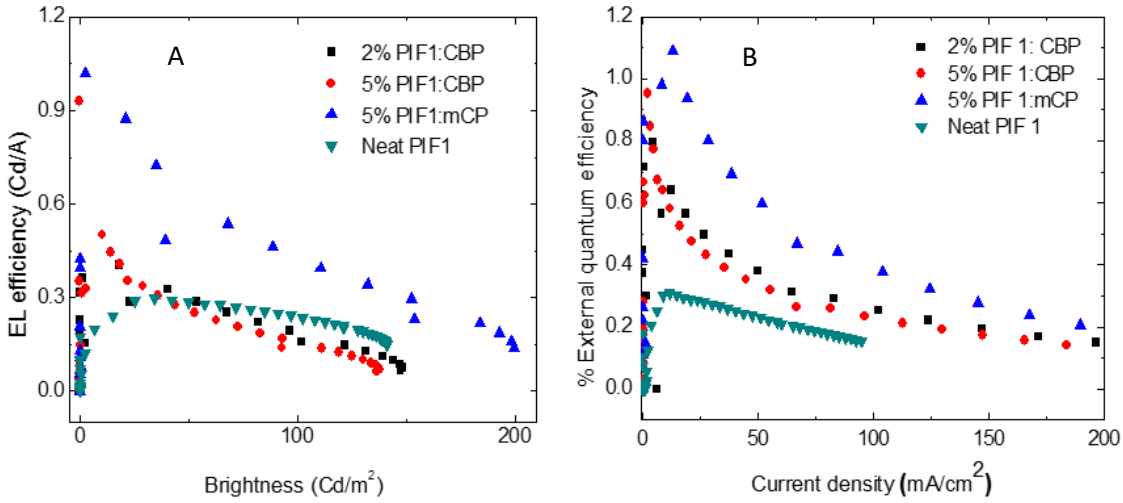

Figure 4.11. A). EL efficiency vs brightness B). External quantum efficiency vs current density.

The electroluminescence spectra of the devices are shown in **Figure 4.12.** All of the spectra for the devices are mostly overlapping each other having emission maxima at 416-417 nm. This value is exactly same as the thin film fluorescence emission. The CIE coordinates of all the devices are (0.16, 0.07) which were very close to the National Television System Committee (NTSC) standard values (0.14, 0.08) for blue electroluminescence in full color displays.

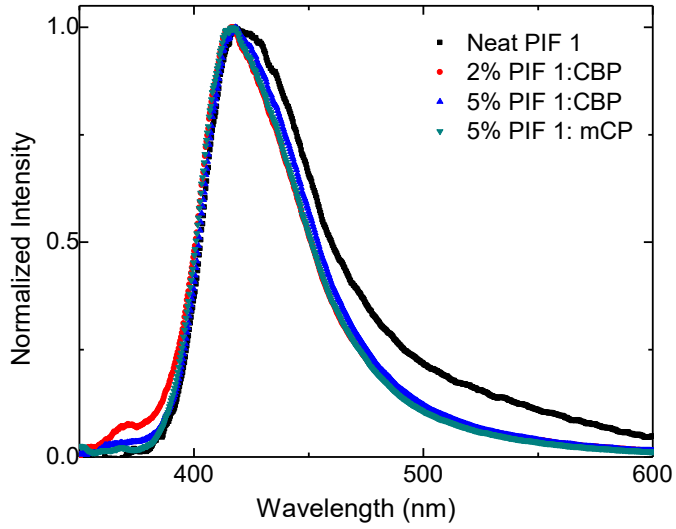

Figure 4.12. The electroluminescence spectra of OLEDs with PIF 1.

4.3.3. Experimental section

OLEDs were fabricated on nominally 25 Ω/in^2, 140 nm thick ITO-coated glass substrates (Colorado Concept coatings). These ITO glass plates (1" x 1") were cleaned in a detergent bath, washed with distilled water, isopropanol and acetone, dried under N_2 and treated with UV/ozone to increase the work function and to improve the hole injection ultimately. A 60 nm layer of high conductivity (902 S cm^{-1}) PEDOT:PSS was spincoated on the cleaned ITO at 1000 rpm for 60 s and annealed for 1 h at 120 °C in air followed by 1 h at 120 °C in the glovebox. The emissive layer was prepared by dissolving (PIF and host compound) in chlorobenzene (9 mg mL^{-1}) and then the mixture was spincoated at 4000 rpm for 60 s on top of the PEDOT: PSS layer in the glovebox. The fabricated structure was then annealed for 1h at 60 °C to obtain the thickness in the range of 30-40 nm. The devices were transferred to a thermal evaporator within the glovebox and then TmPyPb (40 nm), LiF (1 nm) and Al (100 nm) layers were deposited sequentially by thermal evaporation at a base pressure of 10^{-7} mbar. The OLEDs were characterized by monitoring their EL spectra and brightness as a function of the applied voltage, and luminous and external quantum efficiencies.

Figure 4.13. Pictures of some of the steps in the OLED fabrication process

Figure 4.14. The OLED devices I fabricated with PIF 1

4. 4. SUMMARY AND OUTLOOK

The ECL analysis of PIF 1 and PIC showed an intense additional ECL at -1.2 V for both polymer films. Those ECL were stable up to 12s. The ECL efficiency of PIF 1 and PIC were 6.1% and 0.4% respectively which were determined relative to the standard, 9,10 diphenylanthracene with a ECL efficiency of 8%. ECL showed red shifted structureless, broad emission than the fluorescence due to the excimer formation. OLED devices were fabricated using PIF 1 polymer mixed with host materials and 1.1% EQE was achieved with the CIE coordinates of (0.16, 0.07) which were very close to the National Television System Committee (NTSC) standards value for blue light.

4.5. REFERENCES

1. Grimsdale, A. C.; Leok Chan, K.; Martin, R. E.; Jokisz, P. G.; Holmes, A. B., Synthesis of light-emitting conjugated polymers for applications in electroluminescent devices. *Chem. Rev.* **2009,** *109* (3), 897-1091.
2. Leclerc, M.; Morin, J. F., *Design and Synthesis of Conjugated Polymers*. Wiley: 2010.
3. Kalyani, N. T.; Swart, H.; Dhoble, S. J., Chapter 6 - Organic light-emitting diodes: The future of lighting sources. In *Principles and Applications of Organic Light Emitting Diodes (OLEDs)*, Woodhead Publishing: 2017; pp 141-170.
4. Yang, X.; Xu, X.; Zhou, G., Recent advances of the emitters for high performance deep-blue organic light-emitting diodes. *Journal of Materials Chemistry C* **2015,** *3* (5), 913-944.
5. Nau, S.; Schulte, N.; Winkler, S.; Frisch, J.; Vollmer, A.; Koch, N.; Sax, S.; List, E. J. W., Highly efficient color-stable deep-blue multilayer PLEDs: preventing PEDOT:PSS-induced interface degradation. *Advanced Materials* **2013,** *25* (32), 4420-4424.
6. Jeong, S. H.; Lee, J. Y., Dibenzothiophene derivatives as host materials for high efficiency in deep blue phosphorescent organic light emitting diodes. *Journal of Materials Chemistry* **2011,** *21* (38), 14604-14609.
7. Cook, J. H.; Santos, J.; Al-Attar, H. A.; Bryce, M. R.; Monkman, A. P., High brightness deep blue/violet fluorescent polymer light-emitting diodes (PLEDs). *Journal of Materials Chemistry C* **2015,** *3* (37), 9664-9669.
8. Liu, C.; Fu, Q.; Zou, Y.; Yang, C.; Ma, D.; Qin, J., Low Turn-on Voltage, High-power-efficiency, solution-processed deep-blue organic light-emitting diodes based on starburst oligofluorenes with diphenylamine end-capper to enhance the HOMO level. *Chemistry of Materials* **2014,** *26* (10), 3074-3083.
9. Wang, Z.; Liu, W.; Xu, C.; Ji, B.; Zheng, C.; Zhang, X., Excellent deep-blue emitting materials based on anthracene derivatives for non-doped organic light-emitting diodes. *Optical Materials* **2016,** *58*, 260-267.
10. Wettach, H.; Jester, S. S.; Colsmann, A.; Lemmer, U.; Rehmann, N.; Meerholz, K.; Höger, S., Deep blue organic light-emitting diodes based on triphenylenes. *Synthetic Metals* **2010,** *160* (7), 691-700.
11. Hu, L.; Yang, Y.; Xu, J.; Liang, J.; Guo, T.; Zhang, B.; Yang, W.; Cao, Y., Blue light-emitting polymers containing fluorene-based benzothiophene-S,S-dioxide derivatives. *Journal of Materials Chemistry C* **2016,** *4* (6), 1305-1312.
12. Xu, J.; Yu, L.; Hu, L.; He, R.; Yang, W.; Peng, J.; Cao, Y., Color tuning in inverted blue light-emitting diodes based on a polyfluorene derivative by adjusting the thickness of the light-emitting layer. *Journal of Materials Chemistry C* **2015,** *3* (38), 9819-9826.
13. Yu, C.-Y.; Shih, T.-Y., Alternating copolymers containing fluorene and oxadiazole derivatives for fluorescent chemosensors. *Synthetic Metals* **2014,** *191*, 12-18.
14. Zhu, M.; Yang, C., Blue fluorescent emitters: design tactics and applications in organic light-emitting diodes. *Chemical Society Reviews* **2013,** *42* (12), 4963-4976.
15. Keszthelyi, C. P.; Tokel-Takvoryan, N. E.; Bard, A. J., Electrogenerated chemiluminescence. Determination of the absolute luminescence efficiency in electrogenerated chemiluminescence. 9,10-Diphenylanthracene-thianthrene and other systems. *Anal. Chem.* **1975,** *47* (2), 249-256.
16. Suk, J.; Wu, Z.; Wang, L.; Bard, A. J., Electrochemistry, electrogenerated chemiluminescence, and excimer formation dynamics of intramolecular π-stacked 9-naphthylanthracene derivatives and organic nanoparticles. *J. Am. Chem. Soc.* **2011,** *133* (37), 14675-14685.

17. Sartin, M. M.; Camerel, F.; Ziessel, R.; Bard, A. J., Electrogenerated chemiluminescence of B8amide: A BODIPY-based molecule with asymmetric ECL transients. *The Journal of Physical Chemistry C* **2008,** *112* (29), 10833-10841.
18. Sun, C.-L.; Li, J.; Geng, H.-W.; Li, H.; Ai, Y.; Wang, Q.; Pan, S.-L.; Zhang, H.-L., Understanding the unconventional effects of halogenation on the luminescent properties of oligo(phenylene vinylene) molecules. *Chemistry – An Asian Journal* **2013,** *8* (12), 3091-3100.
19. Prieto, I.; Teetsov, J.; Fox, M. A.; Vanden Bout, D. A.; Bard, A. J., A study of excimer emission in solutions of poly (9, 9-dioctylfluorene) using electrogenerated chemiluminescence. *The Journal of Physical Chemistry A* **2001,** *105* (3), 520-523.
20. Friend, R. H.; Gymer, R. W.; Holmes, A. B.; Burroughes, J. H.; Marks, R. N.; Taliani, C.; Bradley, D. D. C.; Santos, D. A. D.; Bredas, J. L.; Logdlund, M.; Salaneck, W. R., Electroluminescence in conjugated polymers. *Nature* **1999,** *397* (6715), 121-128.
21. Carter, S. A.; Angelopoulos, M.; Karg, S.; Brock, P. J.; Scott, J. C., Polymeric anodes for improved polymer light-emitting diode performance. *Applied Physics Letters* **1997,** *70* (16), 2067-2069.
22. Tlach, B. C.; Tomlinson, A. L.; Ryno, A. G.; Knoble, D. D.; Drochner, D. L.; Krager, K. J.; Jeffries-El, M., Influence of conjugation axis on the optical and electronic properties of aryl-substituted benzobisoxazoles. *The Journal of Organic Chemistry* **2013,** *78* (13), 6570-6581.
23. Hellerich, E. S.; Intemann, J. J.; Cai, M.; Liu, R.; Ewan, M. D.; Tlach, B. C.; Jeffries-El, M.; Shinar, R.; Shinar, J., Fluorescent polymer guest:small molecule host solution-processed OLEDs. *Journal of Materials Chemistry C* **2013,** *1* (34), 5191-5199.
24. Zhang, C.-l.; Wang, F.-c.; Zhang, Y.; Li, H.-x.; Liu, S., Studying the attribution of LiF in OLED by the C-V characteristics. *International Journal of Photoenergy* **2010,** *2010*.
25. Shen, H.; Cao, W.; Shewmon, N. T.; Yang, C.; Li, L. S.; Xue, J., High-efficiency, low turn-on voltage blue-violet quantum-dot-based light-emitting diodes. *Nano Letters* **2015,** *15* (2), 1211-1216.
26. Intemann, J. J.; Mike, J. F.; Cai, M.; Bose, S.; Xiao, T.; Mauldin, T. C.; Roggers, R. A.; Shinar, J.; Shinar, R.; Jeffries-El, M., Synthesis and characterization of poly(9,9-dialkylfluorenevinylene benzobisoxazoles): new solution-processable electron-accepting conjugated polymers. *Macromolecules* **2011,** *44* (2), 248-255.
27. Sergent, A.; Zucchi, G.; Pansu, R. B.; Chaigneau, M.; Geffroy, B.; Tondelier, D.; Ephritikhine, M., Synthesis, characterization, morphological behaviour, and photo- and electroluminescence of highly blue-emitting fluorene-carbazole copolymers with alkyl side-chains of different lengths. *Journal of Materials Chemistry C* **2013,** *1* (19), 3207-3216.

CHAPTER V

ATTEMPTED SYNTHESIS OF EUMELANIN-INSPIRED POLYINDOLES TO STUDY THE STRUCTURE-PROPERTY-FUNCTION RELAIONSHIP OF NATURAL EUMELANIN

5.1. INTRODUCTION

Melanin is a class of natural pigments which is biosynthesized in the epidermal pigment cells called melanocytes by tyrosinase-catalyzed oxidation of tyrosine[1] *via* 5,6-dihydroxyindole (DHI) and 5,6-dihydroxyindole-2-carboxylic acid (DHICA), the final monomer precursors. The oxidative polymerization of DHI and DHICA gives rise to eumelanin,[2] the black brown variety of melanin which is commonly found in the human body. Eumelanin exhibits interesting properties such as antioxidant, free radical scavenging behavior,[3] broadband, monotonic UV and visible absorption[4] and strong non-radiative relaxation of photoexcited electronic states which leads to photoprotection against harmful sunrays.[5-6] In addition, eumelanin has fascinating electronic properties such as electronic conductivity varying from 10^{-13} S/cm to 10^{-5} S/cm based on the humidity.[7] Electrical switching work done by McGinness and coworkers first characterized eumelanin as amorphous organic semiconductor.[8] Recent studies by Meredith however has revealed it to be an electronic-

ionic hybrid conductor rather than an amorphous organic semiconductor[9] based on the electrical conductivity, muon spin relaxation and electron paramagnetic resonance measurements. These exciting properties have spurred additional research about this heterogeneous macromolecule. It is more challenging to work on eumelanin due to its insolubility and extremely heterogeneous, amorphous nature. Therefore, to date, the fundamental structure of eumelanin remaines unsolved.[6,10] In order to investigate the fundamental structure of eumelanin, a well-defined, eumelanin-inspired macromolecule could be used to elucidate the structure of natural and synthetic eumelanin The investigation of well-defined, eumelanin-inspired macromolecule properties could be used to study how structures/properties of eumelanins are related. The eumelanin inspired core, methyl 4,7-dibromo-5,6-dimethoxy-1-methyl-1*H*-indole-2-carboxylate (DBI)[11] was used as the template for designing regioregular, soluble eumelanin-inspired polyindoles to study the structure-property-function relationships of natural eumelanins. The attempted synthesis of eumelanin-inspired polyindoles and the synthesis of eumelanin-inspired small molecules are discussed in this chapter.

5.2. DESIGN

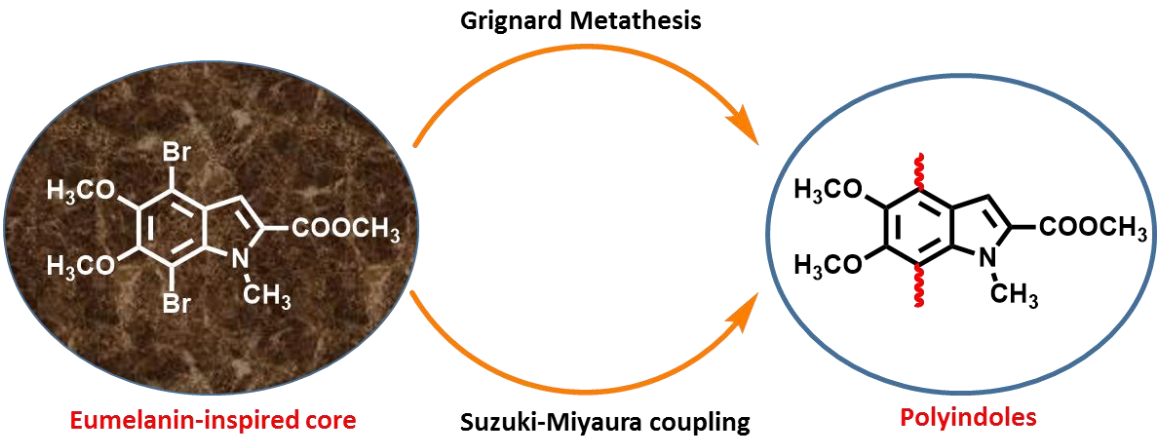

Figure 5.1. Our design of the synthesis of eumelanin-inspired polyindoles.

Our design was to synthesize eumelanin-inspired polyindoles using either a Grignard metathesis (GRIM) polymerization or a Suzuki polymerization reaction. (**Figure 5.1.**) In 1999, McCullough and coworkers developed a method to synthesize head-to-tail (HT) coupled poly(3-alkylthiophenes) using a magnesium-halogen exchange called the GRIM. By treating 2,5-dibromo-3-alkylthiophenes (**1**) with a variety of alkyl and vinyl Grignard reagents they obtained two metalated, regiochemical isomers, namely, 2-bromo-3-alkyl-5-bromomagnesiothiophene (**2**) and 2-bromomagnesio-3-alkyl-5-bromothiophene (**3**) in an 85:15 ratio which has shown in **Scheme 5.1**. A catalytic amount of $Ni(dppp)Cl_2$ was introduced to this isomeric mixture to initiate the Kumada polymerization reaction. The beauty of this specific reaction is only major isomer formed by the Grignard metathesis is involved in to the polymerization reaction. This is due to the steric hindrance of by the alkyl group in the isomer **3** when it is trying to oxidatively insert in to the catalyst system. Therefore, with intermediate **2**, it forms >99% regioregular poly(3-alkylthiophene). The regioregularity of these polymers were very important due to their ability to undergo self-assembly, both in solution and in the solid state. It offered highly ordered two-and three-dimensional polymer structures having greater electronic and photophysical properties compared to regioirregular counterparts containing HH and TT coupling.[12] GRIM polymerization has been used in a number of different conjugated polymer systems.[13-14]

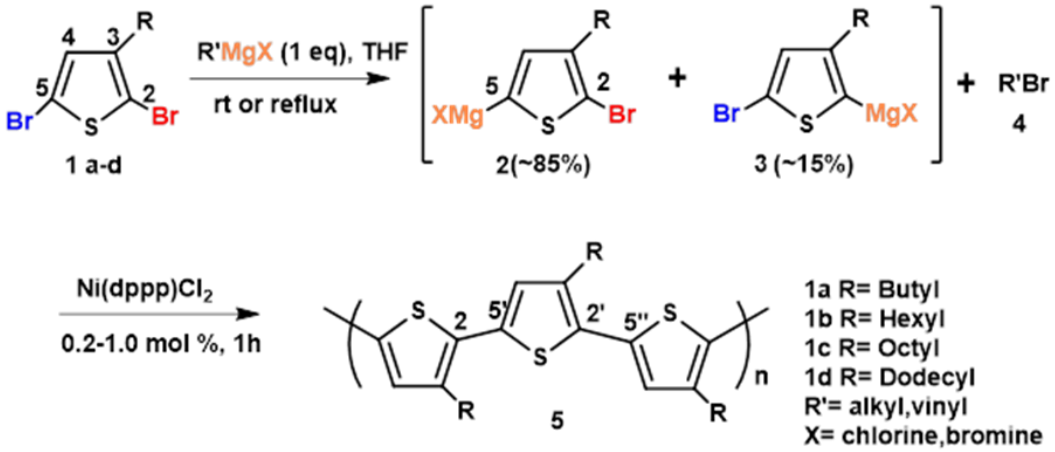

Scheme 5.1. The GRIM polymerization of poly(3-alkylthiophene)s

We designed our experiment based on the GRIM metathesis followed by a Ni initiated Kumada coupling of a eumelanin-inspired core to achieve polyindoles linked at the 4- and 7- positions. The proposed synthesis is shown in **Scheme 5.2.**

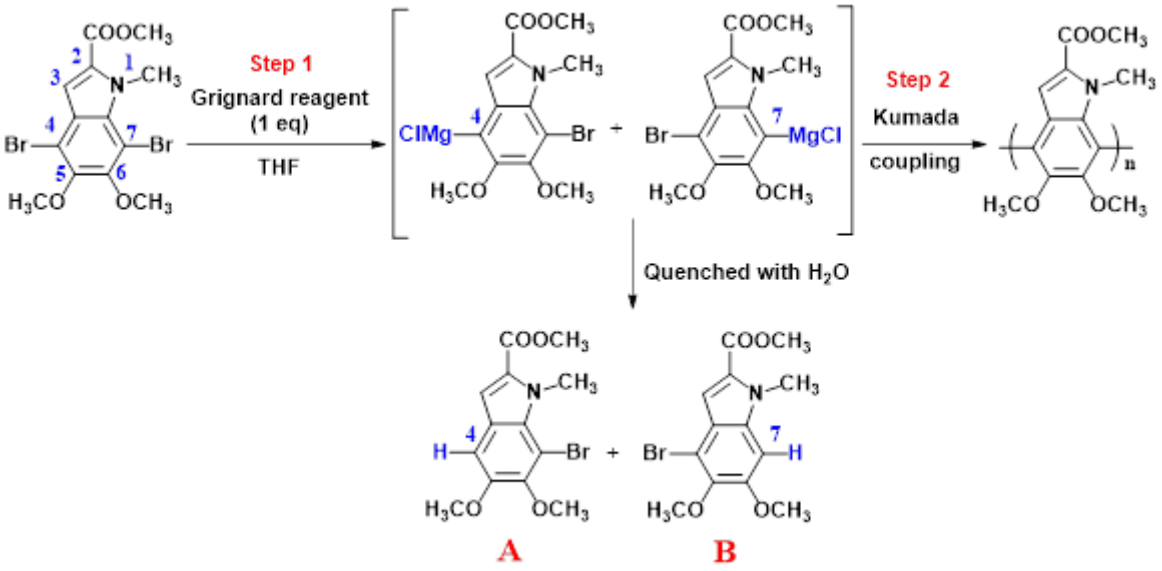

Scheme 5.2. The proposed synthesis scheme of Grignard metathesis polymerization of DBI.

Suzuki polymerization was also planned as an alternative the route for the synthesis of polyindoles. One pot Miyaura borylation and subsequent Suzuki-Miyaura coupling of biindoles was found in the literature[15] and it is shown in **Scheme 5.3**. According to the published procedure, when compound **1** reacts with pinacol borane in the presence of $Pd(dba)_3$, Xphos and Et_3N in dioxane it forms compound **2**. When compound **3** is added to the same reaction pot with DI water, another 1mol % $Pd_2(dba)_3$ and 3 equivalents of K_3PO_4, the biindole **4** is produced.

Here, we designed two ways to synthesize polyindoles which are shown in **Scheme 5.4.** 1) One pot mono borylation of DBI and subsequent Suzuki Miyaura self-polymerization 2) One pot di borylation and subsequent Suzuki Miyaura polymerization with added DBI.

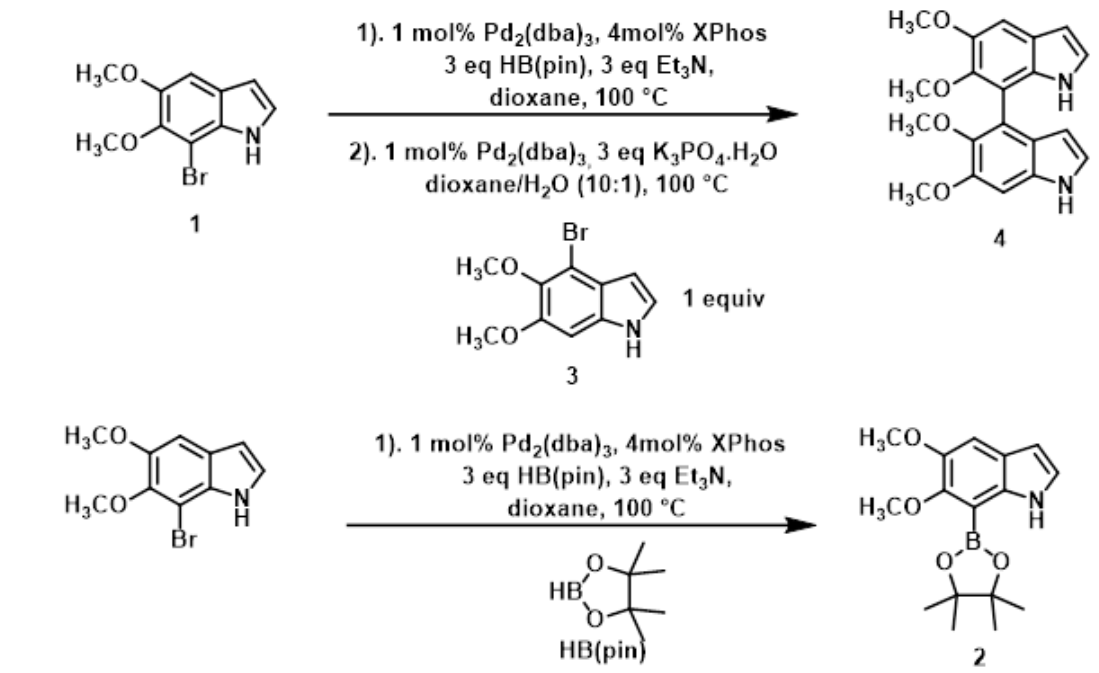

Scheme 5.3. One pot Miyaura borylation and subsequent Suzuki-Miyaura coupling of biindoles[15]

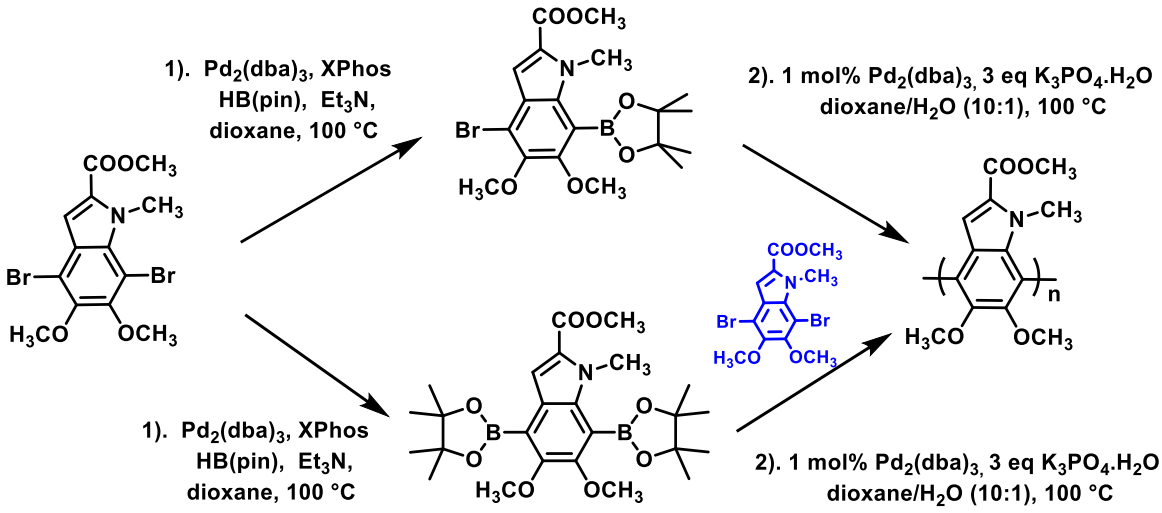

Scheme 5.4. The proposed synthesis of polyindoles via Suzuki polymerization

5.3. RESULTS AND DISCUSSION

First, I tried step 1 of the Grignard metathesis polymerization and quenched it with DI water to determine the ratio between the two possible isomers which is shown in **Scheme 5.5.**

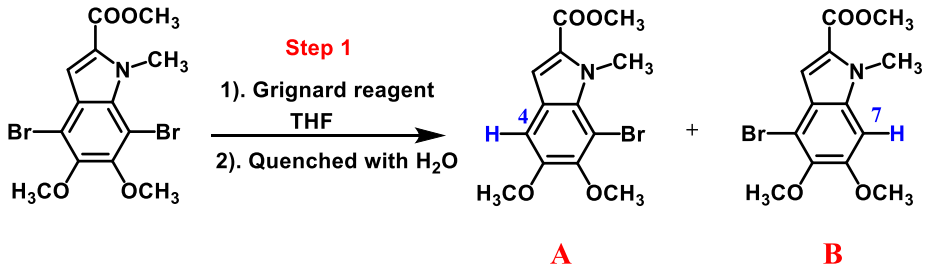

Scheme 5.5. The Grignard metathesis of eumelanin-inspired core.

In the first run, one equivalent of tertiary butyl magnesium chloride was used as the Grignard reagent and the reaction was done in dry THF at r.t. for 2 h. At this time, the conversion of starting material was 5%. Therefore, the optimization study was done with different reaction conditions shown in **Table 5.1.**

Table 5.1. The optimization study of the Grignard metathesis of eumelanin-inspired core.

Run #	Grignard Reagent	Temp. (°C)	Time (h)	SM % [a]	A % [a]	B % [a]
1	t-C_4H_9MgCl	RT	2	95	-	5
2	t-C_4H_9MgCl	RT	24	95	-	5
3	t-C_4H_9MgCl	reflux	24	85	-	15
4	i-C_3H_7MgCl	RT	24	90	-	10
5	CH_3MgCl	RT	24	85	-	15
6	i-C_3H_7MgCl + LiCl (turbo Grignard)	RT	2	67	-	33
7	i-C_3H_7MgCl + LiCl (turbo Grignard)	RT	15	0	-	100

a – ratios are based on ^{1}H NMR

Secondly, the reaction was done under the same conditions while increasing the reaction time to 24 h and the conversion was still 5%. In the third run, the reaction was refluxed for 24 h with tertiary butyl magnesium chloride and improved conversion (15%) of starting material in to product B was observed. Since the conversion is not good even with refluxing, different Grignard reagents were also screened. With isopropyl magnesium chloride and methyl magnesium chloride at room temperature over 24 h, the conversion was same as earlier (run 4 & 5).

Then, a mixture of isopropyl magnesium chloride and anhydrous LiCl (1: 1 molar ratio) was found to be as a strong Grignard reagent with enhanced reactivity which named as "turbo Grignard"[14] in the literature. This turbo Grignard was prepared *in situ* by stirring a 1:1 molar ratio of isopropyl magnesium chloride and anhydrous LiCl in THF for 6 h at room temperature. When the LiCl is added to the Grignard reagent, it breaks the polymeric aggregates formed in the solution to produce a very reactive complex, [*i*-$PrMgCl_2^-Li^+$]. The magnesiate character of this complex may be responsible for the enhanced reactivity of this reagent. The reaction of DBI with the turbo Grignard at room temperature for 15 h resulted in 100% conversion of the DBI to only one regiochemical isomer (product B) via halogen exchange of the bromine at the 7-position. This regiochemical isomer was isolated by quenching with DI water. The structure of this isolated regiochemical isomer, methyl 4-bromo-5,6-dimethoxy-1-methyl-1*H*-indole-2-carboxylate (7*H*-DBI) (**Scheme 5.6**), was confirmed by ^{1}H NMR, ^{13}C NMR, Heteronuclear Multiple Quantum Coherence (HMQC), Heteronuclear Multiple Bond Coherence (HMBC), Nuclear Overhauser Effect (NOE) experiments. The reaction was quenched with D_2O and yielded 52% of the 7*D*-DBI by ^{1}H NMR.

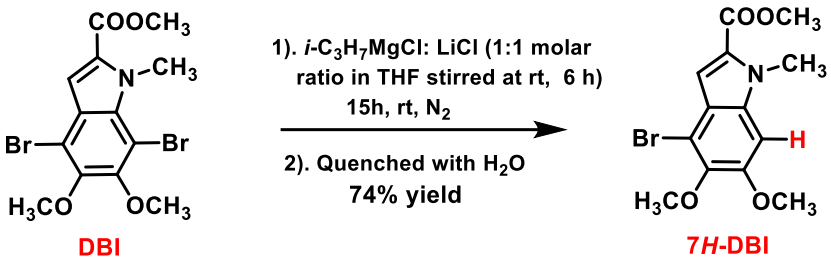

Scheme 5.6. The synthesis of 7*H*-DBI.

Our attempt was to polymerize this GRIM regiochemical isomer by the addition of a Ni catalyst to the same reaction pot. Therefore, Ni(dppp)Cl_2 was first used as the initiator and 5 mol% was added to the reaction mixture under N_2. The reaction was then allowed to stir at room temperature for 24 h and reaction mixture was poured into methanol to precipitate the polymer. There was no solid formed and according to the ^{1}H NMR, the product was 7*H* DBI. Same reaction was done and allowed to polymerize for 48 h. The result was same as for 24 h experiment. Different Ni catalysts such as Ni(dppp)Cl_2, Ni(dppe)Cl_2, Ni(dppf)Cl_2, $NiCl_2$, Ni(acac) and Pd catalyst such as Pd$(PPh_3)_4$ and Pd$(OAc)_2$ were also screened, but the polymerization was not successful and all of the reactions resulted in 7*H*-DBI.

At the same time, an attempt was made to synthesize polyindoles via Suzuki polymerization based on the method proposed in **Scheme 5.4.** Our effort was to borylate the DBI with bis(pinacolato) diborane in the presence of $Pd_2(dba)_3$ as the catalyst and XPhos as the ligand in dioxane, but the conversion of starting material into products was only 30%. To optimize the reaction, the conditions listed below were tested. They involved the use of different boron sources (bis(pinacolato) diborane and pinacol borane), different catalysts (Pd(dppf)Cl_2) other than $Pd_2(dba)_3$ different bases ($K_3PO_4.3H_2O$, Et_3N and KOAc), solvents (dioxane, dioxane : H_2O = 10:1). The equivalents of boron sources and amounts of catalysts and ligands were also varied. All the reactions resulted the desired product in very low yields (e.g.10-20%) with undesired product (7*H*-DBI) and starting material.

Lithiation followed by borylation with 2-isopropoxy-4,4,5,5-tetramethyl-1,3,2-dioxaborolane or bis(pinacolato)diborane was planned with different organolithium reagents. When DBI was reacted with *n*-butyllithium, there was no reaction and starting material was remained. When two equivalencts of *sec*-butyllithium were used, it reacted with the ester group and replaced the ester group with tertiary alcohol group having two *sec*-butyl groups attached to it.

Yamamoto polycondesation is a famous method to synthesize polyarylenes starting from dibromo monomers in the presence of $Ni(COD)_2$ in stoichiometric amounts.[16-18] Yamamoto conditions were also tested to synthesize polyindoles starting from DBI (**Scheme 5.7**) and did not form polymers even after 72 h of heating under the conditions specified in the literature.[18] The solvent system and the amounts of precatalyst and ligands were changed to make the polymerization successful but it resulted in starting material and 7*H* DBI.

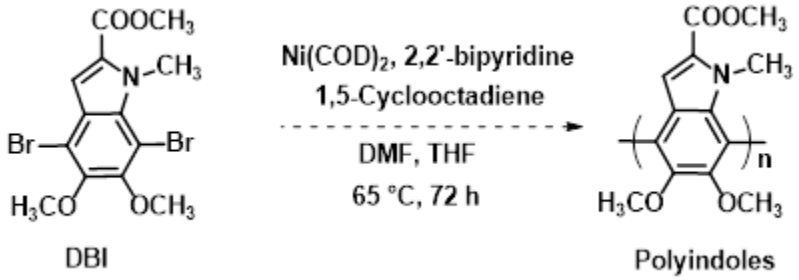

Scheme 5.7. The proposed synthesis of Yamamoto polycondensation of DBI

Our attention was next directed towards the synthesis of eumelanin-inspired dimers and trimers. The idea was to understand the coupling of building blocks of natural eumelanin based on structure-property relationships observed with these small molecules. For this study, we started our synthesis with commercially available ethyl 5,6-dimethoxy-1*H*-indole-2-carboxylate (DMICE) which has a similar structure to our eumelanin-inspired core.

Iridium (Ir) catalyzed, nitrogen directed aryl borylation of DMICE was proposed to synthesize the monoborylated product, ethyl 5,6-dimethoxy-7-(4,4,5,5-tetramethyl-1,3,2-dioxaborolan-2-yl)-1H-indole-2-carboxylate (7-borylated DMICE) which is shown in **Scheme 5.8.** The reaction optimization was done with different conditions, which are summerized in the **Table 5.2.**

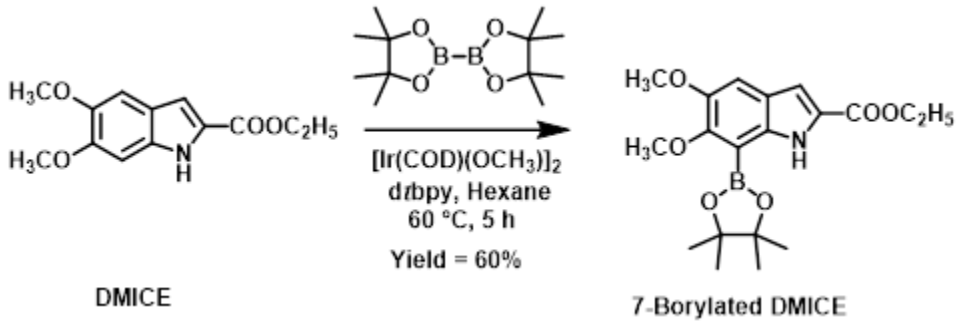

Scheme 5.8. Ir catalyzed nitrogen directed aryl borylation of DMICE

Table 5.2. The optimization study of Ir catalyzed nitrogen directed aryl borylation of DMICE

Entry	Boron source	Boron source Equivalents	Precatalyst mol %	Ligand mol %	Solvent	SM to Product conversion % [a]
1	$(Bpin)_2$	0.50	1.0	3.0	Heptane	10
2	$(Bpin)_2$	0.75	1.0	3.0	Heptane	12
3	$(Bpin)_2$	0.89	1.0	3.0	Heptane	21
4	$(Bpin)_2$	1.00	1.0	3.0	Heptane	40
5	$(Bpin)_2$	1.00	2.0	3.0	Heptane	50
6	HBpin	2.00	1.5	3.0	Hexane	27
7	$(Bpin)_2$	1.50	1.5	3.0	Hexane	70
8	$(Bpin)_2$	1.50	3.0	6.0	Hexane	77
9	$(Bpin)_2$	2.00	3.0	6.0	Hexane	87
10	$(Bpin)_2$	2.00	5.0	10.0	Hexane	100

a – determined with gas chromatography

First, the reaction was done with 0.5 equivalents of the boron compound, 1.0 mol% of $[Ir(COD)(OCH_3)]_2$ precatalyst and 3 mol% of 4,4′-di-*tert*-butyl-2,2′-dipyridyl ligand in *n*-heptane solvent. The starting material to product conversion was 10%. When the number of equivalents of bis(pinacolato)diborane was increased the conversion also increased. (entries 2-3). When the mole percentage of precatalyst and ligand increased with the amount of boron compound, the conversion was further increased to 50%. In these reactions, all reagents were added to a reaction vial inside the glove box followed by solvent. Later, a more detailed procedure for the Ir catalyzed nitrogen directed borylation was found.[19] The current literature procedure mentioned that the reaction yield increased at 60 °C in distilled *n*-hexane.[19] By increasing the boron source, precatalyst and ligand, lower temperature and alternating the order of addition, the conversion was increased to quantitative (entries 7-10) Another reaction was performed with pinacolborane as the boron source and the starting material to product conversion was low (entry 6). For the optimized conditions, the isolated yield of the reaction was 60%.

This borylated DMICE was coupled with the 7*H*-DBI (available from the GRIM reaction) to generate the eumelanin-inspired dimer (**Scheme 5.9**).

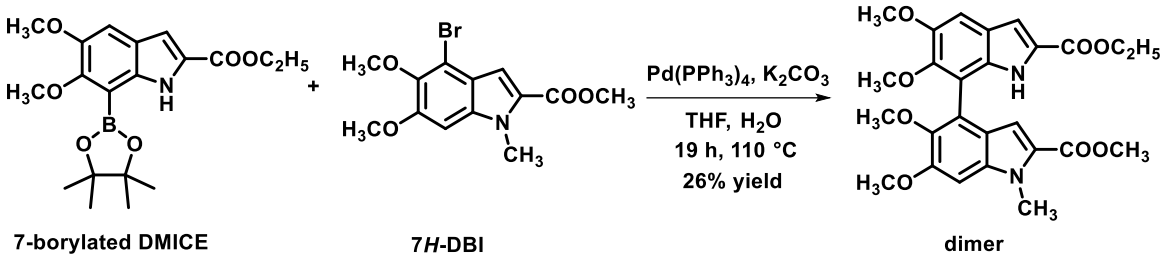

Scheme 5.9. The synthesis of eumelanin-inspired dimer.

5.4. SUMMARY AND OUTLOOK

To understand the structure-property relationship of natural eumelanin, we proposed to synthesize well-defined, soluble eumelanin-inspired polyindoles which could mimic the natural eumelanin. The strategy developed was to polymerize our eumelanin-inspired core through its 4- and 7-

positions *via* a Grignard metathesis (GRIM) reaction followed by a Ni initiated Kumada coupling reaction. Different Grignard reagents were screened under varied temperatures to optimize the conditions for the GRIM reaction. The turbo Grignard reagent (1:1 molar ratio of *i*-C_3H_7MgCl and anhydrous LiCl in THF) at room temperature resulted in 100% conversion of the eumelanin-inspired core to give only one regiochemical isomer *via* halogen-exchange of the bromine at the 7-position. This regiochemical isomer was isolated by quenching with DI water and the structure of this isolated regiochemical isomer, methyl 4-bromo-5,6-dimethoxy-1-methyl-1*H*-indole-2-carboxylate (7*H*-DBI), was confirmed by ^{1}H NMR, ^{13}C NMR, Heteronuclear Multiple Quantum Coherence (HMQC), Heteronuclear Multiple Bond Coherence (HMBC) and Nuclear Overhauser Effect (NOE) experiments. Our attempt was to polymerize this GRIM regiochemical isomer by the addition of a Ni catalyst to the same reaction pot. However, the polymerization was not successful and all the reactions produced 7*H*-DBI. Suzuki polymerization and Yamamoto polycondensation were tested to synthesize polyindoles but those methods were not successful. Ir catalyzed nitrogen directed borylation of DMICE was done and the borylated product was coupled with 7*H*-DBI to synthesize eumelanin-inspired dimers.

5.5. EXPERIMENTAL SECTION

5.5.1. General methods and materials

All the Grignard reagents, lithiating reagents and anhydrous LiCl were purchased from Sigma. Other chemicals purchased from Alfar Aesar and Acros and DMICE was purchased from Oxchem. All the commercial reagents were used as received. Anhydrous *N*,*N*-dimethylformamide (DMF) and tetrahydrofuran (THF) were obtained from solvent purification system under ultra-pure argon. Anhydrous n-heptane was purchased and n-hexane was distilled in the laboratory. Unless otherwise specified, all reactions were run in oven-dried glassware. Reactions were monitored by thin layer chromatography on silica G TLC plates (Silicycle). Purifications were performed by column chromatography on silica gel (Silicycle, 40-63 μm particle size). ^{1}H- and ^{13}C-NMR spectra were

measured on a Bruker Avance 400 MHz instrument or Varian Inova 400 MHz instrument. HMBC and HMQC experiments were done on Agilent Inova using a OneNMR probe, with nominal temperature setting of 25 °C. HSQC spectrum was taken with the gradient CRISIS2 HSQC method using the Agilent gc2hsqc pulse sequence, with 1 s delay between scans, ^{1}H spectral width of 4404.8 Hz, ^{1}H 90 degree pulse width of 6.5 μs, ^{13}C spectral width of 20105.6 Hz, ^{13}C 90 degree pulse width of 6.8 μs, 1322 points, 128 increments, 32 dummy scans before the first increment, and ^{13}C decoupling during the acquisition. The C-H coupling constant parameter j1xh was 146 Hz. HMBC spectrum was taken with the gradient CRISIS2 HMBC method using the Agilent gc2hmbc pulse sequence, with 1 s delay between scans, ^{1}H spectral width of 4404.8 Hz, ^{1}H 90 degree pulse width of 6.5 μs, ^{13}C spectral width of 24125.5 Hz, ^{13}C 90 degree pulse width of 6.8 μs, 1322 points, 200 increments, and 32 dummy scans before the first increment. Coupling constant parameters were j1min 130 Hz, j1max 165 Hz and jnxh 8 Hz. HRMS analysis was performed at Biochemistry and Molecular Biology Recombinant DNA and Protein Core Facility. HRMS data were calculated for compound [Na^{+}].

5.5.2. Synthesis procedures

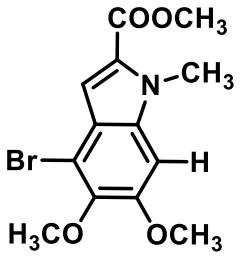

Methyl 4-bromo-5,6-dimethoxy-1-methyl-1*H*-indole-2-carboxylate (7*H*-DBI) : Turbo Grignard reagent was prepared *in situ* prior to the reaction. In a 10 mL clean dry reaction vial was added anhydrous LiCl (11 mg, 0.25 mmol) inside the glove box and the vial was sealed with a crimp cap. Then *i*-PrMgCl (2.0M in THF) (0.12 mL, 0.25 mmol) was added followed by the addition of THF (0.25 mL) at N_2 environment. The reaction was stirred for 6 h at room temperature

under N_2 atmosphere. After 6 h, DBI (100 mg, 0.25 mmol) was dissolved in dry THF (1.0 mL) under N_2 environment was syringed in to the turbo Grignard reagent and allowed to stir another 15 h at room temperature. Then, the reaction was quenched by adding DI water (5.0 mL) and the product was extracted in to diethyl ether (3 x 15 mL) and washed with brine (2 x 30 mL) and dried over anhydrous MgSO4. The solvent was evaporated and the crude product was purified by silica column chromatography using the 4% Ethyl acetate in hexanes as the eluent to give pale orange colored solid. (60 mg, 74 %). H NMR (400 MHz, $CDCl_3$) δ 7.24 (s, 1H), 6.72 (s, 1H), 4.02 (s, 3H), 3.96 (s, 3H), 3.88 (d, J = 11.7 Hz, 6H).^{13}C NMR (101 MHz, $CDCl_3$) δ 162.52, 153.50, 143.34, 136.34, 127.07, 120.82, 111.16, 110.66, 92.28, 76.98, 61.30, 56.58, 51.87, 32.25. HRMS (m/z): calcd. 349.9998; found, 349.9968.

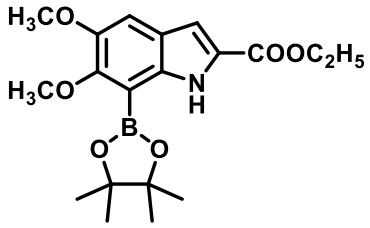

Ethyl 5,6-dimethoxy-7-(4,4,5,5-tetramethyl-1,3,2-dioxaborolan-2-yl)-1H-indole-2-carboxylate: In a 10 mL reaction vial was placed ethyl 5,6-dimethoxy-1*H*-indole-2-carboxylate (DMICE) (50 mg, 0.20 mmol) and dry n-hexane (0.5 mL). Bi(pinacolato) diborane [$(Bpin)_2$] (102 mg, 0.40 mmol) and (1,5-cyclooctadiene)(methoxy)iridium(I) dimer (6 mg, 5 mol %) were added in to a separate test tube and added n-hexane (0.5 mL). 4,4′-Di-*tert*-butyl-2,2′-dipyridyl (6 mg, 0.02 mmol) was placed in another test tube and n-hexane (1.0 mL) was added to dissolve the ligand. Then, ligand dissolved in n-hexane was transferred in to the test tube containing [$(Bpin)_2$] and pre-catalyst. The mixture was stirred for 1 min and the color of the solution turned from yellow to red. Then, this solution was added in to the reaction vial which contained DMICE solution. All these additions were done inside the glove box. The reaction vial was sealed with crimp cap. Outside the glove box, the reaction mixture was heated to 60 °C for 6 h under N_2 atmosphere. After completion

of the reaction, silica (300 mg) was added in to the reaction mixture and solvent was evaporated to form silica dry pack. Silica column was buffered with 4% Et_3N in hexane prior to use. The crude was purified with the buffered silica column chromatography using 18% ethyl acetate in hexane as the solvent to obtain white solid (44 mg, 60%). ^{1}H NMR (400 MHz, $CDCl_3$) δ 9.77 (s, 1H), 7.23 (s, 1H), 7.10 (d, *J* = 2.2 Hz, 1H), 4.39 (q, *J* = 7.1 Hz, 2H), 3.89 (d, *J* = 3.0 Hz, 6H), 1.41 (s, 3H), 1.26 (s, 12H). ^{13}C NMR (101 MHz, $CDCl_3$) δ 162.17, 156.78, 149.34, 137.12, 127.28, 123.04, 108.42, 107.93, 83.98, 76.98, 62.67, 60.94, 56.92, 29.98, 25.23, 14.67.

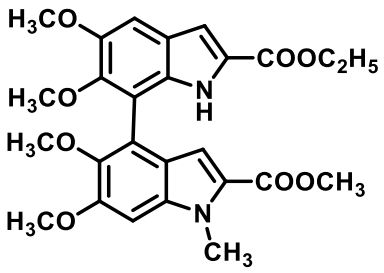

2'-ethyl 2-methyl 5,5',6,6'-tetramethoxy-1-methyl-1H,1'H-[4,7'-biindole]-2,2'-dicarboxylate (dimer): In a 10 mL reaction vial, methyl 4-bromo-5,6-dimethoxy-1-methyl-1*H*-indole-2-carboxylate (25 mg, 0.15 mmol), ethyl 5,6-dimethoxy-7-(4,4,5,5-tetramethyl-1,3,2-dioxaborolan-2-yl)-1H-indole-2-carboxylate (30 mg, 0.16 mmol), $Pd(PPh_3)_4$ (5 mg, 5 mol%) and K_2CO_3 (176 mg, 16.67 mmol) were placed inside the glove box. Then, the vial was sealed with crimp cap. Outside the glove box, vacuum was applied to the reaction mixture for 20 min and refilled with N_2 for 20 min. Dry THF (1.0 mL) and degassed DI water (1.0 mL) was added to the reaction in the N_2 environment. Reaction was heated to 110 °C for 19 h under the N_2. After the reaction was completed 6N HCl (4 mL) was added to neutralize the excess base. Then the product was extracted to chloroform (3 x 10 mL) and washed with brine (2 x15 mL) and dried over anhydrous Na_2SO_4. The crude product was purified with a silica column chromatography starting with 15% ethyl acetate in hexane as the eluent. Product was eluted with 40% ethyl acetate in hexane and white solid was obtained. (20 mg, 26%).^{1}H NMR (400 MHz, $CDCl_3$) δ 8.29 (s, 1H), 7.18 (s, 1H), 7.15

(d, *J* = 2.2 Hz, 1H), 6.90 (s, 1H), 6.77 (s, 1H), 4.29 (dd, *J* = 7.1, 2.0 Hz, 2H), 4.09 (s, 3H), 4.04 (s, 3H), 3.98 (s, 3H), 3.76 (s, 3H), 3.65 (s, 3H), 3.60 (s, 3H), 1.33 (t, *J* = 7.1 Hz, 3H). ^{13}C NMR (101 MHz, $CDCl_3$) δ 162.39, 161.72, 153.14, 149.32, 147.16, 143.57, 136.52, 131.50, 127.34, 126.61, 122.64, 120.02, 119.46, 113.57, 110.46, 108.45, 102.92, 92.91, 77.34, 77.23, 77.02, 76.71, 61.28, 60.72, 56.07, 51.28, 31.93, 31.82, 29.71, 22.70, 14.41.

5.5.3. NMR spectra:

^{1}H NMR of 7*H* DBI

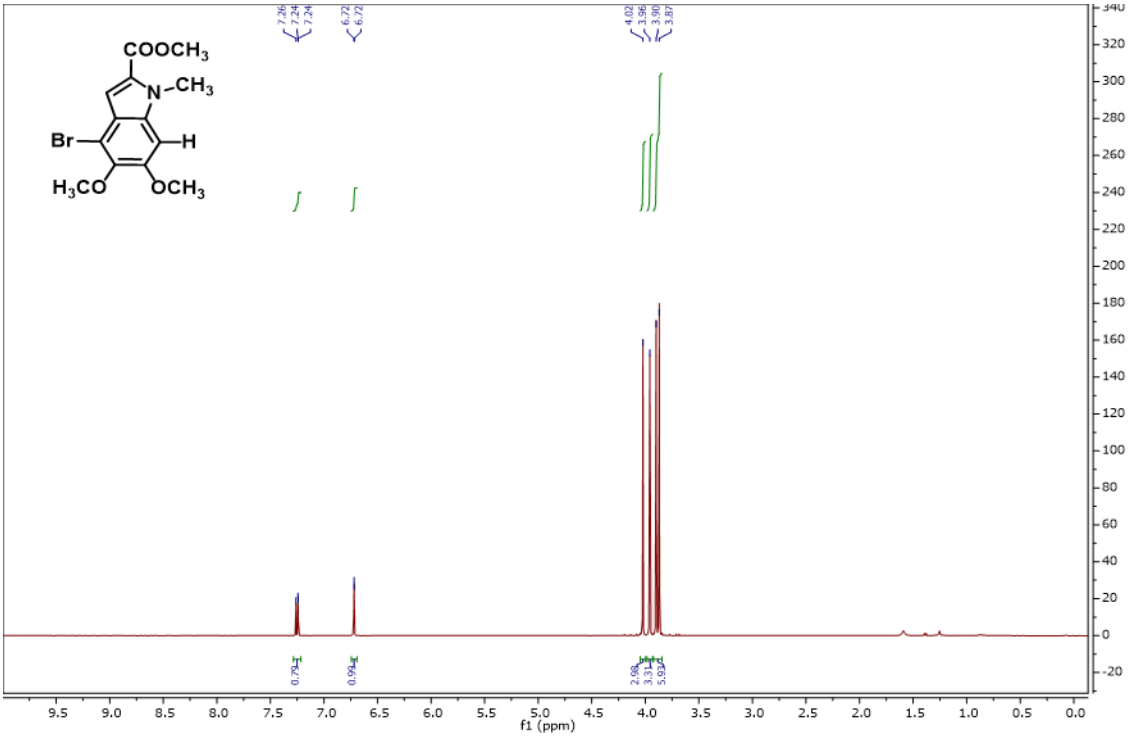

^{13}C NMR of 7*H* DBI

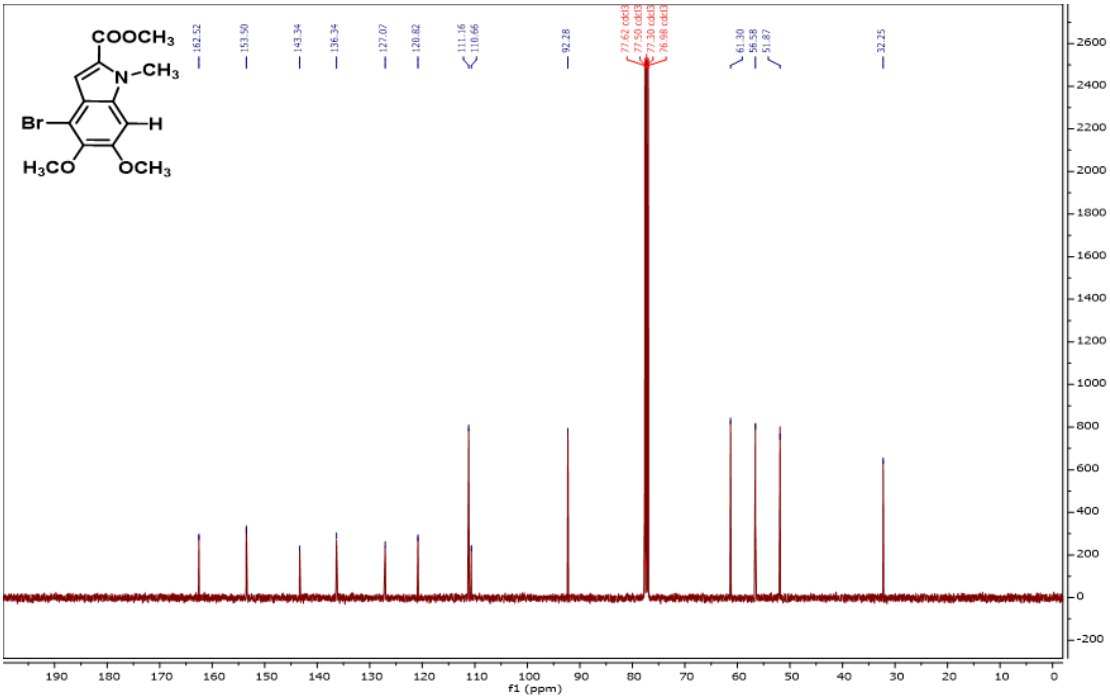

^{1}H {^{13}C} HSQC spectrum of 7*H*-DBI

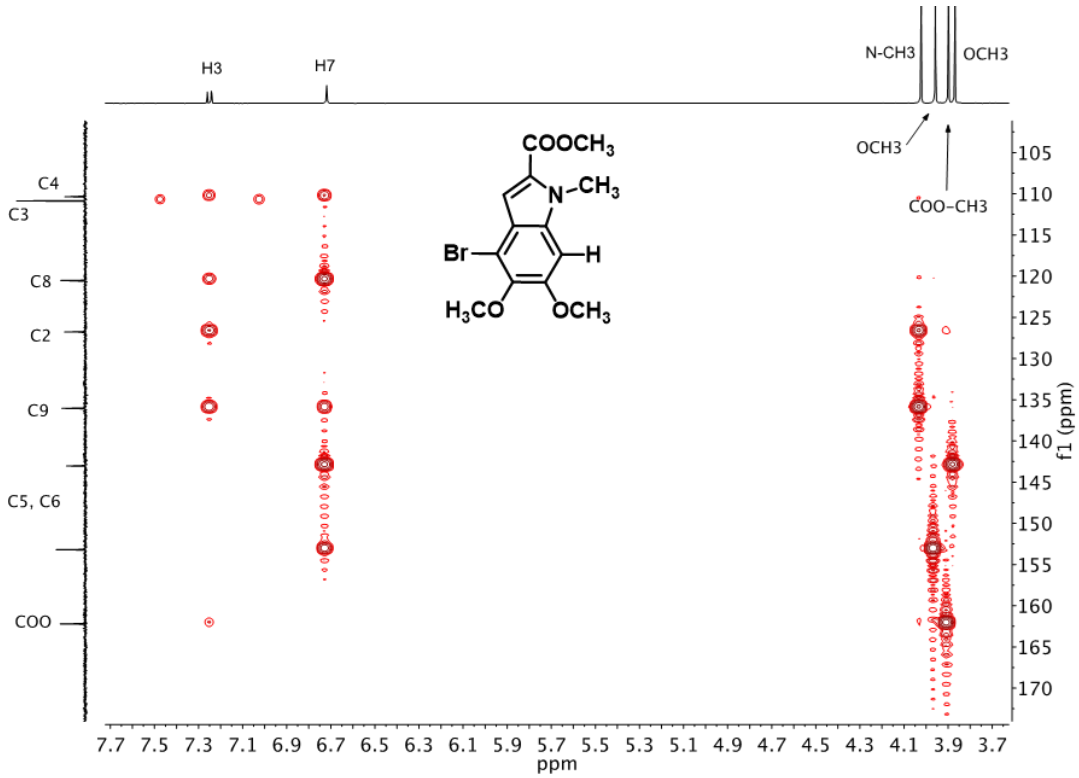

^{1}H {^{13}C} HMBC spectrum of 7*H*-DBI

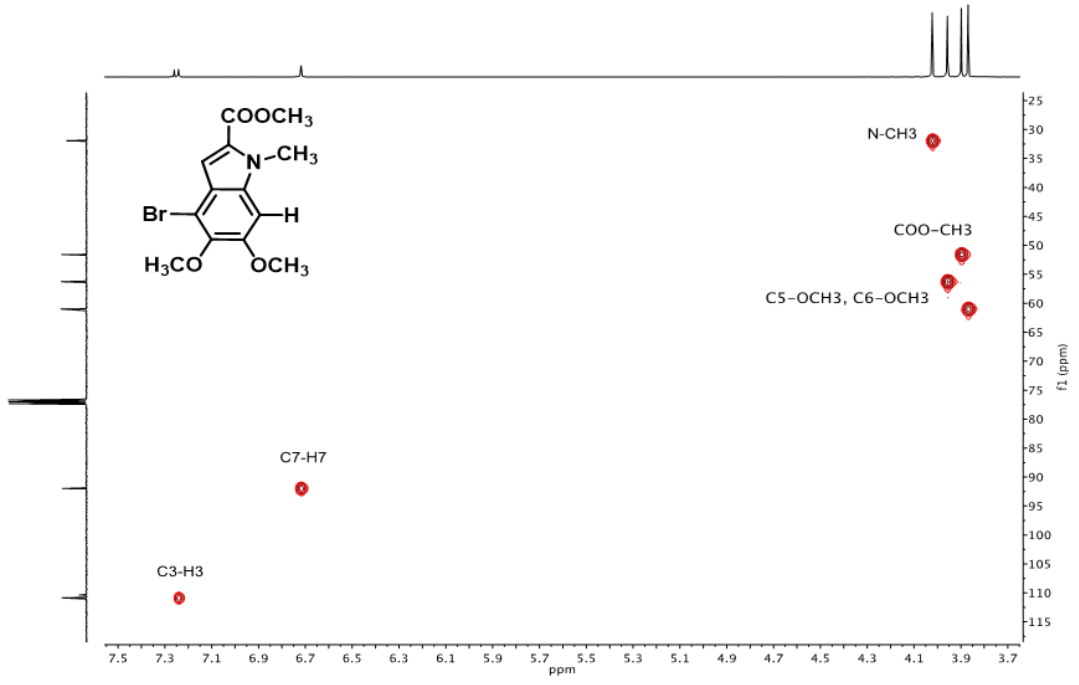

NOE experiment of 7*H*-DBI – 7-position H has irradiated and peaks for N-CH_3 and –OCH_3 at 6-position has enhanced.

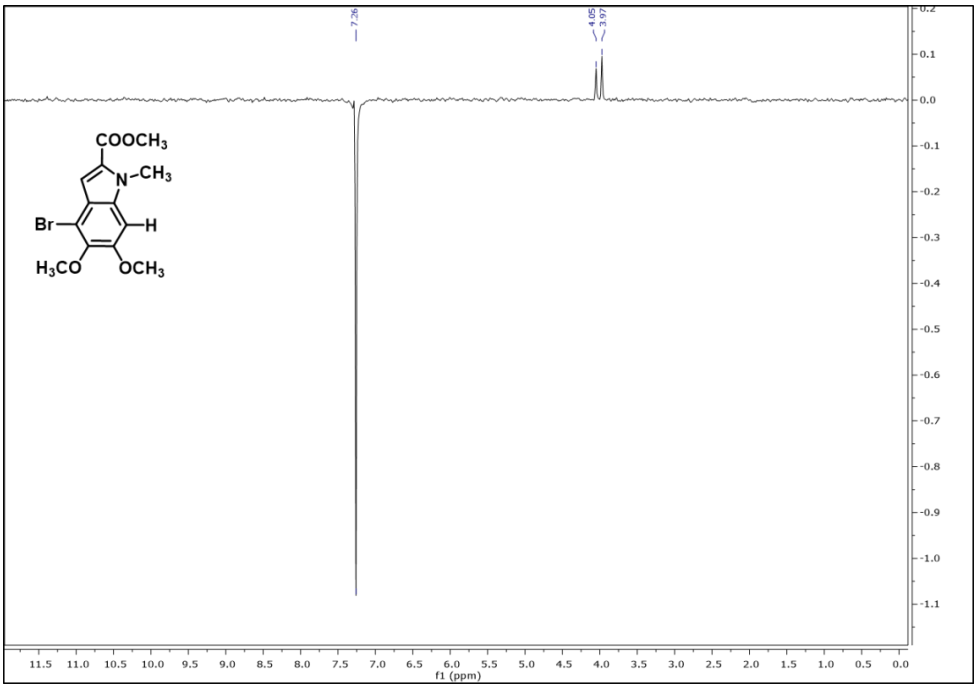

^{1}H NMR of 7-borylated DMICE

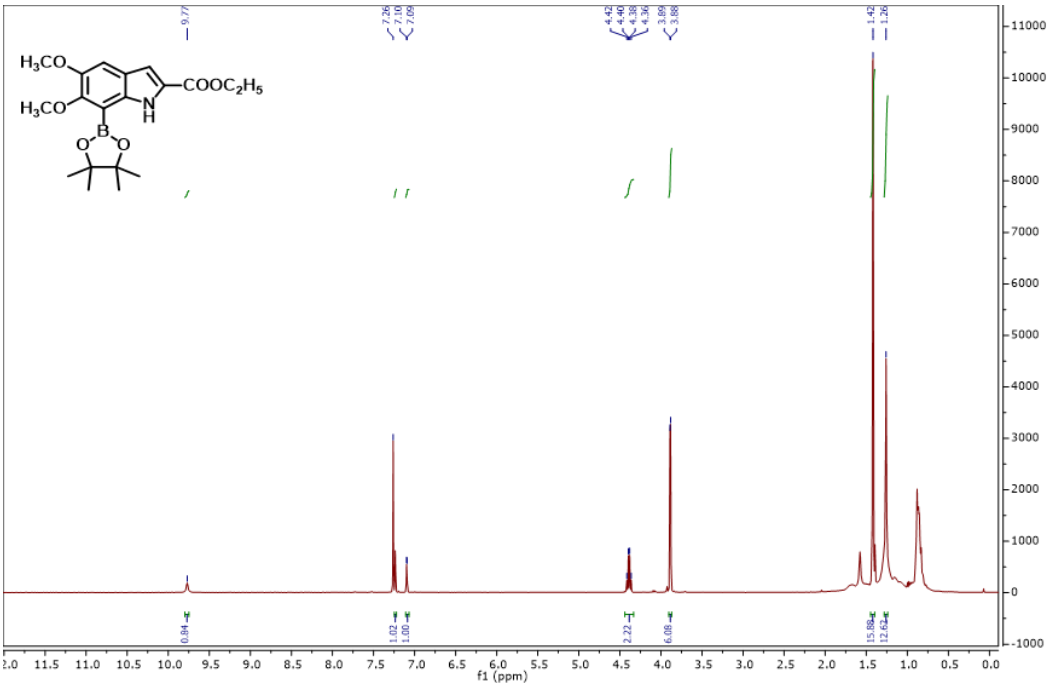

^{13}C NMR of 7-borylated DMICE

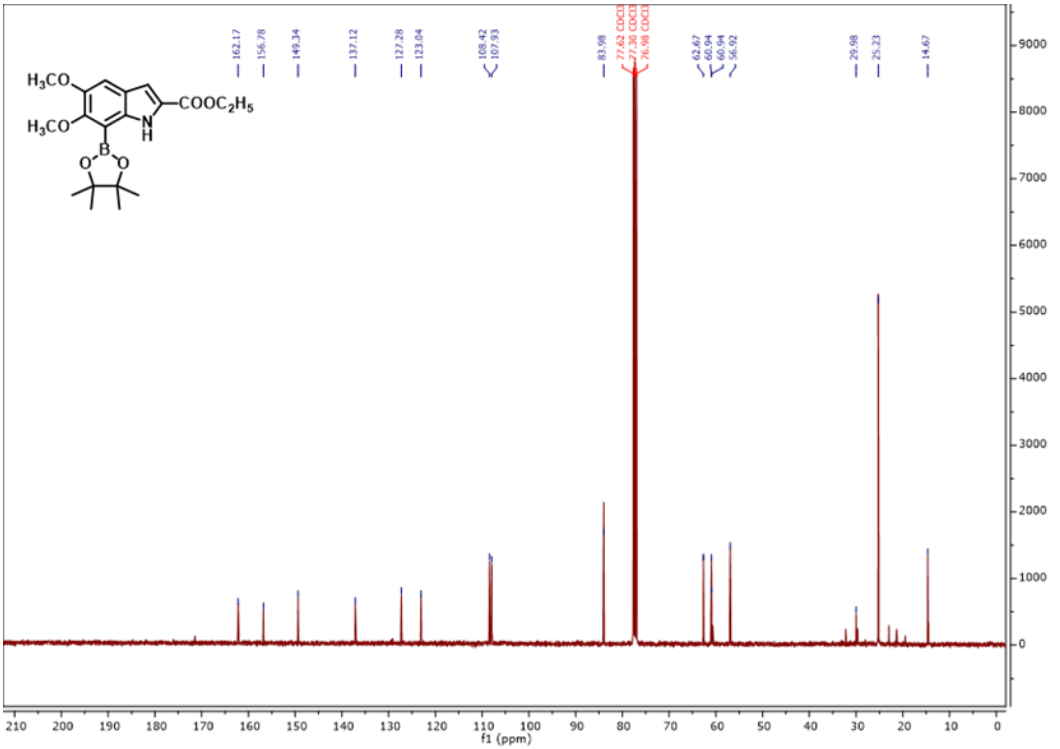

^{1}H NMR of dimer

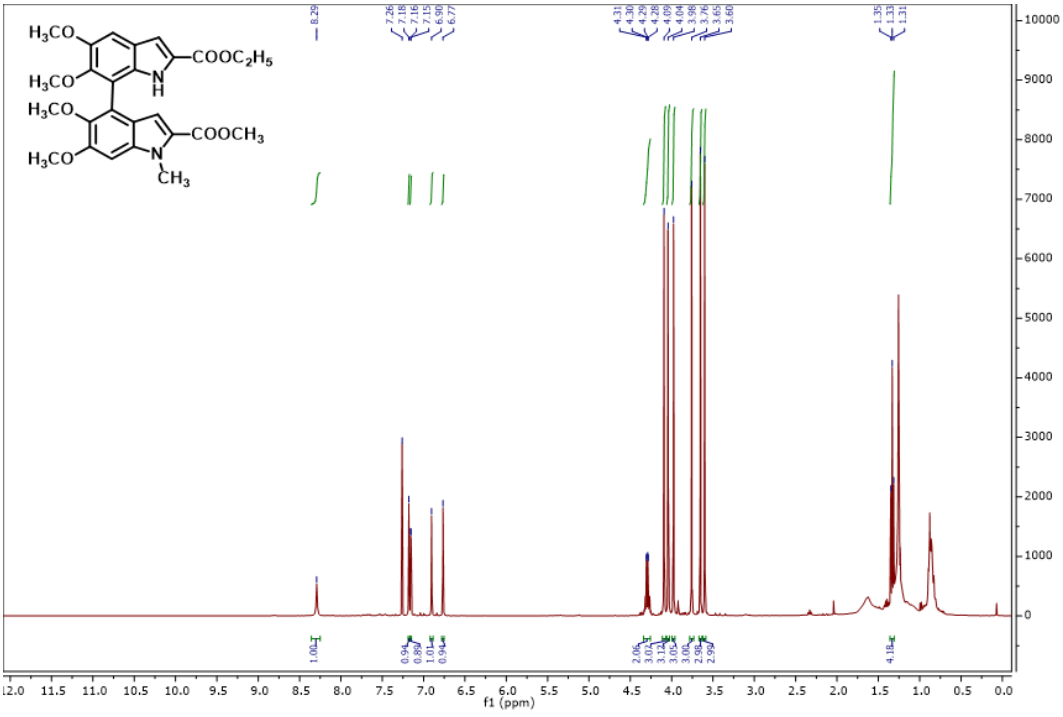

^{13}C NMR of dimer

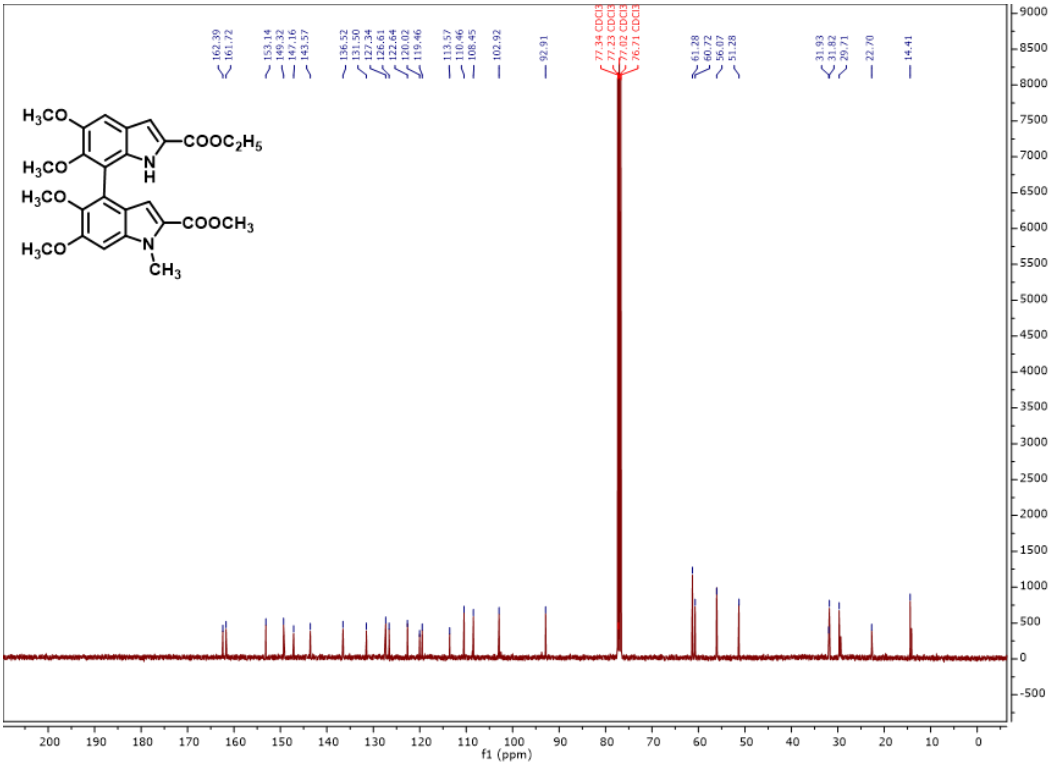

5.6. REFERENCES

1. Land, E. J.; Ramsden, C. A.; Riley, P. A., Tyrosinase autoactivation and the chemistry of ortho-quinone amines. *Accounts of Chemical Research* **2003,** *36* (5), 300-308.
2. d'Ischia, M.; Napolitano, A.; Pezzella, A.; Land, E. J.; Ramsden, C. A.; Riley, P. A., 5,6-Dihydroxyindoles and indole-5,6-diones. In *Adv. Heterocycl. Chem.*, Alan, R. K., Ed. Academic Press: 2005; Vol. Volume 89, pp 1-63.
3. Ju, K.-Y.; Lee, Y.; Lee, S.; Park, S. B.; Lee, J.-K., Bioinspired polymerization of dopamine to generate melanin-like nanoparticles having an excellent free-radical-scavenging property. *Biomacromolecules* **2011,** *12* (3), 625-632.
4. D'Ischia, M.; Crescenzi, O.; Pezzella, A.; Arzillo, M.; Panzella, L.; Napolitano, A.; Barone, V., Structural effects on the electronic absorption properties of 5,6-dihydroxyindole oligomers: The potential of an integrated experimental and DFT approach to model eumelanin optical properties†. *Photochem. Photobiol.* **2008,** *84* (3), 600-607.
5. Meredith, P.; Riesz, J., Radiative relaxation quantum yields for synthetic eumelanin¶. *Photochem. Photobiol.* **2004,** *79* (2), 211-216.
6. d'Ischia, M.; Napolitano, A.; Pezzella, A.; Meredith, P.; Sarna, T., Chemical and structural diversity in eumelanins – unexplored bio-optoelectronic materials. *Angewandte Chemie (International ed. in English)* **2009,** *48* (22), 3914-3921.

7. Jastrzebska, M. M.; Isotalo, H.; Paloheimo, J.; Stubb, H., Electrical conductivity of synthetic DOPA-melanin polymer for different hydration states and temperatures. *J. Biomater. Sci. Polym. Ed.* **1996,** *7* (7), 577-586.
8. McGinness, J.; Corry, P.; Proctor, P., Amorphous semiconductor switching in melanins. *Science* **1974,** *183* (4127), 853-855.
9. Mostert, A. B.; Powell, B. J.; Pratt, F. L.; Hanson, G. R.; Sarna, T.; Gentle, I. R.; Meredith, P., Role of semiconductivity and ion transport in the electrical conduction of melanin. *Proceedings of the National Academy of Sciences* **2012,** *109* (23), 8943-8947.
10. Meredith, P.; Sarna, T., The physical and chemical properties of eumelanin. *Pigment Cell Res.* **2006,** *19* (6), 572-594.
11. Selvaraju, S.; Niradha Sachinthani, K. A.; Hopson, R. A.; McFarland, F. M.; Guo, S.; Rheingold, A. L.; Nelson, T. L., Eumelanin-inspired core derived from vanillin: a new building block for organic semiconductors. *Chemical Communications* **2015,** *51* (14), 2957-2959.
12. Osaka, I.; McCullough, R. D., Advances in molecular design and synthesis of regioregular polythiophenes. *Accounts of Chemical Research* **2008,** *41* (9), 1202-1214.
13. Huang, L.; Wu, S.; Qu, Y.; Geng, Y.; Wang, F., Grignard metathesis chain-growth polymerization for polyfluorenes. *Macromolecules* **2008,** *41* (22), 8944-8947.
14. Stefan, M. C.; Javier, A. E.; Osaka, I.; McCullough, R. D., Grignard metathesis method (GRIM): toward a universal method for the synthesis of conjugated polymers. *Macromolecules* **2008,** *42* (1), 30-32.
15. Duong, H. A.; Chua, S.; Huleatt, P. B.; Chai, C. L. L., Synthesis of biindolyls via palladium-catalyzed reactions. *The Journal of Organic Chemistry* **2008,** *73* (22), 9177-9180.
16. Wakim, S.; Blouin, N.; Gingras, E.; Tao, Y.; Leclerc, M., Poly(2,7-carbazole) Derivatives as semiconductors for organic thin-film transistors. *Macromolecular Rapid Communications* **2007,** *28* (17), 1798-1803.
17. Sergent, A.; Zucchi, G.; Pansu, R. B.; Chaigneau, M.; Geffroy, B.; Tondelier, D.; Ephritikhine, M., Synthesis, characterization, morphological behaviour, and photo- and electroluminescence of highly blue-emitting fluorene-carbazole copolymers with alkyl side-chains of different lengths. *Journal of Materials Chemistry C* **2013,** *1* (19), 3207-3216.
18. Watanabe, M.; Tsuchiya, K.; Shinnai, T.; Kijima, M., Liquid Crystalline polythiophene bearing phenylnaphthalene side-chain. *Macromolecules* **2012,** *45* (4), 1825-1832.
19. Paul, S.; Chotana, G. A.; Holmes, D.; Reichle, R. C.; Maleczka, R. E.; Smith, M. R., Ir-catalyzed functionalization of 2-substituted indoles at the 7-position: nitrogen-directed aromatic borylation. *J. Am. Chem. Soc.* **2006,** *128* (49), 15552-15553.

CHAPTER VI

SYNTHESIS AND OPTICAL PROPERTIES OF BENZODITHIOPHENE-S,S-TETRAOXIDE BASED SMALL MOLECULE AND POLYMER

6.1. INTRODUCTION

Heteroarenes such as benzodithiophenes, benzobisthiazoles, and benzobisoxazoles are essential building blocks used in organic electronic devices like organic photovoltatics, batteries, organic field-effect transistors and organic light-emitting diodes.[1-9] To the best of our knowledge, benzo[1,2-*b*:4,5-*b*']dithiophene-1,1,5,5-tetraoxide (hereafter referred to as benzodithiophene-*S*,*S*-tetraoxide (BDTT)) has seen very limited utility as a building block for the synthesis of organic semiconductors despite it being an electron poor heterocycle with promise for development of electron acceptor materials.[10-12] This lack of effort is likely due to the difficulties of precursor syntheses for carbon-carbon cross coupling reactions that result in low yields.[12] Therefore, we saw an opportunity to employ a more efficient method for the synthesis of 2,6-diarylbenzodithiophene-*S*,*S*-tetraoxide. An efficient copper-catalyzed direct arylation reaction for the regioselective functionalization of BDTT has been developed by Nelson and coworkers.[13] With the optimized

reaction conditions, BDTT was coupled with various aryl iodides to demonstrate the broad scope of the reaction. This optimized condition was also tested using bromobenzene but only starting material was recovered. The reaction's specificity for aryl iodides over the bromides provided an opportunity for the synthesis of new BDTT based small molecules and polymers. Synthesis and optical properties of BDTT-fluorene small molecule and polymer are discussed in this chapter.

6.2. RESULTS AND DISCUSSION

Benzodithiophene-*S,S*-tetraoxide can be characterized as an electron deficient core due to low-lying lowest occupied molecular orbital of and was synthesized according to literature.[14-15] Fluorene is well known as electron rich arene. To illustrate the utility of our copper catalyzed direct arylation reaction's specificity for aryl iodides over the bromides, the donor-acceptor-donor (D-A-D) triad **17** and donor-acceptor (D-A) polymer **18** were synthesized. Compound **16** was synthesized by reacting BDTT with 4-bromo-1-iodobenzene under our copper catalyzed direct arylation condition.[13] In **Scheme 6.1**, the donor-acceptor-donor triad **17** was synthesized by reacting **16** with 9,9-dioctylfluorene-2-boronic acid pinacol ester and the donor-acceptor polymer **18** was synthesized by reacting **16** with 9,9-dioctylfluorene-2,7-diboronic acid bis(1,3-propanediol) ester under Suzuki cross coupling conditions The triad was obtained in 52% isolated yield and poly(benzodithiophene-*S,S*-tetraoxide diphenylene-*co*-fluorene) was isolated in a lower yield (35%). The number averaged molecular weight (M_n) of the polymer was 12.0 kDa and the PDI was 2.84. The low M_n may be due to the low solubility of the polymer in the reaction mixture. There was noticeable precipitation of polymer from the reaction mixture after 24 h which will result in low yields and lower molecular weights.

The optical properties of the two compounds were determined with the UV-vis absorption in $CHCl_3$ and thin films as well as the fluorescence in $CHCl_3$ are shown in **Figure 6.1.**

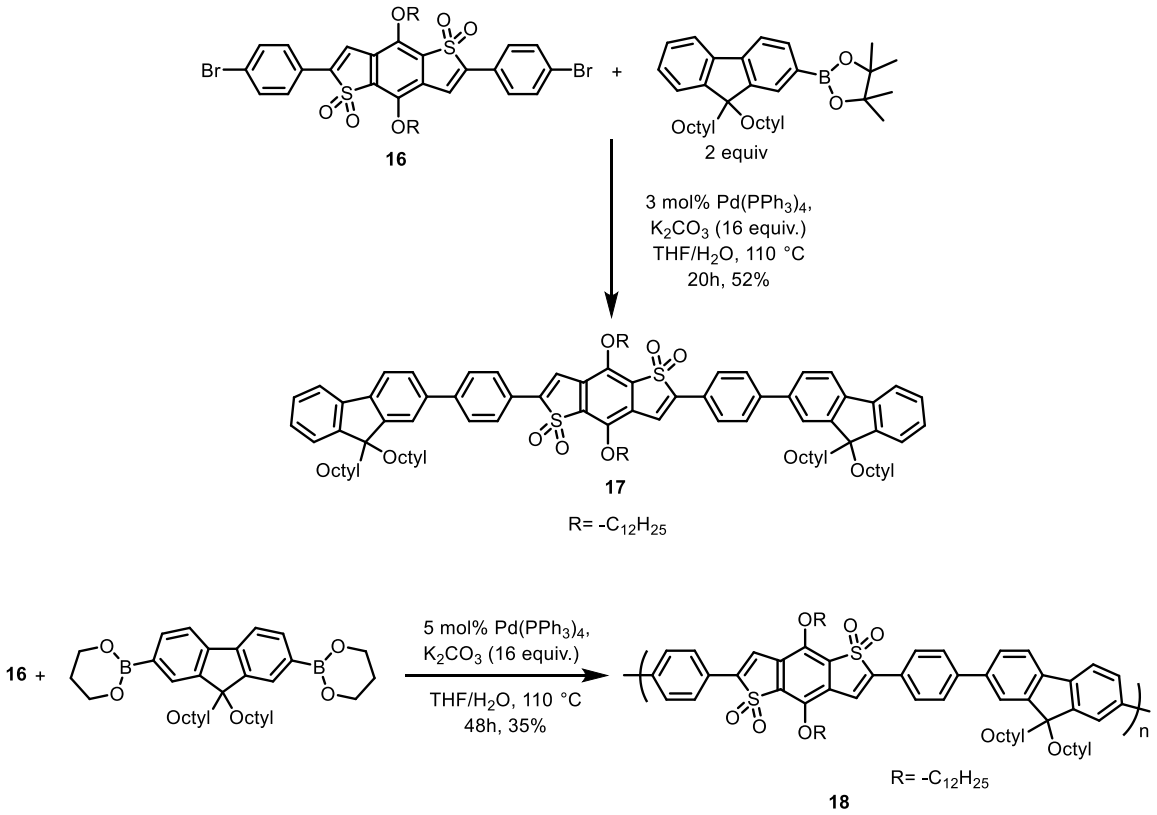

Scheme 6.1. Synthesis of BDTT based donor-acceptor **17** and donor-acceptor polymer **18**

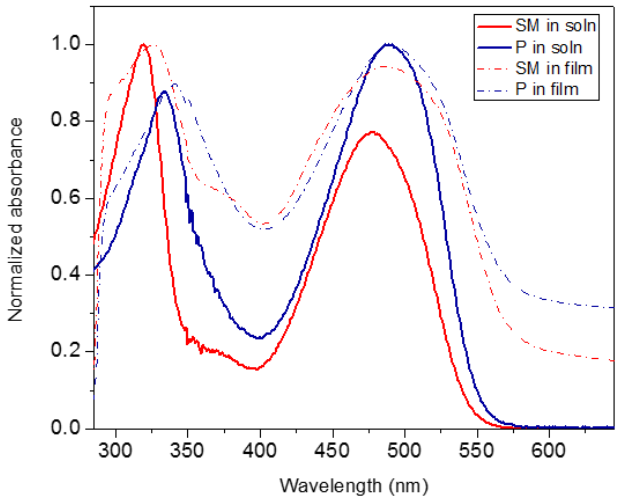

Figure 6.1. A). Absorption spectra of small molecule (**SM**) **17** and polymer (**P**) **18** in solution ($CHCl_3$, solid lines) and thin film (cast from $CHCl_3$, dashed lines)

The absorption spectrum of the D-A-D triad in solution showed two distinct maxima at 319 nm and 478 nm. These two prominent absorption peaks are a common feature for most of the D-A systems.[16-18] The 319 nm peak in the absorption spectrum of SM in dilute solution can be assigned to the π-π* transition whereas the 478 nm peak is due to intramolecular charge transfer (ICT) between the fluorene donor and the BDTT based core acceptor moieties. The absorption of the polymer in solution showed a bathochromic shift compared to the absorbance of SM, due to the increased conjugation length. Similarly, the absorption of the copolymer was characterized by two peaks, one at 334 nm and the other at 488 nm. The former peak can be assigned to π-π* transition whereas the lowest energy band is due to ICT between the donor and the acceptor moieties.[18]

Emission properties of these two compounds were measured and spectra are shown in **Figure 6.2**

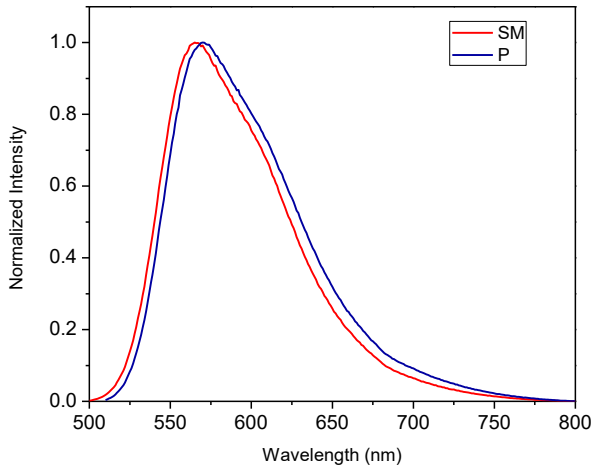

Figure 6.2. The fluorescence spectra of SM and polymer in $CHCl_3$. The excitation wavelength is 478 nm

The emission spectra of two compounds show a similar trend and the polymer spectrum showed a small bathochromic shift indicating the increased conjugation length. The maximum emission of SM and polymer is 565 nm and 570 nm respectively. These compounds dissolved in $CHCl_3$ are

orange in color under visible light and show yellow color emission under 365 nm UV light as shown in **Figure 6.3.**

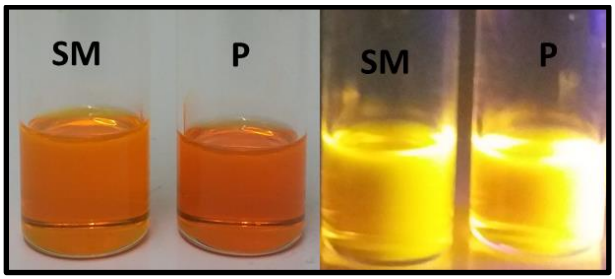

Figure 6.3. Compounds dissolved in chloroform under visible light (left) and under UV light (365 nm)

The optical bandgaps were calculated from a graph of absorption in the thin films, wavelengths corresponding to the energy absorption were measured from the intersection of the leading edge tangent with the *x*-axis. The absoption onsets of SM and P are around 585 nm and 597 nm; thus the optical band gaps (E_g^{opt}) are 2.11 eV and 2.07 eV which is reasonably common in D-A systems.[16,19]

6.3 SUMMARY AND OUTLOOK

The utility of the BDTT based core containing bromine end groups were demonstrated by synthesizing the D-A-D triad and the D-A polymer via Pd(0) catalyzed Suzuki polymerization reaction. The SM and polymer showed interesting absorption and emission properties which are comparable with the other D-A systems. These SMs and polymers showed lower optical band gaps which is promising for solar cell applications.

6.4 EXPERIMENTAL SECTION

6.4.1. Materials

Compound **16** was synthesized according to the previously reported procedure.[13] 9,9-Dioctylfluorene-2,7-diboronic acid bis(1,3-propanediol) ester and 9,9-Dicotylfluorene-2-boronic

acid pinacol ester were purchased from Sigma Aldrich. These compounds were used as received. Anhydrous tetrahydrofuran (THF) and chloroform ($CHCl_3$) were obtained from the solvent purification system under ultrapure argon. Distilled water was degassed with argon by sonicating the flask.

6.4.2. Instrumentation

^1H, and ^{13}C NMR experiments were done to confirm the structures of the compounds. All spectra were acquired on a Varian Inova 400 MHz spectrometer using a OneNMR probe, with nominal temperature setting of 25 °C and chemical shifts were given with respect to TMS ($\delta = 0$ ppm). GPC was performed using a Waters 1515 isocratic pump with a Waters 2410 refractive index detector. THF was used as the solvent at 35 °C with a flow rate of 1.0 mL/min. The polymer molecular weights were estimated with reference to the polystyrene standards. UV–Visible and fluorescence spectra were recorded on a Cary 5000 UV–VIS NIR spectrophotometer and a Cary Eclipse fluorescence spectrophotometer, respectively. Absorption and emission measurements were obtained using compounds in $CHCl_3$ solutions and in thin films which were dropcasted from these solutions.

6.4.3. Synthesis procedures

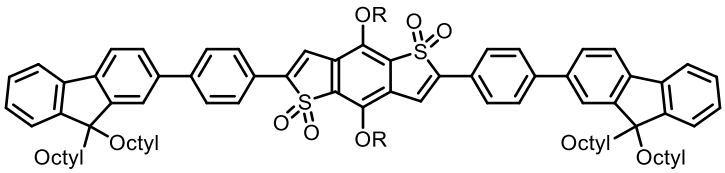

17

2,6-Bis(4-(9,9-dioctyl-9*H*-fluoren-2-yl)phenyl)-4,8-bis(dodecyloxy)benzo[1,2-b:4,5-b']dithiophene-1,1,5,5-tetraoxide (17): In a 10 mL Schlenk flask were added 2,6-Bis(4-bromophenyl)-4,8-bis(dodecyloxy)benzo[1,2-b:4,5-b']dithiophene 1,1,5,5-tetraoxide (50.0 mg,

0.054 mmol), 9,9-dioctylfluorene-2-boronic acid pinacol ester (56.7 mg, 0.109 mmol), $Pd(PPh_3)_4$ (1.8 mg, 3 mol %) and potassium carbonate (123.3 mg, 0.894 mmol) inside the glove box. A condenser with a septum on was connected at the top of the flask. Vacuum was applied to the reaction for 15 min and then it was filled with Ar. Dry THF (1.5 mL) and degassed distilled water (1.5 mL) was added in to the reaction outside the glovebox. The reaction flask was heated to 110 °C for 20 h. After 20 h, distilled water (10 mL) was added to the reaction flask, and crude product was extracted in to ethyl acetate (15 mL x 3). The organic layer was washed with saturated sodium chloride (15 mL x 2) and dried over anhydrous Na_2SO_4. Then the solvent was evaporated and the resulting residue was purified by column chromatography with silica column using dichloromethane/hexanes (2:3), followed by recrystallization with dichloromethane and methanol to afford an orange colored solid. (43.0 mg, 52%) ^{1}H NMR (400 MHz, CDCl3) δ 7.93 (s, 4H), 7.84– 7.56 (m, 12H), 7.49 (s, 2H), 7.36 (s, 6H), 4.55 (s, 4H), 1.99 (s, 12H), 1.57 (s, 9H), 1.17 (d, *J* = 85.6 Hz, 76H), 0.84 (d, *J* = 23.8 Hz, 19H), 0.68 (s, 8H). ^{13}C NMR (101 MHz, $CDCl_3$) δ 151.84, 151.30, 145.33, 144.25, 142.68, 141.56, 140.65, 138.70, 131.94, 128.15, 127.89, 127.57, 127.35, 127.08, 126.20, 125.62, 123.16, 121.60, 120.34, 120.13, 117.98, 55.42, 40.55, 32.15, 31.99, 30.26, 30.22, 29.92, 29.89, 29.86, 29.83, 29.60, 29.43, 29.41, 26.07, 24.01, 22.92, 22.82, 14.36, 14.30. HRMS (m/z): calcd. 1574.0140; found, 1575.0169

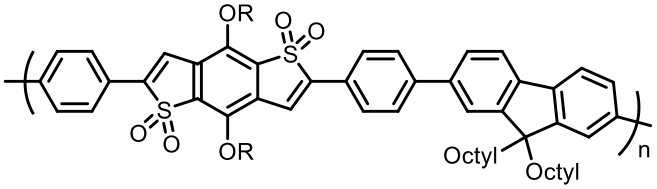

R= $C_{12}H_{25}$

18

Poly(benzodithiophene-*S,S*-tetraoxide diphenylene-*co*-fluorene)(18): To a 10 mL microwave vial were added 2,6-Bis(4-bromophenyl)-4,8-bis(dodecyloxy)benzo[1,2-b:4,5-b']dithiophene 1,1,5,5-tetraoxide (20 mg, 0.027 mmol), 9,9-Dioctylfluorene-2,7-diboronic acid bis(1,3-

propanediol) ester (12 mg, 0.027 mmol), $Pd(PPh_3)_4$ (1.2 mg, 5 mol %) and potassium carbonate (49 mg, 0.447 mmol) inside the glove box and sealed it with a crimp cap. Vacuum was applied to the reaction for 15 min and then it was filled with Ar. Dry THF (1.0 mL) and degassed distilled water (1.0 mL) was added in to the reaction outside the glove box. The reaction was heated to 110 °C for 48 h. Then, 6N HCl (8 mL) was added to the reaction vial, and crude product was extracted in to ethyl acetate (15 mL x 3). The organic layer was washed with saturated sodium chloride (15 mL x 2) and dried over anhydrous Na_2SO_4. Then the solvent was evaporated and the resulting residue was redissolved in THF (1.0 mL) and precipitated in methanol (15.0 mL). The precipitate was collected by filtering through a pipette having a cotton plug. The polymer precipitate was further purified by washing the pipette containing the polymer solid with hot methanol followed by hot hexanes. Then, the polymer was eluted by adding hot chloroform through the pipette and chloroform was evaporated to reduce the amount of chloroform. This concentrated polymer solution was re precipitated on methanol to obtain a dark orange polymer as a solid (10 mg, 35%). ^{1}H NMR (400 MHz, $CDCl_3$) δ 7.95 (t, *J* = 8.9 Hz, 3H), 7.87 – 7.77 (m, 5H), 7.63 (dd, *J* = 18.2, 7.3 Hz, 5H), 7.56 – 7.46 (m, 5H), 4.57 (t, *J* = 6.2 Hz, 4H), 2.17 – 1.88 (m, 8H), 1.67 – 1.50 (m, 8H), 1.49 – 0.99 (m, 52H), 0.88 (t, *J* = 5.9 Hz, 6H), 0.81 (t, *J* = 6.9 Hz, 6H). M_n = 12.0 and PDI = 2.84.

6.4.4. NMR spectra

^{1}H NMR of **17**

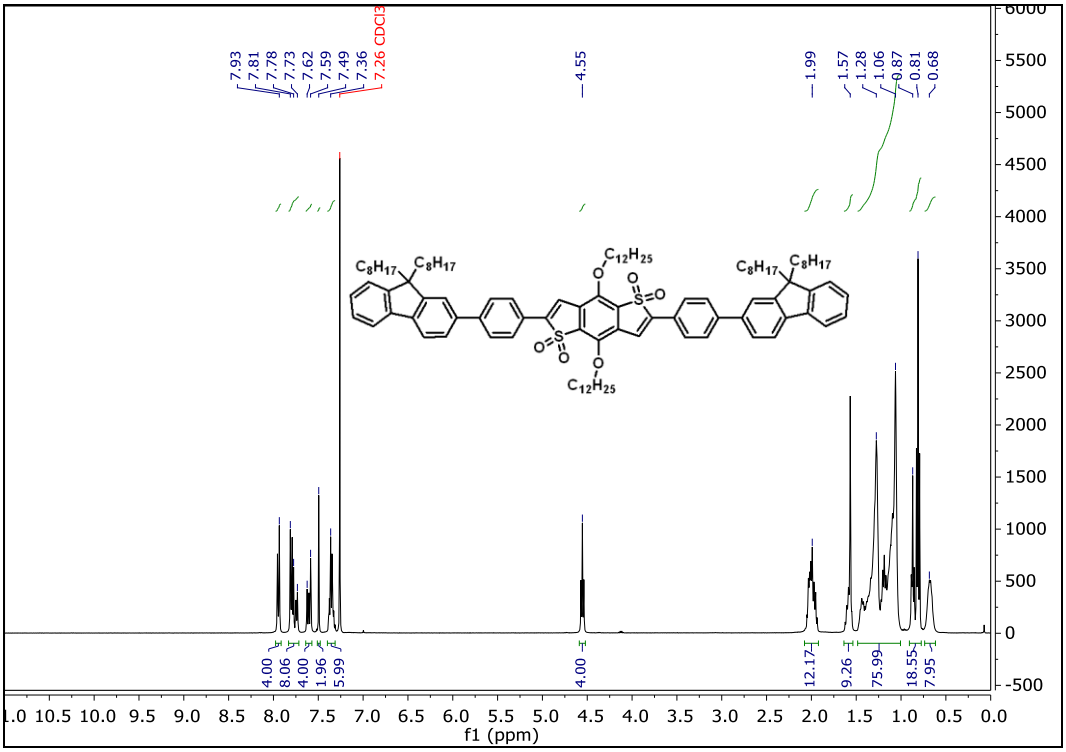

^{13}C NMR of **17**

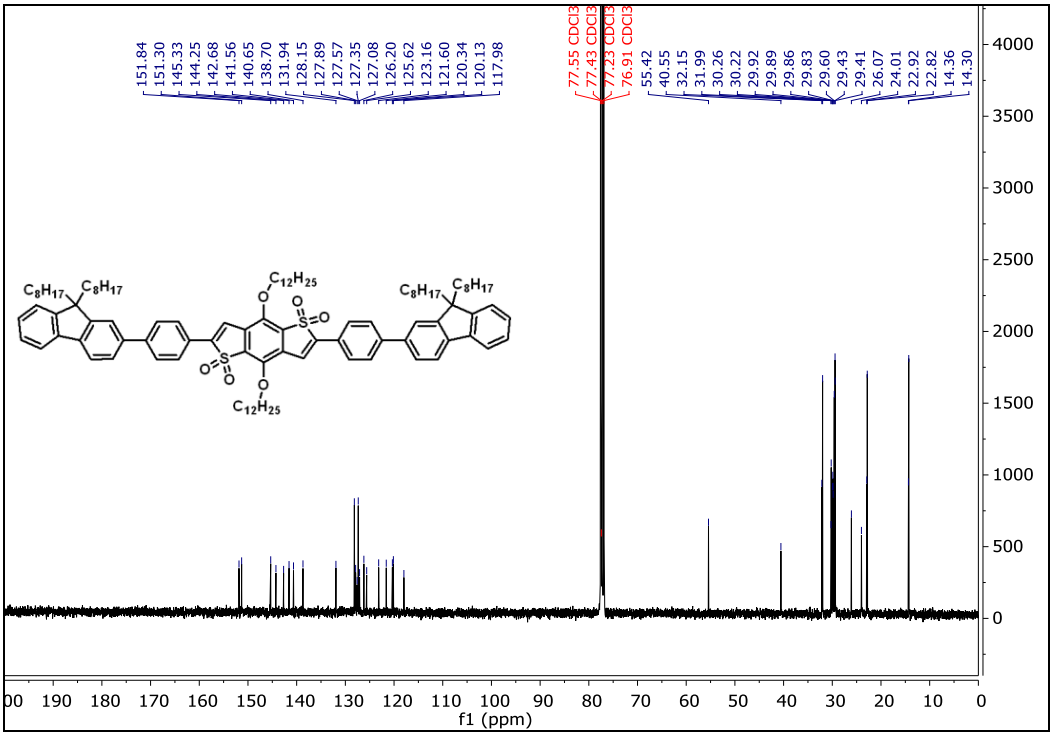

^{1}H NMR of **18**

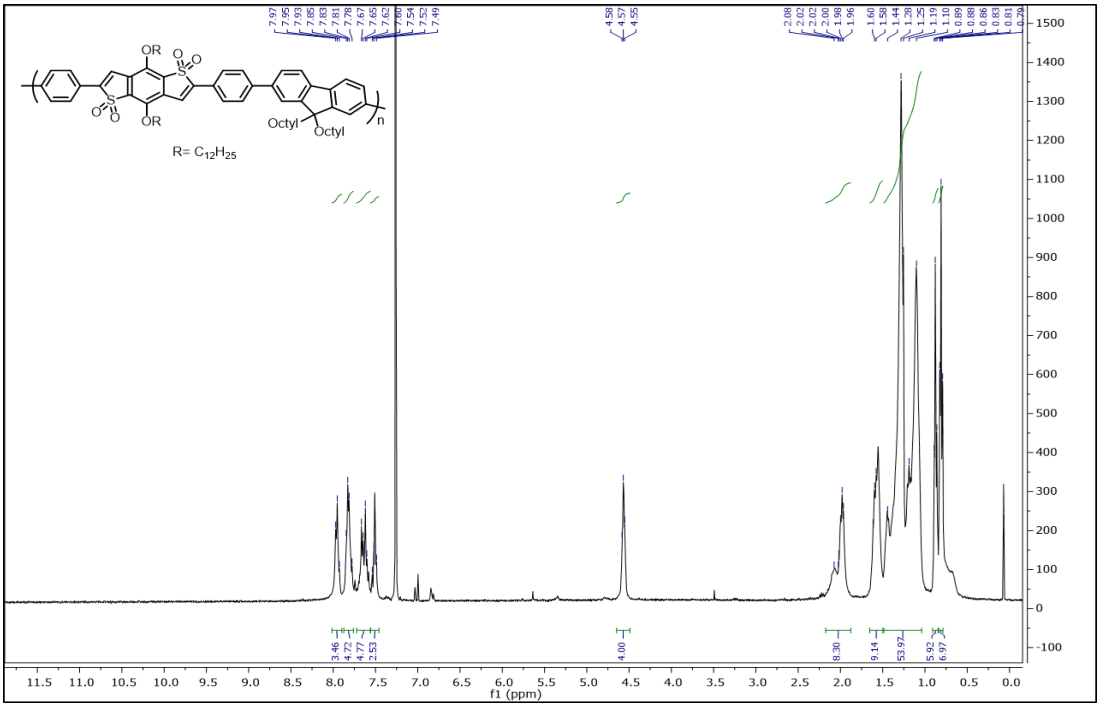

6.4. REFERENCES

1. Ahmed, E.; Subramaniyan, S.; Kim, F. S.; Xin, H.; Jenekhe, S. A., Benzobisthiazole-based donor–acceptor copolymer semiconductors for photovoltaic cells and highly stable field-effect transistors. *Macromolecules* **2011,** *44* (18), 7207-7219.
2. Bhuwalka, A.; Mike, J. F.; He, M.; Intemann, J. J.; Nelson, T.; Ewan, M. D.; Roggers, R. A.; Lin, Z.; Jeffries-El, M., Quaterthiophene–benzobisazole copolymers for photovoltaic cells: effect of heteroatom placement and substitution on the optical and electronic properties. *Macromolecules* **2011,** *44* (24), 9611-9617.
3. Laquindanum, J. G.; Katz, H. E.; Lovinger, A. J.; Dodabalapur, A., Benzodithiophene rings as semiconductor building blocks. *Advanced Materials* **1997,** *9* (1), 36-39.
4. Zhou, J.; Zuo, Y.; Wan, X.; Long, G.; Zhang, Q.; Ni, W.; Liu, Y.; Li, Z.; He, G.; Li, C.; Kan, B.; Li, M.; Chen, Y., Solution-processed and high-performance organic solar cells using small molecules with a benzodithiophene unit. *Journal of the American Chemical Society* **2013,** *135* (23), 8484-8487.
5. Intemann, J. J.; Hellerich, E. S.; Tlach, B. C.; Ewan, M. D.; Barnes, C. A.; Bhuwalka, A.; Cai, M.; Shinar, J.; Shinar, R.; Jeffries-El, M., Altering the conjugation pathway for improved performance of benzobisoxazole-based polymer guest emitters in polymer light-emitting diodes. *Macromolecules* **2012,** *45* (17), 6888-6897.
6. Chavez Iii, R.; Cai, M.; Tlach, B.; Wheeler, D. L.; Kaudal, R.; Tsyrenova, A.; Tomlinson, A. L.; Shinar, R.; Shinar, J.; Jeffries-El, M., Benzobisoxazole cruciforms: a tunable, cross-

conjugated platform for the generation of deep blue OLED materials. *Journal of Materials Chemistry C* **2016,** *4* (17), 3765-3773.
7. Bhuwalka, A.; Ewan, M. D.; Elshobaki, M.; Mike, J. F.; Tlach, B.; Chaudhary, S.; Jeffries-El, M., Synthesis and photovoltaic properties of 2,6-bis(2-thienyl) benzobisazole and 4,8-bis(thienyl)-benzo[1,2-B:4,5-B′]dithiophene copolymers. *Journal of Polymer Science Part A: Polymer Chemistry* **2016,** *54* (3), 316-324.
8. Hao, X.; Zhu, J.; Jiang, X.; Wu, H.; Qiao, J.; Sun, W.; Wang, Z.; Sun, K., Ultrastrong polyoxyzole nanofiber membranes for dendrite-proof and heat-resistant battery separators. *Nano Letters* **2016,** *16* (5), 2981-2987.
9. Hou, J.; Park, M.-H.; Zhang, S.; Yao, Y.; Chen, L.-M.; Li, J.-H.; Yang, Y., Bandgap and molecular energy level control of conjugated polymer photovoltaic materials based on benzo[1,2-b:4,5-b′]dithiophene. *Macromolecules* **2008,** *41* (16), 6012-6018.
10. Jung, I. H.; Lo, W.-Y.; Jang, J.; Chen, W.; Zhao, D.; Landry, E. S.; Lu, L.; Talapin, D. V.; Yu, L., Synthesis and search for design principles of new electron accepting polymers for all-polymer solar cells. *Chemistry of Materials* **2014,** *26* (11), 3450-3459.
11. Nandakumar, M.; Karunakaran, J.; Mohanakrishnan, A. K., Diels–alder reaction of 1,3-diarylbenzo[c]furans with thiophene S,S-Dioxide/Indenone derivatives: A facile preparation of substituted dibenzothiophene S,S-dioxides and fluorenones. *Organic Letters* **2014,** *16* (11), 3068-3071.
12. Pappenfus, T. M.; Seidenkranz, D. T.; Lovander, M. D.; Beck, T. L.; Karels, B. J.; Ogawa, K.; Janzen, D. E., Synthesis and electronic properties of oxidized benzo[1,2-b:4,5-b′]dithiophenes. *The Journal of Organic Chemistry* **2014,** *79* (19), 9408-9412.
13. Khambhati, D. P.; Sachinthani, K. A. N.; Rheingold, A. L.; Nelson, T. L., Regioselective copper-catalyzed direct arylation of benzodithiophene-S,S-tetraoxide. *Chemical Communications* **2017,** *53* (37), 5107-5109.
14. Nakabayashi, K.; Otani, H.; Mori, H., Benzodithiophene-based low band-gap polymers with deep HOMO levels: synthesis, characterization, and photovoltaic performance. *Polym J* **2015,** *47* (9), 617-623.
15. An, C.; Puniredd, S. R.; Guo, X.; Stelzig, T.; Zhao, Y.; Pisula, W.; Baumgarten, M., Benzodithiophene–thiadiazoloquinoxaline as an acceptor for ambipolar copolymers with deep LUMO level and distinct linkage pattern. *Macromolecules* **2014,** *47* (3), 979-986.
16. Jiang, D.; Xue, Z.; Li, Y.; Liu, H.; Yang, W., Synthesis of donor-acceptor molecules based on isoxazolones for investigation of their nonlinear optical properties. *Journal of Materials Chemistry C* **2013,** *1* (36), 5694-5700.
17. Pandey, L.; Risko, C.; Norton, J. E.; Brédas, J.-L., Donor–acceptor copolymers of relevance for organic photovoltaics: A theoretical investigation of the impact of chemical structure modifications on the electronic and optical properties. *Macromolecules* **2012,** *45* (16), 6405-6414.
18. Zhu, Y.; Champion, R. D.; Jenekhe, S. A., Conjugated donor−acceptor copolymer semiconductors with large intramolecular charge transfer: synthesis, optical properties, electrochemistry, and field effect carrier mobility of thienopyrazine-based copolymers. *Macromolecules* **2006,** *39* (25), 8712-8719.
19. Sun, Y.; Ding, X.; Zhang, X.; Huang, Q.; Lin, B.; Yang, H.; Guo, L., Indeno[1,2-b]fluorene-based novel donor–acceptor conjugated copolymers. *High Performance Polymers* **2017**, 0954008316688247.

CHAPTER VII

CONCLUSIONS AND FUTURE DIRECTIONS

7.1. INTRODUCTION

In this chapter, I have summerized all the chapters and have included some possible future directions of those projects.

7.2. CHAPTER 2: CONCLUSIONS AND FUTURE DIRECTIONS

In chapter 2, eumelanin-inspired novel core (DBI) was synthesized starting from vanillin and demonstrated its semiconducting properties by synthesizing poly(indoylenephenyleneethynylene) (PIPE) polymer. PIPE emits green light with the band gap of 2.03 eV and the fluorescence quantum yield is 0.60 which is considerably high value.

In the future, PIPE we made can be used as the emissive material to fabricate OLED devices. Our PIPE has dodecyl alkoxy side chains on the phenylene monomer, instead long branched alkoxy chains, such as ethylhexyl and octyldecyl, and can be used on the monomers. Long chain alkyl and alkoxy chains disrupt the π stacking between the polymer chains and make amorphous polymer

films,[1] which are desirable for OLEDs because they can prevent concentration quenching of emissive material.

7.3. CHAPTER 3: CONCLUSIONS AND FUTURE DIRECTIONS

In chapter 3, eumelanin-inspired blue emitting polymers were synthesized. Here two parameters were varied to investigate the effect on optical, electronic and physical properties of the polymers. The first parameter was the side chain on the monomer. PIF 1 and PIF 2 were synthesized by varying the side chain of the fluorene monomer by choosing two different linear alkyl chains, hexyl and octyl. There was no significant effect from these alkyl groups on the properties of those polymers. The second varied parameter was the arylene group attached to DBI. In this case, fluorene and carbazole were chosen as the two arylene units because they are widely used in the literature as the blue emitting materials. The different arylene groups on these two polymers did not significantly affect the physical and electronic properties but the fluorescence quantum yields of these two polymers were noteworthy.

In the future, the polymers can be end capped to improve the optoelectronic properties as well as avoiding unwanted side reactions possible when the polymers are annealed in the device fabrication process. Conventional Suzuki coupling polymerization takes place for 48 h to achieve high molecular weight polymers. However, using the microwave assisted synthesis, the polymerization can be completed in less than 1 h and even higher molecular weights can be achieved.[2]

7.4. CHAPTER 4: CONCLUSIONS AND FUTURE DIRECTIONS

In chapter 4, the electrogenerated chemiluminescence (ECL) of PIF 1 and PIC was studied to further evacuate their light emitting properties. The PIF 1 and PIC showed ECL values with the efficiencies of 6.1% and 0.4%, respectively, with reference to the standard compound 9,10-diphenylanthracene. Since the ECL efficiency of PIC is very low compared to PIF 1, the OLED

device fabrication was done only using PIF 1 as the emissive material. The maximum EQE of the OLED devices with PIF1 was 1.1% and showed CIE coordinates of (0.16, 0.07) which are much closer to the standard value for blue light. Few preliminary studies have been done with OLED device fabrication.

In the future, the performance of the OLED devices can be improved by optimizing conditions. One condition involves the thickness of the electron transporting layer (ETL). According to the literature, by changing the ETL layer thickness to certain values, the performances of blue emitting OLEDs can be enhanced.[3]

7.5. CHAPTER 5: CONCLUSIONS AND FUTURE DIRECTIONS

In chapter 5, eumelanin-inspired polyindole synthesis was attempted. The Grignard metathesis reaction of DBI resulted 7*H*-DBI with bromine at 4-position and H at 7-position. This 7*H*-DBI was coupled with the 7-borylated DMICE which was prepared by the Ir-catalyzed nitrogen directed borylation reaction via a Suzuki coupling reaction to obtain eumelanin-inspired dimer.

In the future, reacting 2 equivalents of 7-borylated DMICE with DBI, could produce in the trimer **19** (**Scheme 7.1**)

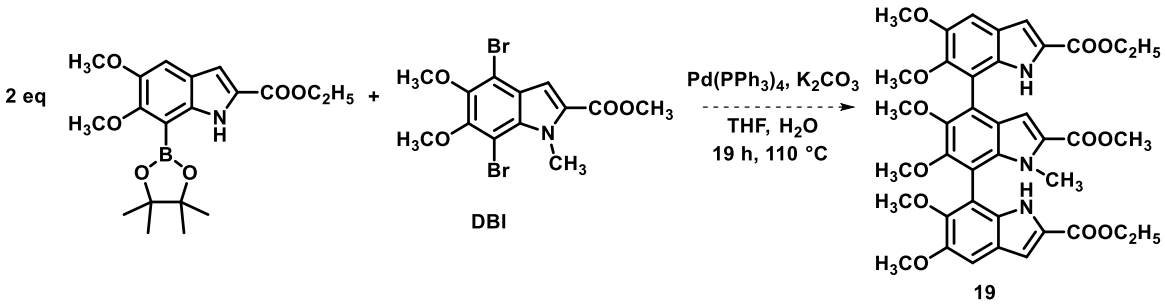

Scheme 7.1. The proposed synthesis of eumelanin-inspired trimer.

The 3-position of DMICE was brominated with *N*-bromosuccinimide to obtain ethyl 3-bromo-5,6-dimethoxy-1*H*-indole-2-carboxylate (3-bromoDMICE) which is shown in **Scheme 7.2.**

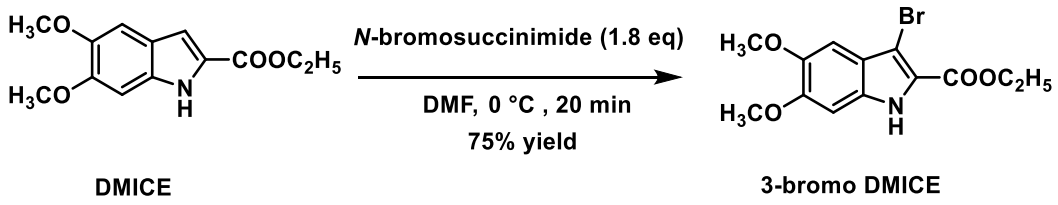

Scheme 7.2. The bromination of the 3-position of DMICE.

By the borylation of the 7-position of 3-bromoDMICE, ethyl 3-bromo-5,6-dimethoxy-7-(4,4,5,5-tetramethyl-1,3,2-dioxaborolan-2-yl)-1*H*-indole-2-carboxylate(7-borylated-3-bromo DMICE) might be obtained. It might also be possible to polymerize the compound under Suzuki conditions to obtain eumelanin-inspired polyindoles through the 3- and 7- positions. (**Scheme 7.3**).

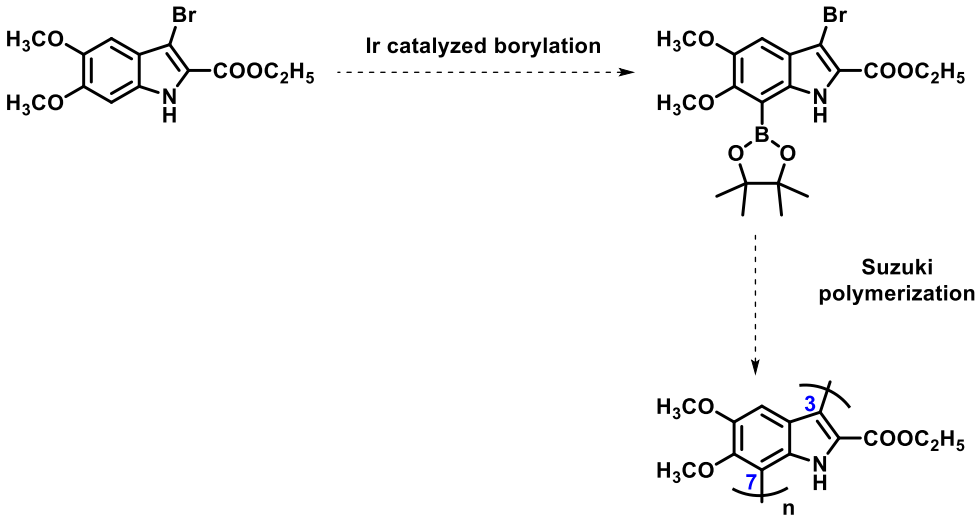

Scheme 7.3. The proposed synthesis of eumelanin-inspired polyindole through the 3- and 7-positions. The absorbance and fluorescence measurements will be performed with these new

eumelanin-inspired materials and compared with properties of natural eumelanin in order to better understand its structure property relationship.

7.6 CHAPTER 6: CONCLUSIONS AND FUTURE DIRECTIONS

In chapter 6, the synthesis and optical characterization of BDTT based donor-acceptor-donor small molecule and donor-acceptor polymer was accomplished. The specificity of the reaction of Cu catalyzed direct arylation of BDTT with aryl iodides over the bromides[4] provided compound **16** which could be further functionalized with conventional coupling methods. The utility of the compound **16** was demonstrated by coupling with a fluorene moiety via a Pd(0) catalyzed Suzuki coupling reaction. These two compounds showed interesting absorption and emission properties with low optical band gaps such as 2.11 eV for the small molecule and 2.07 eV for the polymer. The yield of the polymerization reaction was low which may be due to the less solubility of the polymer in the reaction.

In the future, the solubility of the polymer can be improved by introducing branched alkyl chains or alkoxy groups such as 2-ethylhexyl, octyldecyl and decyldodecyl instead of having a long akyl chain such as dodecyl on BDTT monomer. The band gap of BDTT based D-A polymers can be tailored by introducing strong electron donating arylene moieties.[5] A few thiophene-based strong electron donating groups[6] are shown in **Figure 7.1**. The compounds can be coupled with a BDTT-based core to achieve much lower band gaps.

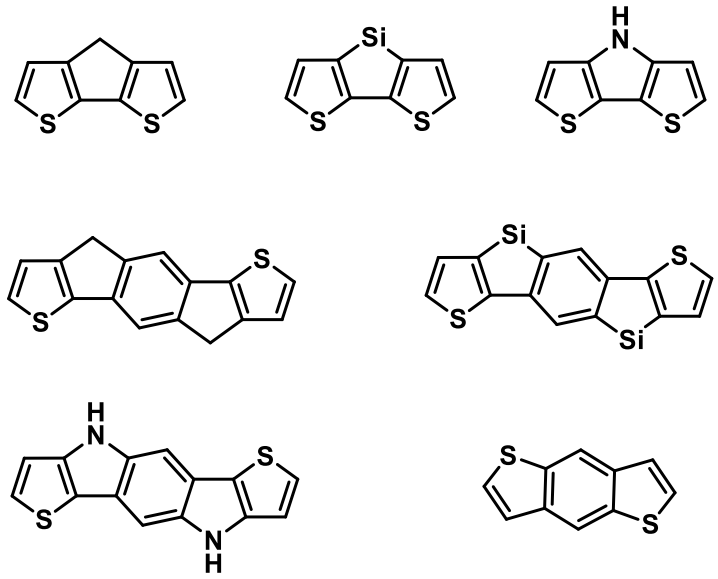

Figure 7.1. Thiophene based strong electron donating groups.

7.7. EXPERIMENTAL SECTION

7.7.1 Materials and Instrumentation

Chemicals for the synthesis were purchased from Oxchem and Alfa Aesar. DMICE was used as recieved and *N*-bromosuccinimide was recrystallized before use. The ^{1}H- and ^{13}C-NMR spectra were measured on a Bruker Avance 400 MHz instrument.

7.7.2. Synthesis procedure

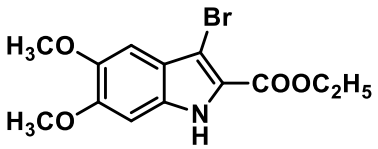

Ethyl 3-bromo-5,6-dimethoxy-1H-indole-2-carboxylate: To a 100mL round bottomed flask was added ethyl 5,6-dimethoxy-1*H*-indole-2-carboxylate (DMICE) (500 mg, 2.00 mmol) and dry DMF (20.0 mL). The mixture was stirred until the solid completely dissolved. Then, the reaction was

cooled to 0 °C and *N*-bromosuccinimide (505 mg, 2.83 mmol) was added in four portions over 10 min. After 20 min, the reaction was poured into ice and DI water mixture (200 mL) The solid formed was collected via the vacuum filtration. The product was dried under high vacuum to obtain a dark purple solid (492 mg, 75%).^{1}H NMR (400 MHz, $CDCl_3$) δ 8.94 (s, 1H), 6.97 (s, 1H), 6.82 (s, 1H), 4.43 (q, *J* = 7.1 Hz, 2H), 3.95 (d, *J* = 12.9 Hz, 6H), 1.44 (t, *J* = 7.1 Hz, 3H). ^{13}C NMR (101 MHz, $CDCl_3$) δ 160.86, 151.02, 146.91, 130.26, 121.20, 100.86, 93.65, 61.11, 56.17, 14.40.

7.8. REFERENCES

1. Lombeck, F.; Di, D.; Yang, L.; Meraldi, L.; Athanasopoulos, S.; Credgington, D.; Sommer, M.; Friend, R. H., PCDTBT: From polymer photovoltaics to light-emitting diodes by side-chain-controlled luminescence. *Macromolecules* **2016,** *49* (24), 9382-9387.
2. Zhang, W.; Lu, P.; Wang, Z.; Ma, Y., Microwave-assisted suzuki coupling reaction for rapid synthesis of conjugated polymer–poly(9,9-dihexylfluorene)s as an example. *Journal of Polymer Science Part A: Polymer Chemistry* **2013,** *51* (9), 1950-1955.
3. Furno, M.; Meerheim, R.; Hofmann, S.; Lüssem, B.; Leo, K., Efficiency and rate of spontaneous emission in organic electroluminescent devices. *Physical Review B* **2012,** *85* (11), 115205.
4. Khambhati, D. P.; Sachinthani, K. A. N.; Rheingold, A. L.; Nelson, T. L., Regioselective copper-catalyzed direct arylation of benzodithiophene-S,S-tetraoxide. *Chemical Communications* **2017,** *53* (37), 5107-5109.
5. Jiang, D.; Xue, Z.; Li, Y.; Liu, H.; Yang, W., Synthesis of donor-acceptor molecules based on isoxazolones for investigation of their nonlinear optical properties. *Journal of Materials Chemistry C* **2013,** *1* (36), 5694-5700.
6. Zhang, Z.-G.; Wang, J., Structures and properties of conjugated Donor-Acceptor copolymers for solar cell applications. *Journal of Materials Chemistry* **2012,** *22*(10), 4178-4187

VITA

K. A. Niradha Sachinthani

Candidate for the Degree of

Doctor of Philosophy

Thesis: DESIGN, SYNTHESIS AND CHARACTERIZATION OF EUMELANIN-INSPIRED SMALL MOLECULES AND POLYMERS AS NOVEL ORGANIC SEMICONDUCTORS

Major Field: Organic Chemistry

Education:
Completed the requirements for the Doctor of Philosophy in Organic Polymer Chemistry at Oklahoma State University, Stillwater, Oklahoma, in July, 2017.

Completed the requirements for the Bachelor of Science in Chemistry at University of Kelaniya, Sri Lanka, in 2010.

Experience:

Graduate Teaching Assistant & Graduate Research Assistant, Department of Chemistry, Oklahoma State University, Stillwater, Oklahoma 2012-2017.

Lab Associate, Ames Laboratory, Iowa State University, Ames, Iowa. Dec 2016.

Temporary Lecturer and Undergraduate Teaching Assistant, Department of Chemistry, University of Kelaniya, Sri Lanka. 2011-2012.

General Assistant, Accounts division, Alliance Five (Pvt) Ltd, Kerawalapitiya, Hendala, Sri Lanka. 2005-2006.

Professional Memberships:

Member of American Chemical Society (ACS), Division of Polymer Chemistry
Member of Phi Kappa Phi Honor Society for excellent academic accomplishments
Departmental representative to The Graduate and Professional Student Government Association (GPSGA) – Oklahoma State University